Imperial College London
Department of Life Sciences

Global Effects of Climate Change on Animal Population Dynamics

Bernardo García-Carreras

June, 2012

Supervised by Dr. D. Reuman

Submitted in part fulfilment of the requirements for the degree of
Doctor of Philosophy in Life Sciences of Imperial College London
and the Diploma of Imperial College London

Declaration

I herewith certify that all material in this dissertation which is not my own work has been properly acknowledged. I have chosen to retain the first-person plural in acknowledgement of Daniel Reuman's (thesis supervisor and co-author) contribution.

Bernardo García-Carreras

Abstract

Climate change affects many statistical descriptions of the environment. The impact of changes in mean environmental conditions on animal populations has been widely reported. The variability and autocorrelation of environmental variables are also changing over time, yet less research has focussed on what impact these changes may have on populations. Is the research focus on changes in mean conditions justified? How do changes in different statistical descriptions of climate change affect populations, and how do the impacts compare? To answer these questions, we developed a simple stochastic population model, explicitly linked to the environment, and compared the impacts of changes in environmental mean and variability. We found, using both the long-term stochastic growth rate and extinction risk as proxies for population fitness, that changes in variability have a significant impact on population dynamics. The main gradient along which the relative importance of changes in environmental mean and variability varied was the population's distance from its ideal environment. We also re-analysed existing population models to yield the sensitivity of the population to changes in environmental mean and variability. Results support the findings from our model, and confirm the importance of changes in variability for population dynamics. Previous theoretical and laboratory studies concluded that the autocorrelation in the environment in part affects the autocorrelation in population time series. So far, this hypothesis has not been tested using empirical data. We used a database of population time series to find that the autocorrelation in mean summer temperature is significantly correlated with the autocorrelation in population time series. Results also show that environmental variables have become less autocorrelated in most geographical regions, suggesting that populations' autocorrelation may also be changing. Autocorrelation in population time series has been linked to extinction; these results may therefore have important implications for animal populations.

Acknowledgements

I would never have managed without the help and support of many people. Thanks are due to:

First and foremost, my supervisor, Dan Reuman, for giving me the opportunity of doing such an exciting project, his pedagogical explanations, infinite patience, enthusiasm, encouragement, and reassurance (basically, everything). I could not have wished for a better supervisor.

My progress review panel, Tim Coulson and Dave Orme, for their advice and comments on individual chapters of this thesis.

Frank van Veen, Owen Jones, Owen Petchey, Ana Bento, Aurelio Malo, Joaquín Hortal, Miguel Olalla-Tárraga, Georgina Mace, Alex Lord, Lisa Signorile, Lawrence Hudson, and two anonymous referees for their useful comments on Chapter 6. Lawrence Sheppard and Martijn van de Pol and an anonymous reviewer for their insights on Chapter 3. Bernt-Erik Sæther, Jarle Tufto, and Stéphanie Jenouvrier, for providing essential information for Chapter 5, and Tim Coulson and Tom Ezard for help with the Soay sheep model.

The Reuman lab, i.e., Lawrence Hudson, Lisa Signorile, Julieta Decarre, Georgina Adams, Emma Defriez, and Lawrence Sheppard for all the chats, help, venting sessions, and surely patience during my multilingual arguments with my computer.

Ana Bento, the first Silwoodian I met, for making my life at Silwood better, and for her help and support throughout the project. Ana has also been my go-to reference for those pesky biological questions. Also Lola Bento, for keeping my sanity in check by taking me on walks and humouring me by fetching any cylindrical or spherical object I dared to throw.

My family, for their patience and unconditional support, without which this thesis would have been much harder to complete.

Contents

List of Figures

List of Tables

1 Introduction

Ongoing climate change presents unprecedented opportunities to understand how a population's environment affects its dynamics. Rapid changes in climate can directly affect the distribution and dynamics of populations through physiological stress (Hughes, 2000), changes in reproductive and survival rates (Walther *et al.*, 2002), and shifts in phenology (McCarty, 2001; Walther *et al.*, 2002; Parmesan, 2006). Other indirect consequences, such as habitat fragmentation or loss, introduction of invasive species, and a change to the competitive interactions between species can also feed back into local abundance and geographic range size (Hughes, 2000). It follows that climate change has been identified as a factor threatening the persistence of populations (Parmesan, 1996; Hughes, 2000; Parmesan, 2006), and both local (Parmesan, 1996; McLaughlin *et al.*, 2002) and global (Pounds *et al.*, 1999; Stuart *et al.*, 2004) extinctions can be expected as a consequence. Significant shifts in range towards higher latitudes and altitudes have been widely documented (Parmesan, 1996; Thomas & Lennon, 1999; Hughes, 2000; McLaughlin *et al.*, 2002; Parmesan & Yohe, 2003; Parmesan, 2006), indicating a pattern of nonrandom local extinctions particularly at lower altitudes and southern borders of populations' ranges (Parmesan, 1996; McCarty, 2001).

Many of these studies focus on the impacts of changes in mean environmental conditions (e.g., Parmesan, 1996; Pounds *et al.*, 1999; Parmesan & Yohe, 2003). This is unsurprising, given that the most commonly measured consequence of climate change is the change in mean state of climate variables (e.g., increases in mean temperature; IPCC, 2007). However, rising levels of greenhouse gases may also alter other statistical moments and descriptions of climate, such as variance and autocorrelation. Changes in variability of climate have received less attention than changes in mean conditions, although they have been studied at various temporal resolutions (e.g., daily: Karl *et al.*, 1995; monthly: Räisänen, 2002; Sun *et al.*, 2010; seasonal: Parker *et al.*, 1994; annual: Vinnikov & Robock, 2002; Boer, 2010), using both empirical data (Michaels *et al.*, 1998; Svoma & Balling, 2010) and forecasts from a range of models (Hunt & Elliott, 2004; Stouffer & Wetherald, 2007; Sakai *et al.*, 2009). Changes in variability have been shown to potentially affect populations' fitness (Schoener & Spiller, 1992; McLaughlin *et al.*, 2002; Tuljapurkar *et al.*, 2003; Tews & Jeltsch, 2004; Altwegg *et al.*, 2006; Chaves *et al.*, 2011). Climate change may also be altering the autocorrelation in environmental variables (Wigley *et al.*, 1998). Both laboratory experiments (Petchey, 2000; Laakso *et al.*, 2003b) and theoretical studies (Roughgarden, 1975; May, 1981; Kaitala *et al.*, 1997b; Laakso *et al.*, 2003a; Greenman & Benton, 2005) conclude that autocorrelation in climate variables at least in part affects autocorrelation in population time series, although empirical support for this hypothesis in the field has so far been lacking. The autocorrelation in population time series has been linked to extinction risk (Lawton, 1988; Halley, 1996; Inchausti & Halley, 2003). Therefore, were the link between autocorrelation in the environment and in population time series to be empirically corroborated, climate change could be affecting extinction risk through changes in autocorrelation of climate variables. Changes in these statistical descriptions of climate (mean, variance, and autocorrelation) may potentially affect populations' dynamics and extinction risk. How do changes in environmental mean, variability, and autocorrelation affect populations, and how do the magnitudes of these effects compare? Is the research bias towards changes in mean conditions justified?

To answer these questions, in Chapters 3 and 4 we develop a simple theoretical framework, where the population is explicitly linked to the environment. This framework is used to compare the effects of changes in different statistical descriptions of climate (specifically mean and variability) on population dynamics. We analyse the sensitivity of two different proxies for population fitness to changes in mean and variability of the environment. In Chapter 3 we use the long-term stochastic growth rate as a measure of population fitness. The model is then extended to estimate extinction risk and its sensitivities to changes in mean and variability of the environment in Chapter 4. The objective of these analyses is to determine how important changes in environmental variability are relative to changes in the mean, and what populations the changes in variability are most likely to affect. We analyse this model applying a suite of tools and methods often applied to matrix population models. These are introduced and described in Section 2.1. There are few empirical studies that aim to compare the sensitivity of a population to changes in environmental mean and variability. In Chapter 5 we re-analyse some existing population models to yield sensitivities to changes in environmental mean and variability, and provide further points of comparison against which to validate the model of Chapters 3 and 4. In Chapter 6, we investigate whether there is a link between the autocorrelation of climate and the autocorrelation of populations by analysing field data of a wide range of species, and a climate data set. Weather station data is also analysed to confirm the hypothesis that climate change is affecting the spectral colour of climate variables likely to be important for populations. Each chapter is presented as a self-sufficient unit, and any supplementary information is provided in the Appendices. Chapter 7 summarises the main results and conclusions.

2 Background

2.1 Population dynamics in stochastic environments

Chapters 3 and 4 develop a theoretical approach for the purpose of comparing the effects of different statistical changes in the environment, such as changes in its mean and variability, on a population. This Section aims to provide the necessary background to the models used in these Chapters. Caswell (2001) provides an excellent introduction to matrix population models; some of the most salient and relevant aspects are summarised in this Section. Many of the tools used to analyse these models, such as approximations to the long-term stochastic growth rate (defined below), are derived in Tuljapurkar (1990).

2.1.1 The Lewontin-Cohen model

The so-called Lewontin-Cohen model (Lewontin & Cohen, 1969) is one of the simplest stochastic population models; it is also frequently used in population dynamics. The reason for its popularity is that there are many tools available to analyse this model (some are used below), and it is analytically tractable. For n_t representing the population in year t, the univariate formulation of the Lewontin-Cohen model (Lewontin & Cohen, 1969) is

$$n_{t+1} = \lambda_t \, n_t, \tag{2.1}$$

where λ_t is the net growth rate of the population in year t. The growth rate λ_t can be averaged over time to obtain the growth rate $\ln \mathrm{E}(\lambda_t)$ of the deterministic skeleton model, $n_{t+1} = \mathrm{E}(\lambda_t) \, n_t$. For the stochastic model, population size asymptotically approaches a lognormal distribution, with mean t times a quantity denoted $\ln \lambda_s$ (a in Tuljapurkar (1982); “infinitesimal mean” μ in Lande & Orzack (1988); $\bar{r}$ in Lande *et al.* (2003)). This mean divided by t (i.e., $\ln \lambda_s$) is the long-term stochastic growth rate (Tuljapurkar, 1982, 1990; Caswell, 2001) and is defined as $\mathrm{E}(\ln \lambda_t)$ (Tuljapurkar, 1990; Lande *et al.*, 2003), and the variance divided by t (σ_r^2; “infinitesimal variance” σ in Lande & Orzack, 1988) is the log variance, which quantifies the variability around the estimate of $\ln \lambda_s$.

The growth rates $\ln \mathrm{E}(\lambda_t)$ and $\ln \lambda_s$ can differ significantly, and can sometimes predict opposite trends (Figure 2.1). The reason lies in the fact that the lognormal distribution of population size becomes more skewed over time, such that $\ln \mathrm{E}(\lambda_t)$ is increasingly dominated by rare but very large populations (Caswell, 2001). Mathematically, the difference between the two growth rates can be explained through Jensen's inequality, which states that $f(\mathrm{E}(X)) \geq \mathrm{E}(f(X))$ if f is a concave function (Ruel & Ayres, 1999; Boyce *et al.*, 2006). In this case f is the log function, so $\ln \lambda_s \leq \ln \mathrm{E}(\lambda_t)$. The long-term stochastic growth rate represents the rate at which almost every realisation of the population grows (Caswell, 2001; Tuljapurkar *et al.*, 2003; Ezard *et al.*, 2008) and is widely studied as a fitness parameter (Boyce *et al.*, 2006). A second-order approximation of $\ln \lambda_s$ for the model of equation (2.1) is

$$\ln \lambda_s \approx \ln \mathrm{E}(\lambda_t) - \frac{\mathrm{Var}(\lambda_t)}{2\,\mathrm{E}(\lambda_t)^2} \tag{2.2}$$

(Tuljapurkar, 1982; Caswell, 2001). This approximation clearly shows how variability in λ_t reduces the population growth rate. Whether the same can be said for variability in the environment will depend on the concavity of the function that links λ_t to the environment (see Section 2.1.5 and Chapter 3).

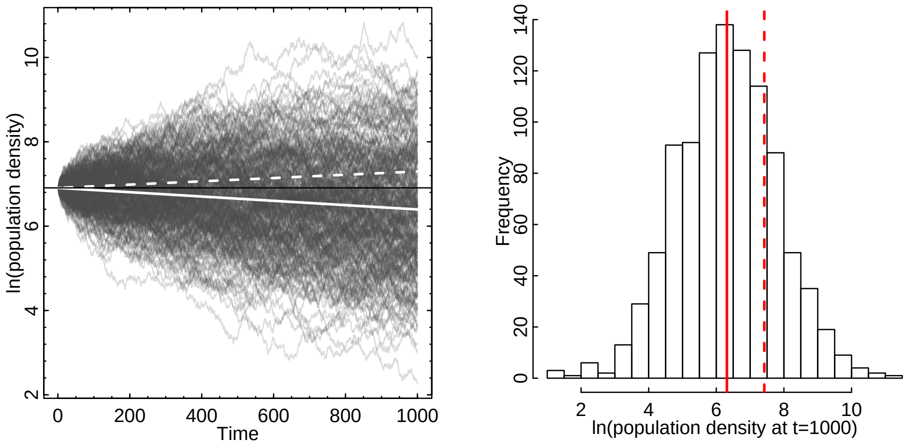

(a) *(b)*

Figure 2.1: (a) 300 stochastic realisations of the Lewontin-Cohen model, with λ_t uniformly distributed between 0.92 and 1.081. The slope of the solid line is $\ln \lambda_s$, and the slope of the dashed line is $\ln \mathrm{E}(\lambda_t)$. (b) Histogram of log-population density at $t = 1000$, for 1000 realisations of the Lewontin-Cohen model. The solid line is $t\ \ln \lambda_s$, and the dashed line is $t\ \ln \mathrm{E}(\lambda_t)$.

2.1.2 Matrix population models

As is apparent from equation (2.2), autocorrelation in the growth rate has no effect on $\ln \lambda_s$, and only becomes relevant once population structure is introduced to the model. For a population with k age-classes, the matrix equivalent of equation (2.1) is

$$\mathbf{n}_{t+1} = \mathbf{\Lambda}_t \, \mathbf{n}_t, \tag{2.3}$$

where

$$\mathbf{\Lambda}_t = \begin{bmatrix} g_0(t) & g_1(t) & g_2(t) & \cdots & g_{k-1}(t) \\ s_0(t) & 0 & 0 & \cdots & 0 \\ 0 & s_1(t) & 0 & \cdots & 0 \\ \vdots & 0 & \ddots & \ddots & \vdots \\ 0 & 0 & 0 & s_{k-2}(t) & 0 \end{bmatrix}, \tag{2.4}$$

is a k x k matrix called the Leslie matrix, and where $g_i(t)$ is the fecundity of age-class i, and $s_i(t)$ is the probability of survival of an individual in age class i (Caswell, 2001). The dominant eigenvalue λ_1 is the deterministic growth rate. It is the long-term growth rate if the environment is assumed to be constant, and is analogous to $\mathrm{E}(\lambda_t)$ in the univariate case above. The right and left eigenvectors $\mathbf{w}_i$ and $\mathbf{v}_i$, correspond to the stable age distribution and age-specific reproductive value respectively, and are scaled such that $\langle \mathbf{w}_i, \mathbf{v}_i \rangle = 1$ for all i (Caswell, 2001). Let

$$\mathbf{\Lambda}_t = \bar{\mathbf{\Lambda}} + \mathbf{D}_t. \tag{2.5}$$

$\bar{\mathbf{\Lambda}}$ is the average matrix, and $\mathbf{D}_t$ is the deviation from the mean. Then,

$$\mathbf{C}_i = \mathrm{E}(\mathbf{D}_{t+i} \otimes \mathbf{D}_t) \qquad i = 0, 1, \ldots \tag{2.6}$$

contains the lag-i autocorrelations of the vital rates (Caswell, 2001). The Kronecker product, denoted $\otimes$, is the product of all possible combinations of the two matrices. $\mathbf{C}_0$ therefore refers to the autocovariances of the elements of $\mathbf{\Lambda}_t$. Tuljapurkar (1990) provides a second-order approximation for $\ln \lambda_s$, analogous to equation (2.2), but for a structured population:

$$\ln \lambda_s \approx \ln \lambda_1 - \frac{\tau^2}{2\,\lambda_1^2} + \frac{\theta}{\lambda_1^2}, \tag{2.7}$$

where

$$\tau^2 = (\mathbf{v_1} \otimes \mathbf{v_1})^{\mathrm{T}} \, \mathbf{C_0} \, (\mathbf{w}_1 \otimes \mathbf{w_1}) \tag{2.8}$$

$$\theta = \sum_{j=2}^{m} (\mathbf{v}_1 \otimes \mathbf{v}_j)^{\mathrm{T}} \left(\sum_{h=1}^{\infty} \left(\frac{\lambda_j}{\lambda_1} \right)^{h-1} \mathbf{C}_h \right) (\mathbf{w}_j \otimes \mathbf{w}_1) \tag{2.9}$$

(Tuljapurkar, 1990; Caswell, 2001). The two terms τ^2 and θ, are the autocovariances (variation within years) and lag-i autocorrelations (variation between years) of the vital rates respectively. The information on the spectral colour of the vital rates is contained within θ. If the vital rates are independent and identically distributed (iid), $\theta = 0$. The univariate model discussed at the beginning of this Section is a special case, where $k = 1$, $\theta = 0$, and $\mathbf{C}_0 = \mathrm{Var}(\lambda_t)$.

The impact of autocorrelation on the $\ln \lambda_s$ of a structured population has been shown to be limited (Tuljapurkar, 1982), but its effect on σ_r^2 can be more substantial (Tuljapurkar & Orzack, 1980; Tuljapurkar, 1982; Runge & Moen, 1998).

2.1.3 Extinction risk

Populations with $\ln \lambda_s \leq 0$ are bound to go extinct with probability 1, whereas for those with $\ln \lambda_s > 0$, extinction is still possible but not certain (Lande & Orzack, 1988). The long-term stochastic growth rate does, *a priori*, have some limitations as a proxy for population fitness, as it is difficult to quantify the actual extinction risk faced by a population from $\ln \lambda_s$ alone. In fact, extinction risk changes very rapidly with $\ln \lambda_s$ (Dennis *et al.*, 1991; Fieberg & Ellner, 2000). Populations described only by equation (2.1) never go extinct, but at most decay exponentially, only asymptotically reaching zero (Caswell, 2001). Lande & Orzack (1988) used a diffusion approximation to derive extinction risk G as

$$G(t|x_0) \approx \Phi\left[\frac{-x_0 - \ln \lambda_s\, t}{\sqrt{\sigma_r^2\, t}}\right] + \exp\left(\frac{-2\, \ln \lambda_s\, x_0}{\sigma_r^2}\right) \Phi\left[\frac{-x_0 + \ln \lambda_s\, t}{\sqrt{\sigma_r^2\, t}}\right], \tag{2.10}$$

(Morris & Doak, 2002), where $\Phi[\cdot]$ is the cumulative distribution function (cdf) of a standard normal, and where $G(t|x_0)$ is the cumulative probability that the population becomes extinct before time t, given an initial population size $x_0 = \ln n_0$. Implicit in equation (2.10) is an extinction threshold of a population size of one individual (Lande & Orzack, 1988). The probability of ultimate extinction is

$$G(t = \infty|x_0) = \begin{cases} 1 & \text{if } \ln \lambda_s \leq 0 \\ \exp\left(\dfrac{-2\, \ln \lambda_s\, x_0}{\sigma_r^2}\right) & \text{if } \ln \lambda_s > 0 \end{cases} \tag{2.11}$$

(Lande & Orzack, 1988; Caswell, 2001). As equation (2.11) shows, the uncertainty around $\ln \lambda_s$, σ_r^2, has important implications for the viability of a population; a population may be expected to grow in the long run ($\ln \lambda_s > 0$), but if the uncertainty around the measure of $\ln \lambda_s$ is large enough, its viability may not be guaranteed. Both $\ln \lambda_s$ and σ_r^2 are therefore necessary inputs to estimate extinction risk (Tuljapurkar & Orzack, 1980).

Extinction risk is important in population viability analysis and conservation biology, where it is a vital statistic. It has the further advantage of being more intuitive to understand than $\ln \lambda_s$. However, the practical use of predicting extinction risk has been questioned, particularly with regards to the amounts of data typically available in ecology (Fieberg & Ellner, 2000). Fieberg & Ellner (2000) point out that reasonably accurate predictions of extinction probabilities can only be made for a short-time horizon (typically 10-20% of the time the population has been monitored). However, in the context of theoretical exploration, extinction risk has advantages: the information contained in σ_r^2 is ignored when using $\ln \lambda_s$ as the sole fitness parameter. How important is σ_r^2 in determining how changes in the vital rates and the environment affect a population? This question is addressed in Chapter 4.

2.1.4 Sensitivity analysis

Often, the objective of studying or parameterising models such as those described in Sections 2.1.1 and 2.1.2 is to perform a sensitivity analysis. A sensitivity analysis provides information on what demographic rates have the largest impact on population fitness, typically as measured by $\ln \lambda_s$ (although extinction risk can also be used, e.g., van de Pol *et al.*, 2010, 2011), and is useful to determine what action is required to protect a population of conservation concern or to control a pest. It consists of perturbing a vital rate to see how the population fitness responds. For example, using the univariate approximation of equation (2.2), one could determine how $\ln \lambda_s$ would respond given a change in the variance of λ_t. More typically, a matrix model could be used to quantify the change in $\ln \lambda_s$ were a vital rate, for instance juveniles' survival, to be perturbed. Mathematically, a sensitivity is the partial derivative of the fitness parameter with respect to the vital rate of interest. For example, $\partial \ln \lambda_s / \partial a_{ij}$ gives the amount by which $\ln \lambda_s$ changes if element a_{ij} of a Leslie matrix is perturbed. The sensitivity is therefore the local slope of $\ln \lambda_s$ as a function of a_{ij}; it is a linear approximation (Caswell, 2001). The sign and magnitude of sensitivities are also indicative of the selection gradient, given that natural selection favours changes in the phenotype that increase fitness (Haridas & Tuljapurkar, 2005).

Elasticities are also often calculated. They are the proportional change in the fitness parameter, for a proportional change in a vital rate, e.g., $E_{ij}^D = \partial \ln \lambda_1 / \partial \ln a_{ij}$, and $E_{ij}^S = \partial \ln \lambda_s / \partial \ln a_{ij}$, where '$D$' and '$S$' stand for deterministic and stochastic respectively (Caswell, 2001; Tuljapurkar *et al.*, 2003). Equations (2.1) and (2.3) show that selection will favour traits that reduce variability in the vital rates and increase their means (Pfister, 1998; Morris & Doak, 2004; Haridas & Tuljapurkar, 2005). However, E^{S}_{ij} perturbs the distribution of a_{ij} uniformly, changing both the mean and variance of a_{ij} while keeping the coefficient of variation constant (Tuljapurkar *et al.*, 2003). To investigate the separate effects of changes in the mean and variability of the vital rates on $\ln \lambda_s$, different elasticities are required. $E^{S\mu}_{ij}$ is the elasticity of $\ln \lambda_s$ to changes in the mean of vital rate a_{ij}, denoted μ_{ij}. $E^{S\mu}_{ij}$ keeps the variance of a_{ij} constant. Likewise, $E^{S\sigma}_{ij}$ perturbs the variability of a_{ij}, denoted σ_{ij}, while keeping μ_{ij} constant (Tuljapurkar *et al.*, 2003; Ezard & Coulson, 2010). These elasticities are dependent:

$$E^{S}_{ij} = E^{S\mu}_{ij} + E^{S\sigma}_{ij}$$

(Tuljapurkar *et al.*, 2003; Haridas & Tuljapurkar, 2005). $E^{S\mu}_{ij}$ is always positive, while the sign of $E^{S\sigma}_{ij}$ is often negative (Haridas & Tuljapurkar, 2005), which is consistent with the idea that variability in vital rates is detrimental to populations. Using empirical data, several studies (e.g., Tuljapurkar *et al.*, 2003; Haridas & Tuljapurkar, 2005; Ezard *et al.*, 2008; Ezard & Coulson, 2010; Jonzén *et al.*, 2010) have shown that in most cases, $E^{S\mu}_{ij} \geq |E^{S\sigma}_{ij}|$, so changes in mean vital rates have a bigger impact on $\ln \lambda_s$ than changes in their variability. Do changes in mean environment analogously have a bigger impact on population fitness than changes in variability? This question is explored in Chapters 3 and 4.

2.1.5 The link between environment & populations

Environmental variables affect population vital rates such as survival probabilities and fecundity rates; it is through vital rates that climate change can affect population growth rates and risks of extinction. Determining the consequences of climatic changes on population growth therefore requires understanding the relationship between environment and vital rates, i.e., how an environmental signal is translated into biological processes (Laakso *et al.*, 2001; Morris *et al.*, 2008).

For some populations, the environment can be simplified down to a discrete set of states which largely determines what the population vital rates will be. For example, a population's vital rates may depend on whether it is a 'good' or 'bad' year (e.g., Jenouvrier *et al.*, 2009; Hunter *et al.*, 2010). Similarly, disturbance-prone populations' response to the environment may mainly depend on events. For these populations, the environment can be modelled as a Markov chain, by ascribing a Leslie matrix to each state and setting the probability of switching from one state to another (e.g., fires: Caswell & Kaye, 2001; Morris *et al.*, 2006; floods: Smith *et al.*, 2005; hurricanes: Tuljapurkar *et al.*, 2003; Horvitz *et al.*, 2005; Morris *et al.*, 2006). If the environment cannot be described as a discrete set of states, it is necessary to understand how the vital rates will vary across the population's environmental range.

For ectotherms, which comprise over 99% of all species (Atkinson & Sibly, 1997), temperature alters the speed at which individuals pass through life stages, thereby influencing population growth rate (Forster *et al.*, 2011). Some studies argue, citing Arrhenius' equation, that the vital rate increases exponentially with temperature (e.g., Drake, 2005). In this case, due to Jensen's inequality, variability in temperature could be interpreted to have a positive effect (Ruel & Ayres, 1999). This view is nevertheless often supported by studies that only record thermal responses for a limited range in temperature, for which the response may indeed be exponential. However, beyond this range, the response is likely to reach an optimum, followed by a monotonic fall (Dell *et al.*, 2011). Therefore, the relationship between temperature and net population growth rate (henceforth called the response function) has typically been shown to have a single peak; there is an ideal temperature that maximises the population's performance (Huey & Stevenson, 1979; Begon *et al.*, 1996; Laakso *et al.*, 2001; Karlsson & Wiklund, 2005; Frazier *et al.*, 2006; Deutsch *et al.*, 2008; Pörtner & Farrell, 2008; Dell *et al.*, 2011). An argument for a single-peaked response function can also be made for endotherms (Boyles *et al.*, 2011) and other environmental variables such as precipitation (Begon *et al.*, 1996). Other than a probable common feature of having one peak, response functions can take different forms depending on species and local environmental conditions. The shape of a response function may determine how variability in temperature or another environmental variable affects the population growth rate (Ruel & Ayres, 1999; Drake, 2005; Boyce *et al.*, 2006; van de Pol *et al.*, 2010). If a response function is log-convex (the log of the function opens up) for the range of an environmental variable that pertains in a locale, then an increase in variability may in fact benefit the population; if the function is log-concave (its log opens down) for the pertinent range of the variable, then variability is detrimental for the population (Ruel & Ayres, 1999; Drake, 2005).

The response function therefore plays an important role in determining the impacts of climate change on populations. There are several important studies that compare the effects of changes in mean and variability of vital rates on population growth rate (e.g., Haridas & Tuljapurkar, 2005; Morris *et al.*, 2008; Ezard & Coulson, 2010; Coulson *et al.*, 2011). However, changes in the mean environment can modify both the mean and standard deviation of vital rates, as can changes in the standard deviation of the environment; understanding the relative importance of changes in means and variabilities of vital rates does not necessarily translate directly to the relative importance of changes in the means and variabilities of environmental variables. *A priori*, the translation from environments to vital rates may affect the relative importance of means and standard deviations. Furthermore, as shown by Jonzén *et al.* (2010), the importance of changes in the variability of the vital rates is not necessarily indicative of the importance of changes in the variability of the environment. It therefore seems necessary to explicitly consider response functions. How important are our assumptions on how climate affects a population's vital rates, in establishing the effect climate change may have on populations? The role of response functions is further investigated in Chapters 3 and 4.

2.2 Spectral colours & population dynamics

Weather and animal population numbers continuously change over time. These fluctuations have been studied with respect to time, but an increasing body of work has focussed on describing the characteristics of these variations in greater detail by analysing the signals with respect to frequency. Concentrating on the oscillations can reveal features that would otherwise have passed unobserved. Furthermore, relationships or correlations could come to light by investigating from this different point of view. This subject is of particular relevance in the context of a changing climate. A change in how the climate fluctuates could lead to the oscillations of populations changing too, so increasing understanding of how the two are related is of vital importance for informing conservation and management policies. The aim of this Section is to review this body of work. Appendix A contains an introduction to spectral analysis and a description of the main statistical tool discussed in this Section: the spectral exponent.

2.2.1 The colour of the environment

The environment is a complex system that fluctuates naturally due to physical processes that are internal to the Earth and its atmosphere (such as ocean circulation and changes in the relative quantities of atmospheric gases) and external factors (such as variation in sunlight intensity). Because of this, climate variables are usually both temporally and spatially autocorrelated, i.e., they are likely to be more similar when close in both space and time than would be expected if they were purely independent.

Environmental noise was, for some time, assumed to be white (Vasseur & Yodzis, 2004). Although this assumption may, according to Steele (1985), hold for shorter terrestrial time series, the consensus is that many climate time series are red: longer-term climatic patterns contribute more to the time series variance than do shorter-term weather fluctuations (Steele & Henderson, 1994; Pelletier & Turcotte, 1997; Cyr & Cyr, 2003; Vasseur & Yodzis, 2004). Possible phenomena that may contribute to redness include inter-annual periodic events such as El Niño-Southern

Oscillation and inter-decadal phenomena such as the North Atlantic Oscillation, the Pacific Decadal Oscillation, or the Atlantic multidecadal oscillation (e.g., see Stenseth *et al.*, 2003). On a longer time-scale yet, climate change over the past century superimposes a longer-term trend.

Whether or not climate spectra are better described by $1/f^\beta$ or autoregressive (AR) noise is less clear (see Appendix A for a comparison between the two). Several studies indicate that they are better approximated by $1/f^\beta$ noise (e.g., Mandelbrot, 1982; Halley, 1996; Halley & Kunin, 1999). However, the recurring presence of a plateaux at low frequencies in the power spectra of temperature time series may be more indicative of an AR process (Talkner & Weber, 2000; Cyr & Cyr, 2003; Vasseur & Yodzis, 2004). Spanning a wide range of time scales (from days to thousands of years), the spectral exponent can vary quite significantly for different frequencies (Pelletier, 1998, 2002), which may suggest that on such a wide range of scales no single, simple $1/f^\beta$ or AR model may suffice.

The spectral colour of mean temperature fluctuations is not only of interest *per se*. How spectral colour is distributed and structured geographically can also provide useful insights not only on how the environment varies in different areas, but also on how that spatial structure may affect other systems (such as animal populations) that to some extent depend on it. Most studies agree that there is indeed a clear spatial distribution of environmental noise colours (Steele, 1985; Steele & Henderson, 1994; Blender & Fraedrich, 2003; Cyr & Cyr, 2003; Fraedrich & Blender, 2003; Vasseur & Yodzis, 2004). Their results show that terrestrial temperature spectra tend to be whiter, and then become systematically redder closer to bodies of water of increasing size. This can be explained by the high heat capacity of water that damps out high-frequency temperature oscillations (Cohen, 1995), thereby increasing autocorrelation. There are, in any case, disagreements. Eichner *et al.* (2003) and Bunde *et al.* (2004), for instance, do not find that the scaling exponent (obtained from Detrended fluctuation analysis (DFA); see Appendix A) depends on the distance of the location from the coastline. In other studies (Koscielny-Bunde *et al.*, 1996, 1998), universal scaling laws were found (also using DFA). In terms of $1/f^\beta$ spectral exponents, they found $\beta \sim -0.3$ to be prevalent. In the latter studies, though, the weather stations used by the authors are relatively coastal. Vasseur & Yodzis (2004) also found a latitudinal pattern, with redder noise found at high latitudes. These findings give rise to an interesting question: does the spectral colour of animal populations exhibit similar patterns?

2.2.2 Animal populations

There has been a lot of interest in the variability of population time series and how this depends on the length of the time series used to measure the variance. Studies using field populations have been constrained by the amount of data available. Pimm & Redfearn (1988), for instance, examined data from four species of insects and a total of 22 species of birds and mammals (no indication as to how many of each is given) from censuses taken annually for over 50 years, and information on 42 species of farmland birds and 32 species of woodland birds spanning 24 years (gathered by the British Trust of Ornithology), and found that in all cases, irrespective of the duration of the census season, the variation in the populations (measured as the standard deviation of the logarithms of annual densities) increased with the number of data points included in calculating this quantity. These conclusions were supported by Lawton (1988), Halley (1996), and Cyr (1997). Cyr (1997) also used the same measure of variability as Pimm & Redfearn (1988) on 70 populations of phytoplankton, zooplankton, and fish sampled over 10 to 51 consecutive years in lakes around the world. The results showed only a moderate increase in variability, although the rate at which this measure changed over time was prone to substantial changes.

Pimm & Redfearn (1988) considered the increase in variability as a surrogate for spectral reddening, arguing that if the spectra of the time series analysed were to be red, its variance would increase over time, as is seen in $1/f^{\beta}$ models. These conclusions were notionally questioned by McArdle *et al.* (1990), who on theoretical grounds argued that these results could be artefactual. Pimm & Redfearn's (1988) conjecture was later supported by Inchausti & Halley (2001, 2002). Inchausti & Halley (2001, 2002) analysed the spectral colour of 544 populations of 123 species (including mammals, insects, birds, bony fish, crustaceans and molluscs) from the Global Population Dynamics Database (GPDD; NERC Centre for Population Biology & Imperial College, 1999) that had been censused for more than 30 years, and found red spectra to be strongly correlated with increase in variance, thereby lending support to the theory that spectral reddening could be the cause of the 'more time-more variation' effect noted by Lawton (1988) and Pimm & Redfearn (1988).

In the studies by Inchausti & Halley (2001, 2002), the mean spectral exponent was -1.022 (SE=0.025), and therefore red. Using the same data, Inchausti & Halley (2002) refined the analysis by looking at trends in different subsets by taxa, body size, trophic level and geographical distribution. They found spectral reddening to be universally prevalent. The results of Ariño & Pimm (1995) also supported this trend, after analysing data of 115 populations comprising 57 different species (including terrestrial birds, birds, mammals, plants, insects, freshwater diatoms, fish, and marine fish) and that had been censused for at least 25 years. They calculated the Hurst exponents for these populations, and found them to range between 0.25 and over 1.3, with a mean of ~ 0.76, corresponding to a spectral exponent range of -1.5 to below -3.6 with a mean of -2.52. The authors furthermore found marine species to be redder than terrestrial species, and terrestrial vertebrates to be redder than insects.

In order to explain the cause of the spectral reddening in populations, Cohen (1995) investigated several simple deterministic population models, and surprisingly found that dynamics predicted by these models tended to be blue. The models he examined were deterministic single-population models (e.g., the Moran-Ricker, the Verhulst, the Hassell, and the Maynard Smith models), many of which have been used in applied contexts, but most of which are now often regarded as mathematical idealisations most useful for simple, general theory. Cohen's (1995) study started a debate as to the suitability and predictive power of the models he chose, and into the reason for this apparent discrepancy between theory and practice (Blarer & Doebeli, 1996; Kaitala & Ranta, 1996; Sugihara, 1996; White *et al.*, 1996b). Some studies misleadingly generalised Cohen's (1995) results stating that "simple population dynamic models are mostly dominated by short-term fluctuations" (Kaitala *et al.*, 1997a). In fact, Cohen (1995) somewhat arbitrarily only investigated single points in the parameter space of each of the selected models, tuned to be in the chaotic regime. Several studies subsequently focussed on specific models and larger parameter ranges, finding that red spectra can also be reproduced (Chapter 6; Blarer & Doebeli, 1996; White *et al.*, 1996a). Unfortunately, most of these studies were formulated as a response to Cohen (1995), and therefore overlooked the need for a comprehensive and systematic approach in order to understand the effect of noise colour over more substantial ranges of the parameter space in the different models.

According to Sugihara (1995), Cohen's (1995) results and the subsequent debate that developed around it prompted three possible explanations that could account for the discrepancy between theory and 'practice': either natural populations are not chaotic, models are fundamentally flawed (or over-simplistic), or there is some extrinsic forcing (most likely climatic), that is the cause of the observed reddening. A further alternative was offered by Akçakaya *et al.* (2003), who used several models with different proportions of density dependence, measurement error, and natural variability (modelled as white noise). Their conclusion was that red population spectra can be explained solely as the effect of a combination of measurement error and natural variability (their results were confirmed by Gao *et al.* (2007) on a spatially structured model). It is important to note, however, that the degree of density dependence is vital in reaching this conclusion. No density dependence gave rise to random walk, whereas when populations were tightly regulated by strong density dependence, the time series were closer to white noise, regardless of the nature of variation. Other explanations were also postulated for populations' red spectra, including the fact that adding a spatial component (White *et al.*, 1996b; but see Gao *et al.*, 2007) and delayed stochastic density dependence (Kaitala & Ranta, 1996) had a reddening effect.

2.2.3 How the environment affects populations

Out of the three alternatives proposed by Sugihara (1995), attention turned to the possible impact that environmental forcing could have on simple population models (Lawton, 1988; Sugihara, 1995, 1996; Ranta *et al.*, 2000). As Roughgarden (1975) and Kaitala *et al.* (1997b) state, population dynamics should be redder in reddened environments than in white environments, if environmental colour were to have any influence on population spectral colour.

Roughgarden (1975) and May (1981) found that population models with a low growth rate (r) are unable to track high-frequency oscillations in the environmental noise, and average these out following only the low-frequency components. Conversely, higher growth-rate populations are capable of tracking all or more components of the noise. Consequently, as Roughgarden (1975) states, for highly autocorrelated environmental noise, the variance of the population tends to equal that of the environment for most values of r. In terms of spectra this would translate to low r populations acquiring the low frequency variance of the environment (thereby becoming red in the process), and high r population spectra more closely mimicking the spectra of the relevant climate variables. Kaitala *et al.* (1997b), on the other hand, found that model-population sensitivity to differences in the noise colour decreases with large growth rates and ultimately disappears in the chaotic range, results largely confirmed in Chapter 6. Kaitala *et al.*'s (1997b) results seem to contradict the aforementioned studies. Roughgarden (1975) and May (1981) concluded that high growth rate populations track noise better, which implies that these populations are likely to be increasingly sensitive to differences in noise. However, Roughgarden (1975) only looked at models that went to equilibrium in the absence of stochasticity (May, 1981 does not state the range of growth rates for which his results hold), whereas Kaitala *et al.* (1997b) went beyond, into the high growth rate and chaos ranges. This distinction could reconcile the apparent differences between their results.

The analysis can be extended by adding complexity and details. The levels of complexity in a field population system can be envisioned as a series of filters between the input environmental signal and the output observed population time series: the environment affects the vital rates of a population; which in turn has a potentially complex impact on the population dynamics; and finally, as discussed by Akçakaya *et al.* (2003), measurement error separates the true and observed population signals. Models investigating the effects of environmental variability on population dynamics can, correspondingly, also be formulated at varying degrees of complexity. In its simplest form, this involves a single-species model. In theory, environmental noise can affect many, or all of the parameters in the model. Furthermore, the dependence of vital rates on environmental variables is likely nonlinear (Vasseur & Yodzis, 2004), an issue that has been addressed using filters describing a range of different functions between climate and vital rates (Laakso *et al.*, 2001, 2003a). Finally, some components, such as density dependence, may also have lags (Kaitala & Ranta, 1996). The single species can then be considered in greater detail, by using a stage structured model, in which the vital rates of different stages can be affected separately (Greenman & Benton, 2005), or by adding a spatial component to the model (White *et al.*, 1996b). Otherwise, two or more species models can be used, to study, for instance, the effects of species interactions (Ripa *et al.*, 1998), or more indirect effects such as perturbations in other parts of the food web (Ruokolainen *et al.*, 2007). The level of potential complexity of the population systems and their interaction with changes in their physical environment has led some researchers to issue a word of warning with respect to seeking generalisations in relation to the cause of reddened spectra (Laakso *et al.*, 2001, 2003a).

Petchey (2000) and Laakso *et al.* (2003b) conducted experimental studies on ciliates to investigate the effect of environmental noise colour on the colour of population spectra. Their results largely confirmed the results obtained by Roughgarden (1975) and May (1981): populations tracked reddened noise more closely than white noise, and populations with higher values of r tracked the noise better than those with low r. Both studies found all populations to be red. According to Petchey (2000), this last result contradicted theory, as the result was independent of environmental noise colour. The author found the contention to be sensible, due to the likely undercompensatory nature of the dynamics of the species studied. This led Petchey (2000) to conclude that spectral reddening was caused by internal population mechanisms, and not by extrinsic factors. The results presented in Petchey (2000) are, however, far from clarifying. Whether or not population spectra are red does not indicate if and how the level of redness, or autocorrelation, changes with different noise colour inputs. On the other hand, Laakso *et al.* (2003b) found the reddest populations, highest variability, and strongest correlation between environment and population in red environments. The results in Petchey (2000) and Laakso *et al.* (2003b) might appear to be contradictory. However, it is not clear from Petchey's (2000) results, whether the populations were affected by noise colour. As shown in Chapter 6 using a stochastic Ricker model, undercompensatory populations can be found to be red regardless of the input noise colour. These are nonetheless clearly affected, given that the redder the noise, the redder the population. Consequently, Petchey's (2000) and Laakso *et al.*'s (2003b) results are not necessarily at odds.

There are several studies that have correlated individual populations with climate using spectra (e.g., Jillson, 1980; Aebischer *et al.*, 1990), but few (if any) have done so on a global scale using multiple populations species, and none on the basis of spectral colour. In their study, Inchausti & Halley (2002) argue that population spectra average -1.022 whereas climate spectra average about -0.5, indicating that the population redness cannot be entirely attributed to climate. They state that evidence shows that on scales of ecological interest, terrestrial populations redden themselves rather than reflect the colour of their environment. This affirmation is nevertheless speculative and unfounded. Their observations, at most, show that the populations do not linearly track the environment. It may even suggest, but not prove, that reddening could be partly caused by internal mechanisms, and not solely due to environmental noise colour. In any case, population redness is likely to occur due to the environment interacting with intrinsic mechanisms in complex ways. There have, to our knowledge, been no studies that explicitly look for correlations between real population spectral exponents with the spectral exponents of climate variables from the same locations. This gap in the literature warrants further investigation, given that large scale correlations using real population data and climate variables could shed some light on the above debate.

2.2.4 Extinction risk & noise colour

Understanding and assessing extinction risk is imperative for conservation and management. For this reason, many of the studies that attempt to elucidate the basic mechanisms by which noise colour can impact populations have been related to extinction risk or persistence time of populations. Some researchers have expressed the intuitive expectation that reddening increases extinction risk (Lawton, 1988; Halley, 1996; Inchausti & Halley, 2003). The reasoning is based on the fact that an autocorrelated environmental time series would have longer runs of unfavourable conditions. This hypothesis is supported by Inchausti & Halley (2003), who found, using the aforementioned 544 populations from the GPDD, that quasi-extinction time (defined as a 90% decline in the population level) was shorter for populations with higher temporal variability and redder dynamics. Similarly, the same conclusion is reached by Pike *et al.* (2004) in an experimental study using springtail (*Folsomia candida*). In this case, the environmental autocorrelation was simulated by regular culling events (the sequence of the magnitude of these events determining the autocorrelation). Results showed that the time to extinction was shortened with increased autocorrelation.

Results from theoretical studies have been ambiguous or have contradicted each other (Heino *et al.*, 2000). In apparent contradiction to the original intuition of

Lawton, Halley, and Inchausti & Halley, Ripa & Lundberg (1996) claimed that red noise decreases extinction risk. Subsequent studies (Petchey *et al.*, 1997; Heino, 1998) were more indecisive on this matter. However, it is unlikely that any general results can be obtained from theoretical studies. How noise affects extinction risk very much depends on several factors, and seemingly subtle differences in the model can result in qualitatively different understandings of how noise colour affects extinction risk (Cuddington & Yodzis, 1999; Ripa & Lundberg, 2000). These factors have been analysed in the literature, and are summarised here.

Model and parameter choice can determine the outcome extinction risk (Heino, 1998; Morales, 1999; Ripa & Heino, 1999; Ripa & Lundberg, 2000). The aforementioned study by Ripa & Lundberg (1996), for example, reached the somewhat surprising conclusion that red noise decreases extinction risk. However, the authors only studied single-species models with parameters chosen so that the models would exhibit overcompensating decay to a stable equilibrium in the absence of stochasticity. Further research showed that reddened noise increased persistence where dynamics were overcompensatory, and decreased it for undercompensatory dynamics (Petchey *et al.*, 1997; Heino, 1998; Cuddington & Yodzis, 1999; Ripa & Heino, 1999; Ruokolainen *et al.*, 2007). Schwager *et al.* (2006) generalised these observations by suggesting that extinction risk depends on the strength of environmental fluctuations and the sensitivity of population dynamics to these fluctuations. Hence, if extreme events can occur (implying strong noise), or the sensitivity of the population is high (overcompensatory dynamics), then temporal correlation decreases extinction risk. These studies examined single-species models that came to equilibrium in the absence of stochasticity.

How and what kind of noise is incorporated into the model can also affect extinction risk (Heino, 1998; Halley & Kunin, 1999; Morales, 1999). For example, choosing a pink or brown noise (of the $1/f^\beta$ family, with $\beta \geq 1$) could result in an inherently non-stationary time series, where populations are allowed to wander to invulnerable population sizes (Halley & Kunin, 1999). This would have the effect of offsetting the increased risk presumed in higher variability. This observation may explain the results obtained by Cuddington & Yodzis (1999), who found that the 'blacker' the noise, the greater the probability of persisting for a very long time ($> 100,000$ generations). Cuddington & Yodzis (1999) furthermore conclude that the probability of a short persistence time in blacker noise is either similar (in strong undercompensation) or far less (strong overcompensation) when compared to red noise.

The choice of noise model is also important. For instance, Cuddington & Yodzis (1999) found that AR processes do not capture the unpredictability of pink or brown ($1/f^\beta$) noise. This, according to them, suggested that using AR noise in models may lead to an overly optimistic view of our ability to predict the effects of environmental noise on populations.

Because of the premise that higher variability will increase extinction risk, the time scale in which the extinctions are scored also requires attention (Halley & Kunin, 1999; Heino *et al.*, 2000). The variance of white and red noise for a given length of time series used to measure the variance are likely to be different, even if the true variances of the underlying stochastic processes are the same, so when making comparisons, Heino *et al.* (2000) emphasise that the variance of noise has to be independent of colour. Heino *et al.* (2000) and Wichmann *et al.* (2005) suggest scaling methods to address this issue. However, according to Heino *et al.* (2000) the need to scale variance depending on the chosen time scale excludes the possibility of achieving any general results.

Most studies mentioned above investigated the impact of environmental noise colour on extinction risk. However, environmental noise does not necessarily affect extinction risk directly, but rather could do so by affecting population spectral colour. This intermediate 'step' is implicitly ignored in the above studies: environmental noise of different kinds and colours is introduced into the population model by varying one or more of its parameters, and the probability of extinction is then analysed. The omission of the intermediate step, population spectral colour, adds to the complexity of the problem and furthermore contributes to creating confusion. In fact, most or all of the aforementioned problems are more likely to relate to how the environment affects populations. Inchausti & Halley (2002) is one of the few exceptions, given that they studied how population spectral colour is correlated with quasi-extinction. Understanding how spectral colour of both environment and population affect extinction risk requires a more systematic approach that explicitly analyses all intermediate steps of the problem.

3 Are changes in the mean or variability of climate signals more important for long-term stochastic growth rate?

Abstract

Population dynamics are affected by changes in both the mean and variability of climate. The impacts of increases in average temperature are extensively researched, while the impacts of changes in climate variability are less studied. Is the greater attention given to changes in mean environment justified? To answer this question we developed a simple population model explicitly linked to an environmental process. We used this model to compare the sensitivities of a population's long-term stochastic growth rate, a measure of fitness, to changes in the mean and standard deviation of the environment. We interpret results in light of a comparative analysis of the relative magnitudes of change in means and standard deviations of biologically relevant climate variables. Results show that changes in variability can be more important for many populations. Changes in mean conditions are likely to have a greater impact than changes in variability on populations far from their ideal environment, e.g., populations near species range boundaries and potentially of conservation concern. Populations near range centres and close to their ideal environment are more affected by changes in variability. Populations of interest in this category include pests and disease vectors; observed changes in variability may benefit these populations.

N. B.: This chapter has been submitted to *PLoS ONE* as: García-Carreras, B. & Reuman, D. C. Are changes in the mean or variability of climate signals more important for long-term stochastic growth rate? Its corresponding supplementary information can be found in Appendix B.

3.1 Introduction

Ongoing climate change is most readily characterised by changes in the mean state of climate variables (e.g., increases in mean temperature; IPCC, 2007), and the impacts on ecosystems of changes in mean environmental state are studied closely (Parmesan *et al.*, 1999; Morris *et al.*, 2008). However, rising levels of greenhouse gases may also affect climate variability (Boer, 2010). An increase in variability could also affect populations' fitness (Schoener & Spiller, 1992; McLaughlin *et al.*, 2002; Tuljapurkar *et al.*, 2003; Tews & Jeltsch, 2004; Chaves *et al.*, 2011). How do changes in the variability of climate compare to changes in the mean values of climate variables in terms of the importance of their impacts on populations? To help answer this question, we here consider the simplest possible population model that can be linked to an environmental process.

Changes in mean climate have been well documented (e.g., IPCC, 2007), and while changes in variability have received less attention, they have been studied at different temporal resolutions (e.g., daily: Karl *et al.*, 1995; monthly: Räisänen, 2002; Sun *et al.*, 2010; seasonal: Parker *et al.*, 1994; annual: Vinnikov & Robock, 2002; Boer, 2010), using both empirical data (Michaels *et al.*, 1998; Svoma & Balling, 2010) and forecasts from a range of models (Hunt & Elliott, 2004; Stouffer & Wetherald, 2007; Sakai *et al.*, 2009). These studies show that for some temporal resolutions, the variability of climate is changing.

Environmental variables affect population vital rates such as survival probabilities and fecundity rates; it is through vital rates that changes in the mean or variability of climate can affect population growth rates. Determining the consequences of climatic changes on population growth therefore requires understanding the relationship between environment and vital rates, i.e., how an environmental signal is translated into biological processes (Laakso *et al.*, 2001; Morris *et al.*, 2008). For ectotherms, which comprise over 99% of all species (Atkinson & Sibly, 1997), temperature alters the speed at which individuals pass through life stages, thereby influencing population growth rate (Forster *et al.*, 2011). In ectotherms, the relationship between temperature and net population growth rate (henceforth called the response function) typically has a single peak; there is an ideal temperature that maximises the population's performance (Huey & Stevenson, 1979; Begon *et al.*, 1996; Laakso *et al.*, 2001; Deutsch *et al.*, 2008; Dell *et al.*, 2011). An argument for a single-peaked response function can also be made for endotherms (Boyles *et al.*, 2011) and other environmental variables such as precipitation (Begon *et al.*, 1996). Other than a probable common feature of having one peak, response functions can take different forms depending on species and local environmental conditions. The shape of a response function may determine how variability in temperature or another environmental variable affects the population growth rate (Ruel & Ayres, 1999; Drake, 2005; Boyce *et al.*, 2006; van de Pol *et al.*, 2010). If a response function is log-convex (the log of the function opens up) for the range of an environmental variable that pertains in a locale, then an increase in variability may in fact benefit the population; if the function is log-concave (its log opens down) for the pertinent range of the variable, then variability is detrimental for the population (Ruel & Ayres, 1999; Drake, 2005).

The response function therefore plays an important role in determining the impacts of climate change on populations. There are several important studies that compare the effects of changes in mean and variability of vital rates on population growth rate (e.g., Haridas & Tuljapurkar, 2005; Morris *et al.*, 2008; Ezard & Coulson, 2010; Coulson *et al.*, 2011). However, changes in the mean environment can modify both the mean and standard deviation of vital rates, as can changes in the standard deviation of the environment; understanding the relative importance of changes in means and variabilities of vital rates does not necessarily translate directly to the relative importance of changes in the means and variabilities of environmental variables. *A priori*, the translation from environments to vital rates may affect the relative importance of means and standard deviations. This possibility can be investigated by explicitly considering response functions.

We know of only two studies that incorporate response functions and compare the effects of changes in mean and variability of the environment, as opposed to vital rates, on a population. Van de Pol *et al.* (2010) and Jonzén *et al.* (2010) parameterised stage-structured stochastic population models using populations of oystercatchers in the Netherlands and red kangaroos in South Australia, respectively. Van de Pol *et al.* (2010) concluded that time to extinction is more sensitive to changes in the environment's mean than its standard deviation, a result further magnified by the fact that climate models predict greater changes in mean temperature than in its standard deviation in the Netherlands. Jonzén *et al.* (2010) also found sensitivity of population growth to be greater to changes in mean rainfall than to changes in the standard deviation of rainfall, although the two sensitivities were similar enough that changes in standard deviation were still important.

In this study we aim to compare the effects of changes in mean and variability of inter-annual environmental conditions on population growth rate, which we use as a measure of fitness, adopting a simple, strategic approach rather than parameterising a complex model of a single population as in Jonzén *et al.* (2010) and van de Pol *et al.* (2010). Both approaches are valuable. We provide a theoretical approach based on an unstructured, annually censused population, which we assume is explicitly linked to an annual environmental variable via a response function. We first derive the population long-term stochastic growth rate as a function of the environment and the response function. We then derive the sensitivity of growth rate to changes in environmental mean and variability. We provide answers based on the model to the following three questions: (1) Given an increase in the mean or standard deviation of the environment, does the growth rate increase or decrease? (2) If mean and standard deviation are perturbed by the same small amount, which causes the greater impact on the growth rate? (3) What are the relative magnitudes of observed changes in mean and standard deviation of climate variables and how do these relate to the sensitivities computed in (2) to yield an overall idea of whether changes in climate means or standard deviations are more important for population dynamics? We discuss results in view of currently ongoing climate change, and identify potential consequences for populations of conservation concern as well as pests, disease vectors, and exploited populations.

3.2 Methods

3.2.1 Theory

For n_t representing the population in year t, the base model (Lewontin & Cohen, 1969) is

$$n_{t+1} = \lambda_t \, n_t, \tag{3.1}$$

where λ_t is the net growth rate of the population in year t. We assume $\lambda_t = f(w_t)$, where w_t is the environmental variable and f is the response function. Let $p(w_t) = \ln f(w_t)$ be the log of the response function. The growth rate λ_t can be averaged over time to obtain the growth rate $\ln \mathrm{E}(\lambda_t)$ of the deterministic skeleton model, $n_{t+1} = \mathrm{E}(\lambda_t)\, n_t$. For the stochastic model, population size asymptotically approaches a lognormal distribution, with mean t times a quantity denoted $\ln \lambda_s$ (a in Tuljapurkar, 1982; "infinitesimal mean" μ in Lande & Orzack, 1988; $\bar{r}$ in Lande *et al.*, 2003); $\ln \lambda_s$ is the long-term stochastic growth rate (Tuljapurkar, 1982, 1990; Caswell, 2001),

$$\ln \lambda_s = \mathrm{E}(\ln \lambda_t) = \int_{-\infty}^{\infty} p(w_t)\, \varphi_{\mu,\sigma}(w_t)\, \mathrm{d}w_t, \tag{3.2}$$

where $\varphi_{\mu,\sigma}$ is the probability density function (pdf) of w_t, with mean parameter μ and standard deviation parameter σ (Tuljapurkar, 1990; Lande *et al.*, 2003). Second-order approximations to $\ln \lambda_s$ (Tuljapurkar, 1982, 1990) are used, but equation (3.2) is an exact formula that applies in the case of an unstructured population. The growth rates $\ln \mathrm{E}(\lambda_t)$ and $\ln \lambda_s$ can differ significantly, but $\ln \lambda_s$ represents the rate at which almost every realisation of the population grows (Caswell, 2001; Tuljapurkar *et al.*, 2003; Ezard *et al.*, 2008) and is widely studied as a fitness parameter (Boyce *et al.*, 2006). The sensitivities of $\ln \lambda_s$ to changes in mean and standard deviation of the environment are obtained simply by taking the partial derivatives of equation (3.2) with respect to μ and σ, moving the partial derivatives under the integral symbol and applying them to $\varphi_{\mu,\sigma}(w_t)$. This approach applies generally, for any $p(w_t)$.

For concreteness, we adopt a flexible parameterisation for p. Without loss of generality we transform w_t such that its distribution in the focal location is $\mathcal{N}(0, 1)$ (see Section B.1 in the Appendix). If $h(w_t) = w_t^\alpha$ for some $\alpha > 0$, $p(w_t)$ is taken to be $a_1 \, h(-w_t + b) + c$ for $w_t \leq b$ and $a_2 \, h(w_t - b) + c$ for $w_t \geq b$ (Figure 3.1). This function is single peaked with maximum height c occurring at the ideal environment, b. The rate of falloff of p as w_t decreases (respectively, increases) from the ideal environment is controlled by a_1 (respectively, a_2); both are taken to be negative. The ratio $f_s = a_1/a_2$ is a measure of asymmetry of the response function around b. The examples of Figure 3.1 are similar to reported response functions (Huey & Stevenson, 1979; Begon *et al.*, 1996; Deutsch *et al.*, 2008; Dell *et al.*, 2011). The value of b is the difference between the local environment and the population's ideal environment, measured in units equal to the standard deviation of the local environment because we re-scaled w_t to make it standard normally distributed. Larger values of $|b|$ describe populations living in a suboptimal environment (for example, those living in environmental range margins or struggling to adapt to climate change), whereas $|b| \sim 0$ represents populations living in a close-to-ideal environment.

Substituting the above parameterisation of $p(w_t)$ into equation (3.2), we get $\ln \lambda_s$ as a function of the parameters that define the log response function,

$$\ln \lambda_s = a_1 \int_{-\infty}^{b} (-w_t + b)^\alpha \, \varphi_{\mu,\sigma}(w_t) \, \mathrm{d}w_t + a_2 \int_{b}^{\infty} (w_t - b)^\alpha \, \varphi_{\mu,\sigma}(w_t) \, \mathrm{d}w_t + c \qquad (3.3)$$

(Section B.2 in the Appendix), where $\varphi_{\mu,\sigma}$ now represents the pdf of the normal distribution with mean μ and standard deviation σ. It is straightforward to compute the partial derivatives of $\ln \lambda_s$ with respect to μ and σ at $\mu = 0$ and $\sigma = 1$ (Sections B.3 and B.4 in the Appendix). These are the instantaneous rates of change of $\ln \lambda_s$ per unit change in μ and σ respectively, where the unit of change in μ and σ is one standard deviation of w_t. The signs of these sensitivities indicate whether a small increase in mean or standard deviation of the environment increases or decreases $\ln \lambda_s$. Following the rationale of van de Pol *et al.* (2010), the relative magnitudes of these sensitivities provide an estimate of whether small changes in environmental mean or standard deviation have a bigger influence on $\ln \lambda_s$.

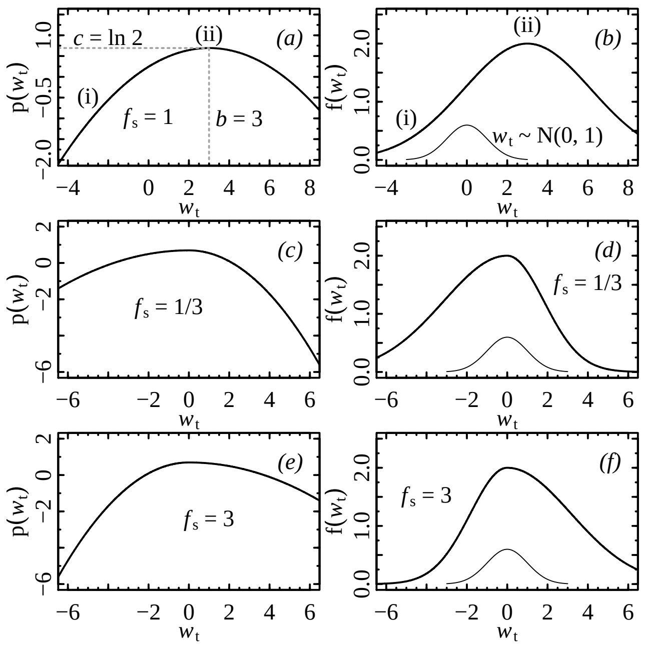

Figure 3.1: A log response function $p(w_t)$ (a) and corresponding linear-scale response function $f(w_t)$ (b) for $\alpha = 2$, $a_1 = a_2 = -0.05$, $b = 1$, and $c = \ln 2$. Region (i) represents a suboptimal environment and region (ii) represents an optimal environment. Examples are also shown for asymmetric response functions with $f_s = 1/3$ ($a_1 = -0.05$, $a_2 = -0.15$) (c, d) and $f_s = 3$ ($a_1 = -0.15$, $a_2 = -0.05$) (e, f), on the log (c, e) and linear (d, f) scales, for $b = 0$, $c = \ln 2$, and $\alpha = 2$. Standard normal distributions (b, d, f) represent the population's local environment w_t. In (b), the population is in a suboptimal environment, for instance at the periphery of the species' range. In (d, f) the population is close to its ideal environment.

3.2.2 Analysis of climate data

To analyse changes in environmental variables, we downloaded Version 2 of the United States Historical Climatology Network database (USHCN; Menne *et al.*, 2009; National Climatic Data Center, National Oceanic and Atmospheric Administration, 2011) and extracted annual time series of mean summer temperatures, minimum winter temperatures, maximum summer temperatures, and total spring precipitation for locations in the conterminous United States (Section B.5 in the Appendix). Annual time series were used because our model is more consistent with annually measured populations and environmental variables. We chose weather variables that are likely to be biologically meaningful to populations living in temperate latitudes. The USHCN data were filtered to include only time series that covered the entire 1911-2010 period. Each time series was then split into two periods (1911-1945 and 1976-2010), each of 35 years length. We calculated the mean and standard deviation of the climate variables listed above, for the two periods separately. Prior to calculating the standard deviation, each time period was detrended to remove quadratic and linear trends that could otherwise inflate the amount of variability measured. To approximate normality, the square root of the precipitation data was used.

3.3 Results

3.3.1 Theoretically predicted sensitivities

We now provide answers to questions (1) and (2) posed in the Introduction by considering a simple special case and then by showing the general case produces largely the same results. The special case is $\alpha = 2$ (so $h(w_t) = w_t^2$) and $a_1 = a_2 = a$ (so $f_s = 1$). For this special case, the log response function is symmetric (Figure 3.1a and b) and $\ln \lambda_s$ and sensitivities can be calculated entirely analytically:

$$\ln \lambda_s = a\,(b^2 + 1) + c \tag{3.4}$$

$$\left.\frac{\partial \ln \lambda_s}{\partial \mu}\right|_{\substack{\mu=0\\ \sigma=1}} = -2\,a\,b \tag{3.5}$$

$$\left.\frac{\partial \ln \lambda_s}{\partial \sigma}\right|_{\substack{\mu=0\\ \sigma=1}} = 2\,a \tag{3.6}$$

(Section B.6 in the Appendix). The signs of the sensitivities of $\ln \lambda_s$ to changes in μ and σ provide an answer to the first question posed in the Introduction: given a change in the mean or standard deviation of the environment, does the growth rate increase or decrease? The sign of the sensitivity of $\ln \lambda_s$ to changes in μ is the same as the sign of b, since $a < 0$; hence any change in the mean environment toward a population's optimum will increase $\ln \lambda_s$, as expected. The sensitivity to changes in σ is always negative; hence any increase in σ is detrimental to the population. Analysis of the ratio of the two sensitivities, which is $-b$, answers our second question: if mean and standard deviation are perturbed by the same amount, which causes the greater impact on the growth rate? For $|b| < 1$, changes in σ have a greater effect, whereas for $|b| > 1$, changes in mean environment are more important. For fixed values of a and c, larger $\ln \lambda_s$ happens only through smaller $|b|$, which means the absolute ratio of the two sensitivities is smaller; so larger growth rates mean greater relative sensitivity of the growth rate to changes in environmental variability.

Log response functions may often be asymmetric and α may differ from 2, so how contingent are the above results on the assumptions made by the special case? We numerically analysed the sensitivities of $\ln \lambda_s$ for a range of values of f_s and for $\alpha = 1/2, 1$ and 2 and results remain largely the same. Figure 3.2a-c shows that $\partial \ln \lambda_s / \partial \mu$, plotted against b, changes sign from negative to positive at a value of b close to 0, with some small variation in the value of b at which the sign changes, depending on the values of f_s and α. Figure 3.2d-f illustrates that for $\alpha \geq 1$, $\partial \ln \lambda_s / \partial \sigma$ is always negative. For $\alpha < 1$, this sensitivity can be positive for larger values of $|b|$. Figure 3.3 compares the absolute magnitudes of the sensitivities. For b close to 0, the sensitivity of $\ln \lambda_s$ to changes in σ is generally comparable in magnitude to or larger in magnitude than the sensitivity to changes in μ. The specific interval of b in which the sensitivity of $\ln \lambda_s$ to changes in σ is larger varies depending on f_s and α. But regardless of this variation the conclusion holds that for $|b| \lesssim 2$, changes in environmental standard deviation are expected to be comparably or more important for long-term stochastic growth rate than changes of the same magnitude in the mean environment. Figure 3.3g-i shows that for given c and a, larger values of $\ln \lambda_s$ are within the range for which $|\partial \ln \lambda_s / \partial \sigma| > |\partial \ln \lambda_s / \partial \mu|$, i.e., across a species environmental range, populations with comparatively higher growth rates are likely to be more affected by changes in variability of the environment than changes in mean.

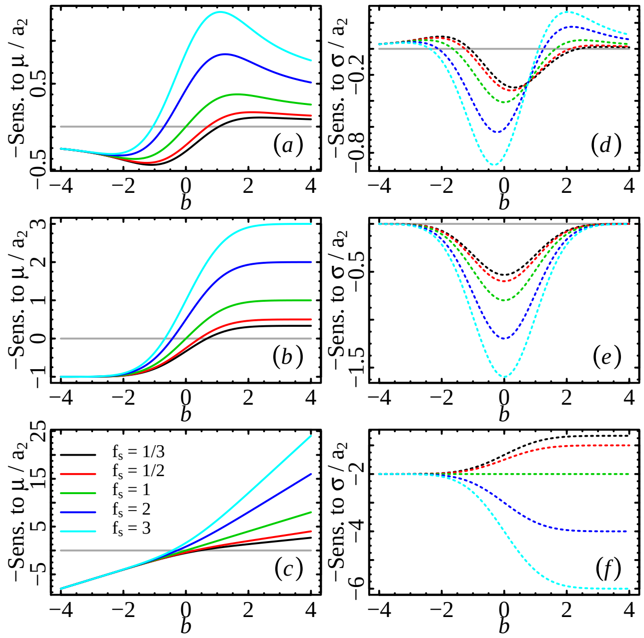

Figure 3.2: The quotients $-\partial \ln \lambda_s / \partial \mu / a_2$ (a-c) and $-\partial \ln \lambda_s / \partial \sigma / a_2$ (d-f), which have the same signs as the sensitivities $\partial \ln \lambda_s / \partial \mu$ and $\partial \ln \lambda_s / \partial \sigma$, respectively, and which were calculated numerically (Sections B.3 and B.4 in the Appendix). Here, $a_2 = -1$, and $\alpha = 1/2$ (a, d), $\alpha = 1$ (b, e), and $\alpha = 2$ (c, f). Sensitivities did not depend on c.

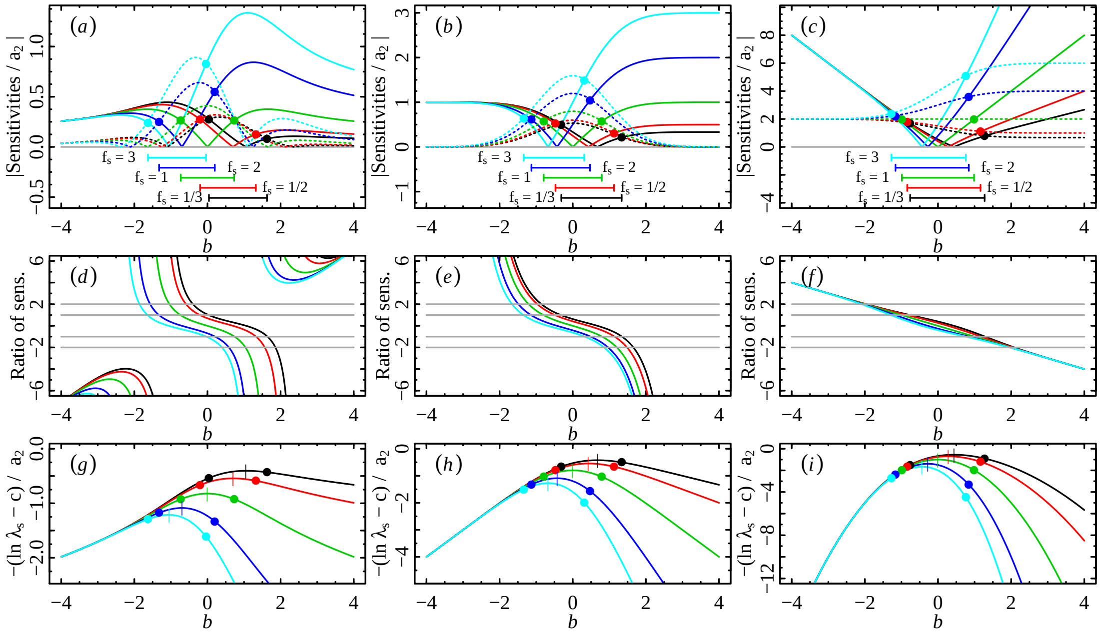

Figure 3.3: (a-c) Absolute values of the sensitivities of Figure 3.2. Solid lines are $|\partial \ln \lambda_s / \partial \mu / a_2|$ and dotted lines are $|\partial \ln \lambda_s / \partial \sigma / a_2|$. Dots indicate points at which solid and dotted lines of the same color cross; dots line up with the endpoints of the ranges below each plot and indicate the b for which $|\partial \ln \lambda_s / \partial \sigma| > |\partial \ln \lambda_s / \partial \mu|$. (d-f) The ratio of the two sensitivities, $(\partial \ln \lambda_s / \partial \mu)/(\partial \ln \lambda_s / \partial \sigma)$. Horizontal lines at absolute ratios equal to one and two are for reference and correspond, respectively, to changes in mean environment being as important and doubly as important, respectively, for long-term stochastic growth rate, compared to changes in the standard deviation of the environment. (g-i) The quotient $-(\ln \lambda_s - c)/a_2$, which shows how $\ln \lambda_s$ depends on b. Dots line up with those in panels (a-c). Vertical lines indicate maxima. (a, d, g) is for $\alpha = 1/2$, (b, e, h) is for $\alpha = 1$, and (c, f, i) is for $\alpha = 2$.

3.3.2 Results of climate data analysis

The third question posed in the Introduction was what are the relative magnitudes of observed changes in mean and standard deviation of climate variables? Results are shown for winter mean temperature and total spring precipitation in Figure 3.4, and for summer mean temperature, winter minimum temperature, and summer maximum temperature in Figure B.1 in the Appendix. The magnitudes of changes in the means of all variables, except total spring precipitation, were generally slightly but not markedly larger than those of standard deviations. For total spring precipitation, changes in mean and standard deviation were of almost the same magnitude. Results are also spatially heterogeneous. The only variable for which changes in standard deviation are of the same sign throughout most of the United States is minimum winter temperature (Figure B.1e in the Appendix), where variability decreased from

1911-1945 to 1976-2010. For all other variables, the sign and magnitude of changes depend on location. Changes in mean were generally slightly but not markedly bigger in magnitude than changes in standard deviation at local scales, too (Figure 3.4e-f), although there are many locations and weather variables where the reverse is true (e.g., for summer mean temperature and precipitation). Although changes in means were more often larger than changes in standard deviation, both types of changes were similar in size, so results comparing relative sensitivities of long-term stochastic growth rate can also be interpreted as approximately reflecting the relative importance of the two types of change for population dynamics.

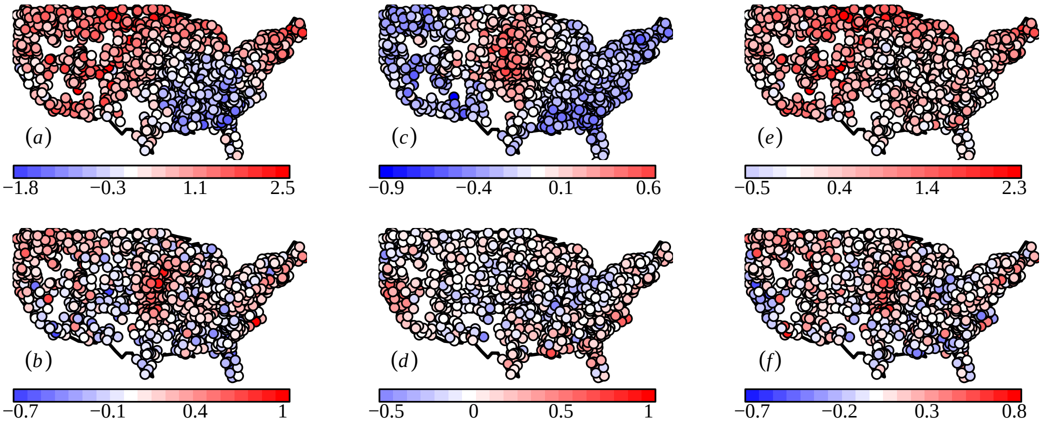

Figure 3.4: Mean (a, b) and standard deviation (c, d) values for 1976-2010 minus values for 1911-1945, and absolute values of changes in mean minus absolute values of changes in standard deviation (e, f), for winter mean temperature (a, c, e) and total spring precipitation (b, d, f). For instance, if m_1 and sd_1 are the mean and standard deviation of winter temperature in a location for the period 1911-1945, and m_2 and sd_2 are the mean and standard deviation of winter temperature in the same location for the period 1976-2010, then panel (a) shows $m_2 - m_1$, panel (c) shows $sd_2 - sd_1$, and panel (e) shows $|m_2 - m_1| - |sd_2 - sd_1|$. White corresponds to no change. Mean and standard deviation of total spring precipitation (b, d, f) use the square root of the precipitation values (Methods). Other weather variables are shown in Figure B.1 in the Appendix.

3.4 Discussion

We showed for a simple model how the effects on population dynamics of changes in the mean and variability of an environmental variable compare. Our results show that for $|b| \lesssim 2$, changes in the standard deviation of the environment are at least comparably important to changes in the mean environment. The units of b are equal to the standard deviation of the local environment. Hence results suggest that whenever the ideal environment is within two standard deviations of the local mean environment, changes in environmental variability will be comparably or more important than changes in environmental mean for a population's growth rate. We discuss the contrasting implications of these results for two different kinds of populations: those living close to their ideal environment and those far from it.

Populations living close to their ideal environment, such as those in the centre of the species environmental range, are interpreted in our model as those having $|b| \lesssim 2$. Populations of interest that live close to their ideal environment include populations of pests and disease vectors (Reuman *et al.*, 2006, 2008; Chaves *et al.*, 2011). The regions of most concern for pests and disease vectors are those near the centre of the range of the species, where growth rates are highest and associated economic and health problems are worst. Other populations of interest that may fall into this category include exploited populations (e.g., fish) or populations which provide a major food supply for exploited populations (e.g., copepods), for which centres of species environmental ranges are also of most economic importance. For these species, our results show that any increase in variability of the environment is detrimental, and that furthermore, changes in variability are more important than changes in mean. Given that the variability of temperature has decreased in many locations of the United States over the past 100 years, our model suggests that pests and disease vectors, but also potentially some exploited species, may stand to benefit from ongoing climate change.

Climate change has led to shifts and contractions in range size (Parmesan *et al.*, 1999; Thomas & Lennon, 1999) compounded by habitat loss and fragmentation (Sala *et al.*, 2000). Populations struggling to adapt to rapid climate changes are also likely to be those living on the periphery of species ranges, where environmental conditions are suboptimal. Such populations may be of conservation interest; they are interpreted in our model as having $|b| \gtrsim 2$. For these populations, environmental variability can, for the larger values of $|b|$, be beneficial if the log response function is described by $\alpha < 1$. This result may seem surprising, given that variability in net growth rate or in vital rates reduces $\ln \lambda_s$ (McLaughlin *et al.*, 2002; Lande *et al.*, 2003; Tuljapurkar *et al.*, 2003; Tews & Jeltsch, 2004; Haridas & Tuljapurkar, 2005). However, the effect of a change in environmental variability on $\ln \lambda_s$ is contingent on the concavity of the response function (Ruel & Ayres, 1999; Drake, 2005; Boyce *et al.*, 2006; van de Pol *et al.*, 2010). Our results also show that for these populations, changes in mean environmental conditions have a greater effect than changes in variability.

Prior studies have compared the impacts of changes in mean and variability of vital rates on $\ln \lambda_s$. For instance, Haridas & Tuljapurkar (2005) and Ezard & Coulson (2010) found that perturbations in mean vital rates cause a greater change in $\ln \lambda_s$ than perturbations in the variance of vital rates. Coulson *et al.* (2011) reached a similar conclusion using an integral projection model of wolves in Yellowstone National Park, USA. Morris *et al.* (2008) concluded that although all species they examined were more sensitive to changes in vital rate means than variance, the greater importance of changes in means was reduced for shorter-lived, faster growing species.

The above results may appear to be directly comparable to our results; however, as pointed out by Jonzén *et al.* (2010), the importance of changes in the variability of vital rates need not be indicative of the importance of changes in environmental variability. The crucial difference between our study and the above results is that we link to the environment via a biologically reasonable response function, considering sensitivities to changes in environmental means and variances rather than vital rate means and variances. The key parameters in our model turned out to be the response function parameters b, the distance from the ideal environment, and α, the shape of the function $h(w_t)$; response functions are not considered in the earlier studies. Our result that populations for which the ideal environment is within two standard deviations of the local mean environment are likely to be more sensitive to changes in environmental variability than to changes in environmental mean in some ways parallels part of the result of Morris *et al.* (2008) described above. However, whereas the populations of Morris *et al.* were all more sensitive to changes in vital rate means than variances, our results show that changes in environmental variability can sometimes be more important than changes in environmental mean. Comparing the results of Morris *et al.* with ours illustrates that the relative importance of changes in mean and variability can differ depending on whether one considers environments or vital rates.

Only two empirical studies currently exist that can be directly compared to our theoretical predictions, and they provide some support for our conclusions; a principle value of our model is in guiding future work. The only prior studies we know of that have directly compared the importance of changes in mean and variability of the environment for populations are those of van de Pol *et al.* (2010) and Jonzén *et al.* (2010). They used structured population models, parameterised for a population of oystercatchers (van de Pol *et al.*, 2010) and a population of red kangaroos (Jonzén *et al.*, 2010). The oystercatcher population has been declining at a rate of $\sim 5\%$ per year (van de Pol *et al.*, 2010); it therefore lives in less than ideal conditions. Van de Pol *et al.* conclude, as our model would suggest, that changes in mean environmental conditions will have a greater effect on this population than do changes in variability. The red kangaroo population of Jonzén *et al.* (2010) probably lives in a closer-to-ideal environment for the species, as it has a substantially positive $\ln \lambda_s$: the authors estimate that growth rate will be greater than 1 even with annual harvesting up to 20%. Consistent with our model, the sensitivity of $\ln \lambda_s$ to changes in mean rainfall (after converting the elasticities provided in Jonzén *et al.* (2010) to sensitivities) is only ~ 2.4 times greater in magnitude than that to changes in the standard deviation of rainfall: sensitivity to changes in standard deviation is important for the kangaroo population. More insight can be gained in future work by replicating these efforts for other populations. This is a non-trivial effort. Many years worth of data are necessary for each population (e.g., 25 years of data were used in van de Pol *et al.*, 2010). Each monitored population would correspond to a single point in parameter space of a general theoretical analysis. Our findings help inform what populations may be of interest to compare. We suggest the comparison of populations thought to be living in close-to-ideal conditions with those far from ideal conditions. For example, one could replicate the study of van de Pol *et al.* with other oystercatcher populations across a gradient of environmental conditions, including expanding populations.

Insight might also be gained by introducing more biological detail into our model in future work, for instance by including age or stage structure. For a stage-structured model, n vital rates or stochastic matrix elements would be linked to n potentially different environmental variables $w_i(t)$ $(i = 1, \ldots, n)$ by different response functions, each with its own α_i, $a_{1,i}$, $a_{2,i}$, b_i, and c_i, resulting in n sensitivities of $\ln \lambda_s$ to changes in μ_i and σ_i. It is realistic to expect the n response functions to differ in concavity and other respects (van de Pol *et al.*, 2010). In addition, the w_i may be correlated and this correlation structure may be affected in unknown ways by climate change. Managing this complexity is a challenge. Alternative modelling frameworks (e.g., Runge & Moen, 1998; Steinsaltz *et al.*, 2011) face similar problems. If a general model proves too complicated to immediately provide insight, a sensible next step may be a 2 x 2 matrix model of a population with juveniles and adults (non-semelparous, as semelparous populations are covered by our model; Section B.8 in the Appendix). Such a model would make it possible to study the differing impacts of climate change on fecundity and survival rates, as well as effects that may only emerge when some stage structure is present. For an age or stage structured model, the exact formulation of $\ln \lambda_s$ used in this study would no longer be valid, but Tuljapurkar's (Tuljapurkar, 1982, 1990) approximation could be used. For the unstructured case, the approximation yields qualitatively similar results to the ones presented here (results not shown). The long-term stochastic growth rate for a stage-structured model is also affected by autocorrelation in the environment (Tuljapurkar, 1982, 1990; Caswell, 2001). The autocorrelation of environmental variables is also changing due to climate change (García-Carreras & Reuman, 2011). It would be possible, using a stage-structured model, to compare the relative effects of changes in mean, variance, and autocorrelation of the environment on population dynamics (as done for a single oystercatcher population in van de Pol *et al.*, 2011). Finally, the sensitivities of $\ln \lambda_s$

are linear approximations of the functions that relate $\ln \lambda_s$ to μ and σ, and therefore assume small changes in the environment. More substantial environmental changes may entail nonlinearities for which a linear approximation is no longer sufficient. An examination of such nonlinear effects may be analytically intractable, though simulations and numeric work may provide insights.

4 Are changes in the mean or variability of climate signals more important for extinction risk?

Abstract

Climate change affects the extinction risk faced by animal populations by altering their dynamics. While greater attention has been devoted to the impacts of readily measured changes in the means of environmental variables such as temperature, climate change also entails changes in the variability of environmental variables. Is the greater attention given to changes in mean environment justified? To help answer this question we formulated a simple stochastic population model explicitly linked to an environmental process, and used it to compare the sensitivities of a population's extinction risk to changes in mean and standard deviation of the environment. Results show that changes in environmental standard deviation can be more important than changes in the mean of the environment for populations living close to their ideal environment, but that still face the threat of extinction. Changes in mean conditions are more important than changes in environmental standard deviation for populations living further from their ideal environment.

N. B.: This chapter is in preparation for *PLoS ONE*. Its corresponding supplementary information can be found in Appendix C.

4.1 Introduction

Extinction risk is a vital statistic in population viability analysis and conservation biology (Lande & Orzack, 1988; Caswell, 2001; Morris & Doak, 2002). Ongoing climate change, among other factors, has been shown to increase current rates of extinction (Hassan *et al.*, 2005). Rapid changes in climate can directly affect the distribution and dynamics of populations through physiological stress (Hughes, 2000), changes in reproductive and survival rates (Walther *et al.*, 2002), and shifts in phenology (McCarty, 2001; Walther *et al.*, 2002; Parmesan, 2006). Other indirect consequences, such as habitat fragmentation or loss, introduction of invasive species, and a change to the competitive interactions between species can also feed back into local abundance and geographic range size (Hughes, 2000). It follows that climate change has been identified as a factor threatening the persistence of populations (Parmesan, 1996; Hughes, 2000; Parmesan, 2006), and both local (Parmesan, 1996; McLaughlin *et al.*, 2002) and global (Pounds *et al.*, 1999; Stuart *et al.*, 2004) extinctions can be expected as a consequence. Significant shifts in range towards higher latitudes and altitudes have been widely documented (Parmesan, 1996; Thomas & Lennon, 1999; Hughes, 2000; McLaughlin *et al.*, 2002; Parmesan & Yohe, 2003; Parmesan, 2006), indicating a pattern of nonrandom local extinctions particularly at lower altitudes and southern borders of populations' ranges (Parmesan, 1996; McCarty, 2001). Although risk of extinction is faced by populations of every continent and ocean and of most major taxonomic groups (Parmesan, 2006), high extinction risk has been associated with populations possessing a number of attributes: high-trophic level; low population density; slow life history; and particularly a small or restricted range (Purvis *et al.*, 2000; Parmesan, 2006).

Many of these studies focus on the impacts of changes in mean conditions (e.g., Parmesan, 1996; Pounds *et al.*, 1999; Hughes, 2000; Parmesan & Yohe, 2003). Yet, climate change also manifests itself as changes in other statistical descriptions (Chapters 3 and 6). Changes in the variability of temperature and precipitation have also been reported (Michaels *et al.*, 1998; Svoma & Balling, 2010, Chapter 3) and forecast (Hunt & Elliott, 2004; Stouffer & Wetherald, 2007; Sakai *et al.*, 2009), and have been shown to potentially affect populations' fitness (Schoener & Spiller, 1992; McLaughlin *et al.*, 2002; Tuljapurkar *et al.*, 2003). In order to compare the impacts of changes in mean and variability of environmental conditions on a population, in Chapter 3 we proposed a simple population model linked to an environmental variable via a response function, which translated the environmental signal into a biological process. We found that changes in mean conditions are likely to have a greater impact than changes in variability on populations near species environmental range boundaries or of conservation concern, whereas faster-growing populations such as pests and disease vectors, and other populations near range centres are more likely to be affected by changes in climate variability.

Our proxy for population fitness in Chapter 3, the long-term stochastic growth rate $\ln\lambda_s$, is a common choice in population dynamics (e.g., Tuljapurkar *et al.*, 2003; Haridas & Tuljapurkar, 2005; Ezard & Coulson, 2010). It is an estimate of the most likely rate at which the population will grow in the long run. In the context of extinction risk, populations with $\ln\lambda_s \leq 0$ are bound to go extinct with probability 1, whereas for those with $\ln\lambda_s > 0$, extinction is possible but not a certainty (Lande & Orzack, 1988). It does however have, *a priori*, some limitations, as it is difficult to quantify the actual extinction risk faced by a population from $\ln\lambda_s$ alone. There is also uncertainty around $\ln\lambda_s$, referred to as the log variance (denoted σ_r^2 henceforth, but frequently σ^2 in the literature, e.g., Caswell, 2001 and infinitesimal variance in Lande & Orzack, 1988). This uncertainty may have important implications for the viability of a population; a population may be expected to grow in the long run ($\ln\lambda_s > 0$), but if the uncertainty around the measure of $\ln\lambda_s$ is large enough, its persistence may not be guaranteed. This information is ignored when using $\ln\lambda_s$ as the sole fitness parameter. Both $\ln\lambda_s$ and σ_r^2 are therefore necessary inputs to estimate extinction risk (Tuljapurkar & Orzack, 1980).

In this study we compare the effects of changes in mean and variability of environmental conditions on population extinction risk. We build on the theoretical approach developed in Chapter 3 by deriving σ_r^2 and extinction risk as a function of the environment and the response function. We then derive the sensitivity of σ_r^2 and extinction risk to changes in environmental mean and variability. We provide answers to the following questions: (1) Given an increase in the mean or standard deviation of the environment, does extinction risk increase or decrease? (2) If mean and standard deviation are perturbed by the same small amount, which causes the greater impact on extinction risk? We also compare the results to those in Chapter 3 to assess the merits of using extinction risk as a population fitness parameter in comparison to $\ln\lambda_s$, and discuss results in view of currently ongoing climate change.

4.2 Methods

For n_t representing the population in year t, the base model (Lewontin & Cohen, 1969) is

$$n_{t+1} = \lambda_t\, n_t, \tag{4.1}$$

where λ_t is the net growth rate of the population in year t. We assume $\lambda_t = f(w_t)$, where w_t is the environmental variable and f is the response function. The response function describes how an environmental variable is translated into a biological process

(Laakso *et al.*, 2001; Morris *et al.*, 2008, Chapter 3). The function typically has a single peak. Let $p(w_t) = \ln f(w_t)$ be the log of the response function.

For the stochastic model, log population size asymptotically approaches a normal distribution with mean $t \ln \lambda_s$ and standard deviation $t\, \sigma_r^2$. The mean divided by t (i.e., $\ln \lambda_s$) is the long-term stochastic growth rate (Tuljapurkar, 1982, 1990; Caswell, 2001), and the variance divided by t (σ_r^2) is the log variance, which quantifies the variability around the estimate of $\ln \lambda_s$. For our model, these are

$$\ln \lambda_s = \mathrm{E}(\ln \lambda_t) = \int_{-\infty}^{\infty} p(w_t)\, \varphi_{\mu,\sigma}(w_t)\, \mathrm{d}w_t, \tag{4.2}$$

and

$$\sigma_r^2 = \mathrm{Var}(\ln \lambda_t) = \int_{-\infty}^{\infty} p(w_t)^2\, \varphi_{\mu,\sigma}(w_t)\, \mathrm{d}w_t - (\ln \lambda_s)^2, \tag{4.3}$$

(Section C.1 in the Appendix), where $\varphi_{\mu,\sigma}$ is the probability density function (pdf) of w_t, with mean parameter μ and standard deviation parameter σ (Tuljapurkar, 1990; Lande *et al.*, 2003). Second-order approximations are often used to estimate $\ln \lambda_s$ and σ_r^2 (Tuljapurkar, 1982, 1990), but equations (4.2) and (4.3) are exact formulae that apply in the case of an unstructured population. Populations described only by equation (4.1) never go extinct, but at most decay exponentially, only asymptotically reaching zero (Caswell, 2001). We consider extinction to have occurred when the population goes below the threshold of one. Lande & Orzack (1988) used a diffusion approximation to derive extinction risk G as

$$G(t|x_0) \approx \Phi\left[\frac{-x_0 - \ln \lambda_s\, t}{\sqrt{\sigma_r^2\, t}}\right] + \exp\left(\frac{-2\, \ln \lambda_s\, x_0}{\sigma_r^2}\right) \Phi\left[\frac{-x_0 + \ln \lambda_s\, t}{\sqrt{\sigma_r^2\, t}}\right], \tag{4.4}$$

(Morris & Doak, 2002), where $\Phi[\cdot]$ is the cumulative distribution function (cdf) of a standard normal random variable, and where $G(t|x_0)$ is the cumulative probability that the population becomes extinct before time t, given an initial positive log population size $x_0 = \ln n_0$. All results are substantially the same for any other choice of extinction threshold. The sensitivities of extinction risk to changes in mean and standard deviation of the environment are

$$\frac{\partial G(t|x_0)}{\partial \mu} = \frac{\partial G(t|x_0)}{\partial \ln \lambda_s} \frac{\partial \ln \lambda_s}{\partial \mu} + \frac{\partial G(t|x_0)}{\partial \sigma_r^2} \frac{\partial \sigma_r^2}{\partial \mu} \tag{4.5}$$

$$\frac{\partial G(t|x_0)}{\partial \sigma} = \frac{\partial G(t|x_0)}{\partial \ln \lambda_s} \frac{\partial \ln \lambda_s}{\partial \sigma} + \frac{\partial G(t|x_0)}{\partial \sigma_r^2} \frac{\partial \sigma_r^2}{\partial \sigma}. \tag{4.6}$$

The sensitivities of $\ln \lambda_s$ and σ_r^2 can be calculated by taking the partial derivatives of equations (4.2) and (4.3) with respect to μ and σ. We do this by moving the partial derivatives under the integral symbol and applying them to $\varphi_{\mu,\sigma}(w_t)$. The other derivatives that appear in equations (4.5) and (4.6) are straightforward to calculate. This approach applies generally, for any specified $p(w_t)$, yielding sensitivities expressible as integrals which can easily be calculated numerically.

For concreteness, we adopt a flexible parameterisation for p. Without loss of generality we transform w_t such that its distribution in the focal location is $\mathcal{N}(0,1)$ (see Section C.2 in the Appendix). If $h(w_t) = w_t^\alpha$ for some $\alpha > 0$, $p(w_t)$ is taken to be $a_1\, h(-w_t+b)+c$ for $w_t \leq b$ and $a_2\, h(w_t-b)+c$ for $w_t \geq b$ (Figure 4.1). This function is single peaked with maximum height c occurring at the ideal environment, b. The rate of falloff of p as w_t decreases (respectively, increases) from the ideal environment is controlled by a_1 (respectively, a_2); both are taken to be negative. The ratio $f_s = a_1/a_2$ is a measure of asymmetry of the response function around b. The examples shown in Figure 4.1 are similar to response functions reported in the literature (Chapter 3). The value of b is the difference between the local environment and the population's ideal environment, measured in units equal to the standard deviation of the local environment because we re-scaled w_t to make it standard-normally distributed. Larger values of $|b|$ describe populations living in a suboptimal environment (for example, those living in environmental range margins or struggling to adapt to ongoing climate change), whereas $|b| \sim 0$ is more indicative of populations living in a close-to-ideal environment.

Substituting the above parameterization of $p(w_t)$ into equation (4.2), we get $\ln\lambda_s$ and σ_r^2 as functions of the parameters that define the log response function,

$$\ln\lambda_s = a_1 \int_{-\infty}^{b} (-w_t+b)^\alpha\, \varphi_{\mu,\sigma}(w_t)\,\mathrm{d}w_t + a_2 \int_{b}^{\infty} (w_t-b)^\alpha\, \varphi_{\mu,\sigma}(w_t)\,\mathrm{d}w_t + c \qquad (4.7)$$

$$\sigma_r^2 = a_1^2 \int_{-\infty}^{b} (-w_t+b)^{2\,\alpha}\, \varphi_{\mu,\sigma}(w_t)\,\mathrm{d}w_t + a_2^2 \int_{b}^{\infty} (w_t-b)^{2\,\alpha}\, \varphi_{\mu,\sigma}(w_t)\,\mathrm{d}w_t - (\ln\lambda_s - c)^2 \qquad (4.8)$$

(Chapter 3 and Section C.1 in the Appendix), where $\varphi_{\mu,\sigma}$ now represents the pdf of the normal distribution with mean μ and standard deviation σ. It is straightforward to compute the partial derivatives of $\ln\lambda_s$ and σ_r^2 with respect to μ and σ and the partial derivatives of G with respect to $\ln\lambda_s$ and σ_r^2 at $\mu = 0$ and $\sigma = 1$ (Chapter 3, Sections C.3, C.4, and C.5 in the Appendix). These partial derivatives allow us to calculate the sensitivity of extinction risk to changes in μ and σ using equations (4.5) and (4.6). These are the instantaneous rates of change of G per unit change in μ and σ respectively, where the unit of change in μ and σ is one standard deviation of w_t.

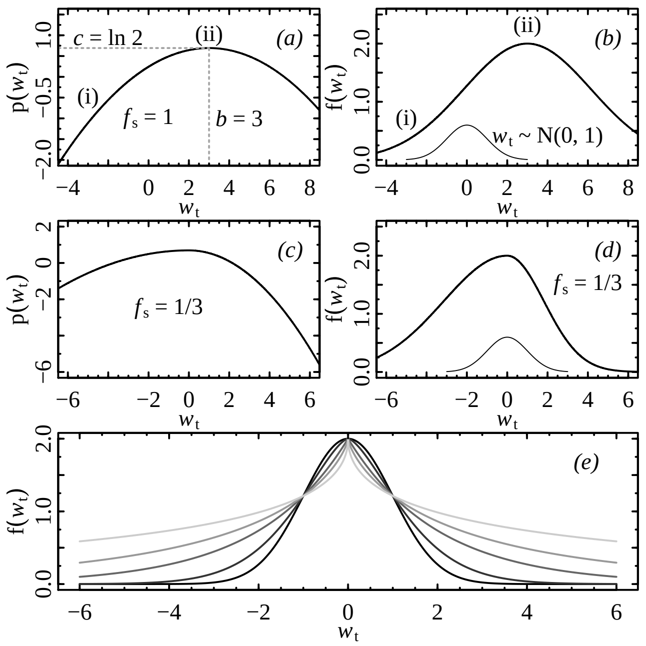

Figure 4.1: A log response function $p(w_t)$ (a) and corresponding linear-scale response function $f(w_t)$ (b) for $\alpha = 2$, $a_1 = a_2 = -0.05$, $b = 1$, and $c = \ln 2$. Region (i) represents a suboptimal environment and region (ii) represents an optimal environment. An example is also shown for an asymmetric response function with $f_s = 1/3$ ($a_1 = -0.05$, $a_2 = -0.15$) (c, d) on the log (c) and linear (d) scales, for $b = 0$, $c = \ln 2$, and $\alpha = 2$. Standard normal distributions (b, d, f) represent the population's local environment w_t. In (b), the population is in a suboptimal environment, for instance at the periphery of the species' range. In (d, f) the population is close to its ideal environment. Response functions on the linear scale for different values of α (e), ranging from $\alpha = 2$ for the black line, to $\alpha = 0.5$ for the light grey line, for $f_s = 1$, and $a_1 = a_2 = -0.5$. The intermediate values of α are 1.5, 1, and 0.75.

The signs of these sensitivities indicate whether a small increase in mean or standard deviation of the environment increases or decreases extinction risk. Following the rationale of van de Pol *et al.* (2010), the relative magnitudes of these sensitivities provide an estimate of whether small changes in environmental mean or standard deviation have a bigger influence on G.

4.3 Results

We now provide answers to the questions posed in the Introduction by analysing a specific, representative case, and then examining deviations from this special case. For this representative case, $\alpha = 2$ and $f_s = 1$, so the log response function is symmetric (and qualitatively similar to Figure 4.1a and b). The signs of the sensitivities of extinction risk to changes in μ and σ provide an answer to the first question posed in the Introduction: given a change in the mean or standard deviation of the environment, does the extinction risk increase or decrease? Panels (a) and (c) in Figure 4.2 show $\partial G/\partial\mu$ and its sign respectively for the representative case. The sign of the sensitivity of extinction risk to changes in μ is the opposite sign of b; hence any change in the mean environment toward a population's optimum will decrease extinction risk, as expected. Panels (b) and (e) in Figure 4.2 shows $\partial G/\partial\sigma$ and its sign respectively. The sensitivity to changes in σ is negative over most of parameter space; hence any increase in σ is detrimental to the population. For populations with $G(t=5) \gtrsim 0.9$, particularly those with higher values of c and $|b|$, $\partial G/\partial\sigma$ can be positive, albeit small in magnitude, but this is of little consequence since these populations have such high near-term extinction risk that climate change will not have time to affect them before they disappear.

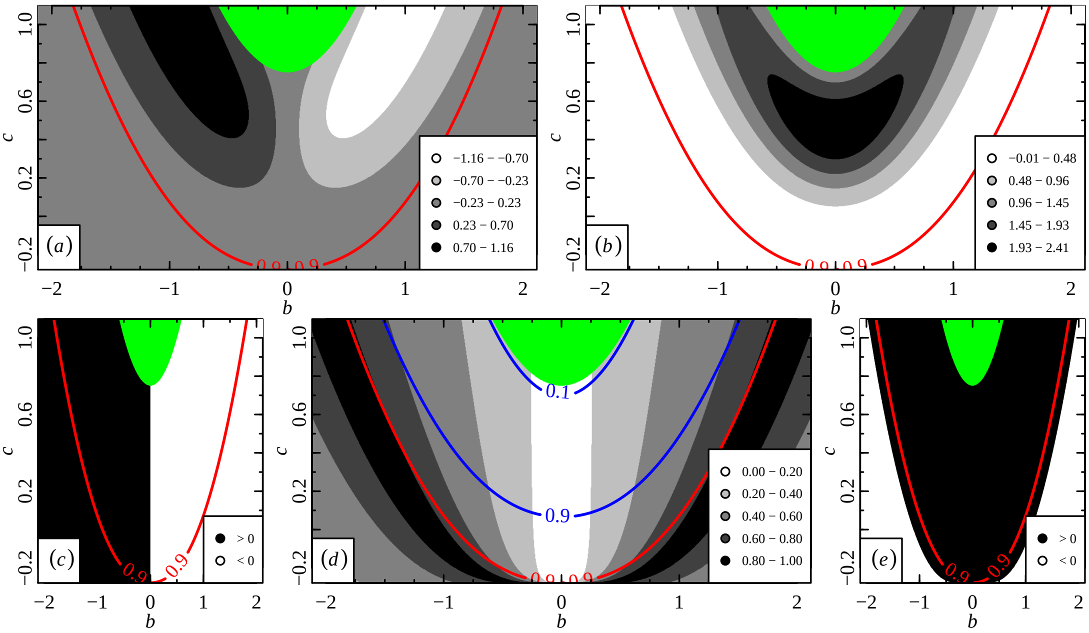

Figure 4.2: (a) $\partial G/\partial\mu$, (b) $\partial G/\partial\sigma$, (c) the sign of the sensitivity shown in panel (a), (d) the relative importance of the sensitivity to changes in μ, i.e. $|\partial G/\partial\mu|/(|\partial G/\partial\mu| + |\partial G/\partial\sigma|)$, (e) the sign of the sensitivity shown in panel (b), for $\alpha = 2$, $a_2 = -0.5$, $f_s = 1$, $t = 10$, and $x_0 = \ln 10$. The red contour line is $G(t=5) = 0.9$, so populations below this line are doomed to extinction. Blue contour lines are for $G(t=10) = 0.1, 0.9$. The green area corresponds to populations with $G(t=100) \leq 0.1$ that are relatively safe from extinction.

Analysis of the magnitude of absolute sensitivities answers the second question posed in the Introduction: if mean and standard deviation are perturbed by the same amount, which causes the greater impact on the extinction risk? Panel (d) in Figure 4.2 shows the value of P_μ

$$P_\mu = \frac{\left| \left. \frac{\partial G(t|x_0)}{\partial \mu} \right|_{\substack{\mu=0\\ \sigma=1}} \right|}{\left| \left. \frac{\partial G(t|x_0)}{\partial \mu} \right|_{\substack{\mu=0\\ \sigma=1}} \right| + \left| \left. \frac{\partial G(t|x_0)}{\partial \sigma} \right|_{\substack{\mu=0\\ \sigma=1}} \right|} \tag{4.9}$$

For $P_\mu < 0.5$, the sensitivity of G to changes in σ is bigger in magnitude than its sensitivity to changes in μ, and for $P_\mu > 0.5$, the sensitivity of G to changes in μ is bigger in magnitude than its sensitivity to changes in σ. For $|b| \lesssim 1$, changes in σ have a greater effect on extinction risk. For a fixed value of b, as c increases, changes in environmental variability become progressively more important. Changes in mean environment become more important when $|b|$ increases while holding c constant, and as $|b|$ increases while holding extinction risk constant.

We numerically examined deviations from the above special case by analysing the sensitivities of extinction risk for all combinations of the following parameters: $\alpha = 0.5, 0.75, 1, 1.5, 2$, $f_s = 1/3, 1, 3$, and $a_2 = -0.1, -0.5, -1, -1.5$. Some additional results are shown in Section C.6 in the Appendix. The main observations remain largely the same. The main effect of altering the value of α and a_2 is to change the size of parameter space. As α is decreased, parameter space becomes progressively larger, because populations are capable of surviving further away from their ideal environment (Figure 4.1(e)). Similarly, for large values of $|a_2|$, the fall-off in population fitness from the ideal environment is steep, and therefore populations cannot survive far from their ideal environment, whereas when $|a_2|$ is small, populations can persist in locations far from their ideal environment. Changing the value of f_s such that $f_s \neq 1$ means that the sensitivities of G to changes in μ and σ are no longer symmetric along the $b = 0$ line, as would be expected (Figure 4.3). Therefore, the sign of $\partial G/\partial \mu$ in the example shown in Figure 4.3 no longer changes at $b = 0$, but at values between ~ -0.2 and -0.5. Similarly, for $f_s = 1/3$, the sign of the sensitivity of G to changes in μ changes at values close to $b = 0$ (Section C.6 in the Appendix).

To understand the contributions of the different partial derivatives that compose the sensitivity of G to changes in μ and σ (equations (4.5) and (4.6)), and to inform the Discussion, we also analysed the sensitivity of σ_r^2 to changes in μ and σ, as well as the sensitivity of G to changes in $\ln \lambda_s$ and σ_r^2. Figure 4.4 shows $\partial \sigma_r^2/\partial \mu$ and $\partial \sigma_r^2/\partial \sigma$, for the specific case considered above ($\alpha = 2$, $f_s = 1$). The log variance is always more sensitive to changes in σ than to changes in μ. An increase in σ always increases σ_r^2.

The sensitivity of extinction risk to changes in $\ln \lambda_s$ and σ_r^2 is shown in Figure 4.5. Extinction risk is more sensitive to changes in $\ln \lambda_s$ than to changes in σ_r^2, although changes in log variance become increasingly important as α decreases (Section C.7 in

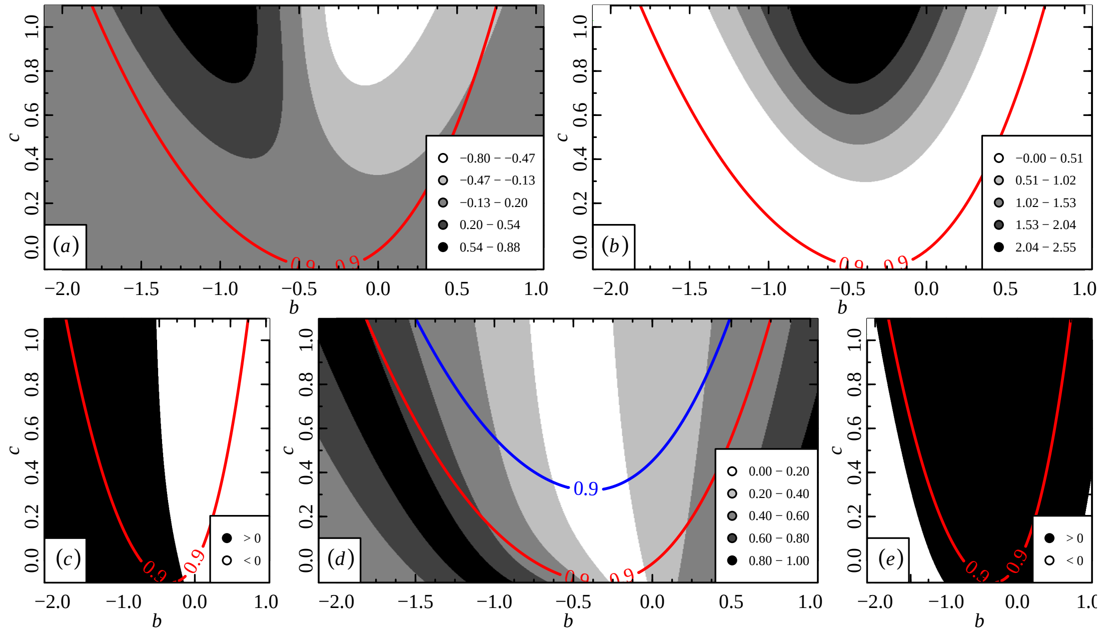

Figure 4.3: (a) $\partial G/\partial\mu$, (b) $\partial G/\partial\sigma$, (c) the sign of the sensitivity shown in panel (a), (d) the relative importance of the sensitivity to changes in μ, i.e. $|\partial G/\partial\mu|/(|\partial G/\partial\mu| + |\partial G/\partial\sigma|)$, (e) the sign of the sensitivity shown in panel (b), for $\alpha = 2$, $a_2 = -0.5$, $f_s = 3$, $t = 10$, and $x_0 = \ln 10$. The red contour line is $G(t = 5) = 0.9$, so populations below this line are doomed to extinction. Blue contour lines are for $G(t = 10) = 0.1, 0.9$. The green area corresponds to populations with $G(t = 100) \leq 0.1$ that are relatively safe from extinction.

the Appendix). The effect of increasing $\ln\lambda_s$ is to decrease extinction risk, as would be expected, whereas $\partial G/\partial\sigma_r^2$ is mostly positive, except at higher extinction risk, when the sensitivity can be negative, albeit small in magnitude.

4.4 Discussion

Our results show how the effects of changes in the mean and the variability of an environmental variable on extinction risk compare. For populations living close to their ideal environment ($|b| \lesssim 1$), changes in the standard deviation of the environment are at least comparable, although usually more important than changes in the mean environment. On the other hand, populations living further away from their ideal environment, particularly those with higher values of c and high extinction risk, are more affected by changes in mean conditions. The units of b are equal to the standard deviation of the local environment. Hence, results suggest that whenever the ideal environment is within a standard deviation of the local mean environment, changes in environmental variability will be comparably or more important than changes in

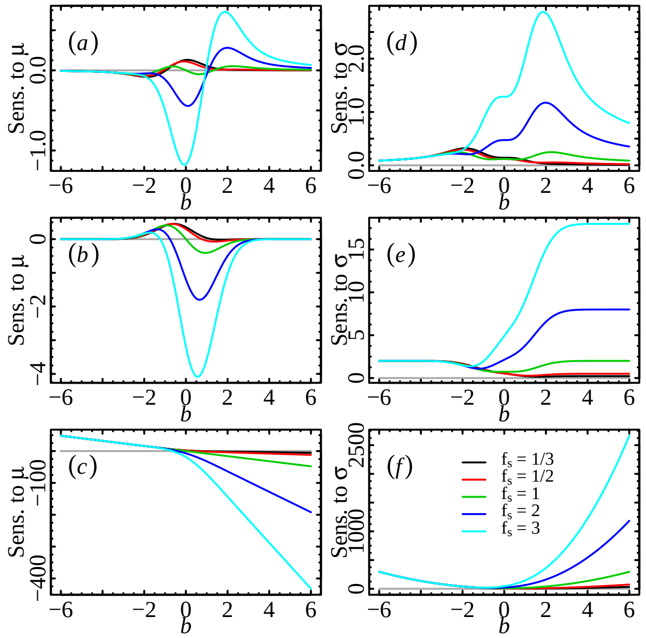

Figure 4.4: $\partial\sigma_r^2/\partial\mu$ (a-c) and $\partial\sigma_r^2/\partial\sigma$ (d-f), which were calculated numerically (Sections C.3 and C.4 in the Appendix). Here $a_2 = -1$, $\alpha = 1/2$ (a, d), $\alpha = 1$ (b, e), and $\alpha = 2$ (c, f). Sensitivities did not depend on c.

environmental mean for extinction risk. We discuss the contrasting implications of these results for two different kinds of populations: those living close to their ideal environment, and those living further from it and typically characterised by higher maximum population growth rates.

Populations described by $|b| \lesssim 1$ in our model are populations living close to their ideal environment but that yet have a non-zero extinction risk in the long run. These combination of features – living in an ideal environment but yet risking extinction – would seem to suggest an unviable population. However, these populations may still be of conservation concern. Populations recently object of conservation programs living in protected habitats may only recently be experiencing their ideal environment, and would still be described in our model by $|b| \lesssim 1$. The relatively low growth rate at their ideal environment suggests these populations may be characterised by a slow life history and larger body size (Blueweiss *et al.*, 1978), coinciding with several of the attributes associated with higher extinction risk (Purvis *et al.*, 2000). Alternatively, factors extrinsic to the population, such as competition from recently introduced species, shrinking or fragmentation of habitat, or unmanaged exploitation or fishing, may be increasing mortality rates and threatening viability. Any change in the mean environmental conditions is likely to be detrimental for these populations. However, changes in the variability of climate will cause a larger change in extinction risk. Given that the variability of temperature has decreased in many locations of

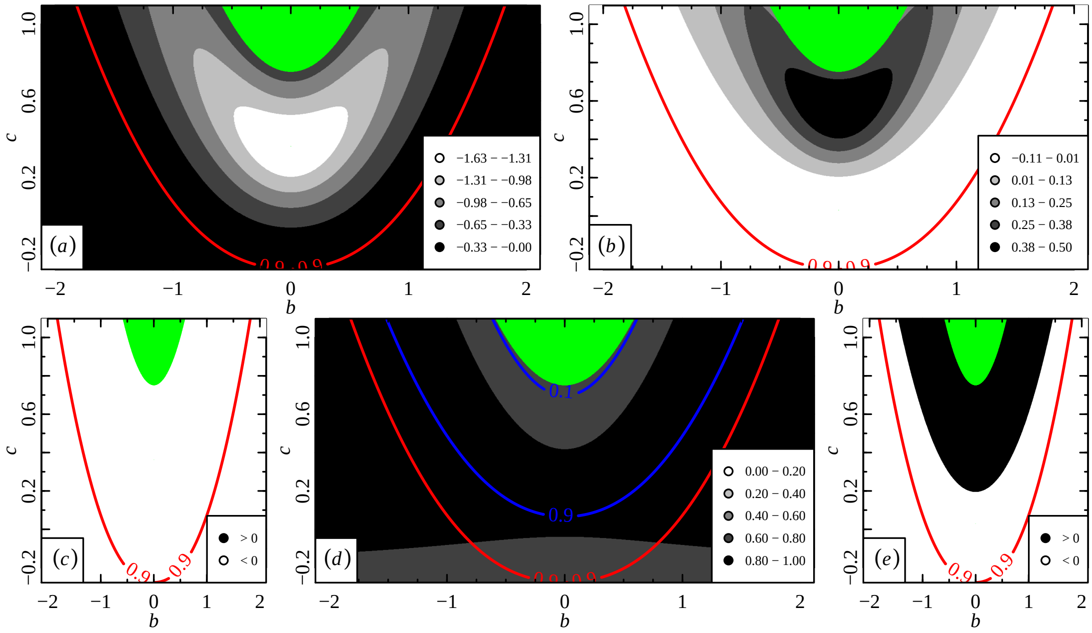

Figure 4.5: (a) $\partial G/\partial \ln \lambda_s$, (b) $\partial G/\partial \sigma_r^2$, (c) the sign of the sensitivity shown in panel (a), (d) the relative importance of the sensitivity to changes in $\ln \lambda_s$, i.e. $|\partial G/\partial \ln \lambda_s|/(|\partial G/\partial \ln \lambda_s|+|\partial G/\partial \sigma_r^2|)$, (e) the sign of the sensitivity shown in panel (b), for $\alpha = 2$, $a_2 = -0.5$, $f_s = 1$, $t = 10$, and $x_0 = \ln 10$. The red contour line is $G(t = 5) = 0.9$, so populations below this line are doomed to extinction. Blue contour lines are for $G(t = 10) = 0.1, 0.9$. The green area corresponds to populations with $G(t = 100) \leq 0.1$ that are relatively safe from extinction.

the United States over the past century (Chapter 3), our model suggests that these populations may stand to benefit from ongoing climate change.

The second group of populations is endangered and is characterised by a high maximum intrinsic growth rate (value of $\exp(c)$), an unrealised potential because these populations live further away from their ideal environment ($|b| \gtrsim 1$). Maximum intrinsic growth rate is negatively correlated with body size (Blueweiss *et al.*, 1978), therefore, populations that are more likely to fit in this group are those smaller in size but also with faster life histories. Specific relevant examples may include lower trophic level fish of commercial interest (for example anchovies or sardines: Chavez *et al.*, 2003) and their food supply (e.g., plankton: Hays *et al.*, 2005), and endangered small mammals (e.g., lagomorphs: Beever *et al.*, 2003; Anderson *et al.*, 2009), amphibians (e.g., frogs: Pounds *et al.*, 1999; Stuart *et al.*, 2004), and arthropods (e.g., butterflies: Parmesan, 1996; Thomas & Lennon, 1999; McLaughlin *et al.*, 2002 and spiders: Schoener & Spiller, 1992). The only attribute these species are likely to possess that may predispose them to a higher extinction risk of those listed in Purvis *et al.* (2000) is that of a small range size. For these populations, changes in mean environmental conditions are more important than changes in variability.

The above results resemble those in Chapter 3, where we used $\ln \lambda_s$ as a fitness indicator. Both when using $\ln \lambda_s$ and G as fitness parameters, the distance from the ideal environment b was identified as the most important gradient along which the relative contributions of changes in μ and σ changed. Extinction risk is more sensitive to changes in $\ln \lambda_s$ than to changes in σ_r^2, so the sensitivities of $\ln \lambda_s$ to changes in μ and σ have a greater weight on the sensitivity of extinction risk than do the sensitivities of σ_r^2. Chapter 3 showed that $\ln \lambda_s$ of populations populations of conservation concern was more affected by changes in μ. When using extinction risk as a proxy for fitness, we necessarily focus on populations of conservation concern, which might explain why the area of parameter space for which changes in σ are more important, is smaller ($|b| \lesssim 1$) when using G, than when using $\ln \lambda_s$ ($|b| \lesssim 2$; Chapter 3).

Our results in part justify the use of $\ln \lambda_s$ as a fitness parameter; it requires fewer assumptions than the estimation of extinction risk, and produces qualitatively similar results. Using extinction risk as a fitness measure is, however, advantageous when analysing populations of conservation concern. It allows to distinguish between groups of populations, such as the two considered above, that would not have been possible by using $\ln \lambda_s$ alone.

5 Are changes in the mean or variability of climate more important for populations?

Abstract

Changes in the variability of climate are likely to impact the dynamics of populations, yet have received less attention than changes in mean conditions. To what extent is this imbalance in research focus justified? Results from a theoretical model explicitly linked to the environment developed in Chapters 3 and 4 show that changes in environmental variability can be more important than changes in mean, particularly for populations living close to their ideal environment. However, there are few empirical studies we can use to validate our model with. We extend the number of studies we can use for validation by re-analysing existing population models linked to the environment, and comparing the relative effects of a change in mean environment on the population with the impact of a change in variability. Results show that across different taxa and modelling approaches, changes in variability are important for population dynamics. For one of the studies analysed, changes in variability had a clearly greater effect on the population than changes in mean. The main conclusion from Chapters 3 and 4 was that changes in variability deserve greater attention because of the impact these changes can have on animal populations. This conclusion is supported by the empirical studies analysed here.

5.1 Introduction

Climate change entails not only changes in mean conditions of climate (IPCC, 2007), but also changes in other statistical descriptions of climate change, such as variability (Michaels *et al.*, 1998; Räisänen, 2002; Boer, 2010) and autocorrelation (García-Carreras & Reuman, 2011). While changes in mean environment have garnered widespread attention, changes in variability have been the focus of fewer studies. To address whether the imbalance in research efforts is justified, we developed a simple theoretical model to compare the impacts of changes in mean environment to those due to changes in variability, and showed that changes in variability may in fact be more important for some populations (Chapters 3 and 4). However, do these results find support in existing empirical studies? There are only three studies which can be used to directly validate our predictions. We here re-analyse a selection of population models that are linked to the environment, to provide further empirical points of comparison for our model's results.

To elucidate how changes in the mean and standard deviation of the environment affect populations, and how their impacts compare, in Chapters 3 and 4 we used a simple, strategic approach, based on an unstructured population explicitly linked to an environmental variable via a flexible formulation of a response function. The results showed that changes in variability can be expected to be important for populations, even when compared to the impacts of changes in mean conditions. We furthermore offered insight into what populations are likely to be more vulnerable to changes in variability. The main gradient along which the relative importance of changes in mean and variability of environment varied was the population's distance from its ideal environment. Populations living close to their ideal environment are predicted to be more susceptible to changes in environmental variability, whereas those living in suboptimal conditions are expected to be more vulnerable to changes in mean conditions.

The credibility of any theoretical model depends on empirical validation. Without support from laboratory and field studies, it is very difficult to establish whether the approach taken and the assumptions made are appropriate. We know of only three empirical studies that compared the population's sensitivity to changes in mean and variability of the environment. They are those by van de Pol *et al.* (2010), Jonzén *et al.* (2010), and more indirectly, Jenouvrier *et al.* (2012); they are described below. While their findings broadly provide support for our theoretical predictions, they represent only three data points against which to validate our model. In Chapter 3 we encouraged replicating these efforts, preferably across environmental ranges (from ideal to suboptimal). However, this requires a non-trivial effort, with a substantial investment in both time and money.

Climate change has motivated a wealth of studies on how climate affects population dynamics. Most empirical studies focus on single populations, often of conservation concern. These studies often perform a sensitivity analysis, to see how different vital rates contribute to population fitness (e.g., Haridas & Tuljapurkar, 2005; Morris *et al.*, 2008; Ezard & Coulson, 2010; Coulson *et al.*, 2011). These sensitivities can provide indirect information on what climatic changes could be detrimental for a population. For example, short-lived plants were found to be very susceptible to variability in reproductive rates (Morris *et al.*, 2008), so they are probably sensitive to changes in climate that increase variation in these vital rates. However, changes in mean and variability of climate have the potential to change both the mean and variability of vital rates. To gain a better understanding of how climate change affects a population requires understanding the relationship between environment and vital rates (see Chapter 3). Some studies explicitly link vital rates to environmental variables, and estimate the impact of a predicted climatic change (e.g., an increase in mean temperature: Sæther *et al.*, 2000, or a change in variability: Lawler *et al.*, 2009) on the population. While these studies do not compare the effects of a change in mean and variability of the environment, they often provide a parameterised model set up to calculate at least one of these two sensitivities. It should therefore be possible, given the necessary information, to calculate the second sensitivity.

In this study we aim to re-analyse a select number of studies, to provide direct comparisons between the effects of changes in mean environment with changes in variability. The studies chosen needed to be fully parameterised, explicitly linked to an environmental variable, provide information on how the environment affects population vital rates, and preferably have originally estimated the sensitivity of the population to changes in mean and/or variability of climate. The results from this meta-analysis will provide further data points against which to validate the theoretical model developed in Chapters 3 and 4.

5.2 Selected studies

The studies chosen (Sæther *et al.*, 2000; Coulson *et al.*, 2008; van de Pol *et al.*, 2010; Jonzén *et al.*, 2010; Jenouvrier *et al.*, 2012) are described below. We summarise their model and original conclusions, and where necessary use the model to obtain the missing sensitivities to changes in climate.

5.2.1 Dippers

Sæther *et al.* (2000) conducted a study on a population of a small songbird, and one of their main objectives was to predict the impact of climate change. They studied a population of dippers (*Cinclus cinclus*) in southern Norway for 20 years, and developed a stochastic population model that included density dependence and climate effects (mediated through winter temperature) to model the dynamics of the population. They found that the predicted increase in mean winter temperature of 2.5°C would increase the carrying capacity and expected value of the distribution of population size by over 50%. How would the dynamics of the population be affected by a change in the variability of mean winter temperature?

Their model can be summarised as follows: the log growth rate of the population is drawn from a normal distribution:

$$\ln\left(\frac{X_{t+1} - M_{t+1}}{X_t}\right) \sim \mathcal{N}\left(r - \alpha\, X_t + \beta\, C_t, \sigma_e'^2 + \frac{\sigma_d^2}{X_t}\right), \tag{5.1}$$

where X_t is the number of breeding pairs in year t, M_t is the number of immigrants, r is the population growth rate, α is the strength of density dependence, and σ_d^2 is the demographic variance. C_t is the climatic variable, β alters the strength of the effect of the climatic variable, and $\sigma_e'^2$ is the residual variance not accounted for by variation in C_t. The environmental variance is

$$\sigma_e^2 = \sigma_e'^2 + \beta^2\,\mathrm{Var}(C_t). \tag{5.2}$$

The number of immigrants M_t is drawn from a Poisson distribution with parameter λ_t, where

$$\ln \lambda_t \sim \mathcal{N}(\mu_0 + \mu_1\, C_t, \sigma_\lambda^2). \tag{5.3}$$

Here, σ_λ^2 is the variance of $\ln M_t$, μ_0 is the mean log immigration rate at $C_t = 0$, and μ_1 measures the dependence of the immigration rate on C_t. The climatic variable C_t is modelled as a first-order autoregressive process

$$C_{t+1} - c \sim \mathcal{N}(a\,(C_t - c), \sigma_c^2), \tag{5.4}$$

where c and σ_c^2 are the mean and variance respectively, and a determines the return time of the process. The posterior distribution of the parameters of equations (5.1) and (5.3) were estimated using Markov Chain Monte Carlo methods (Sæther *et al.*, 2000). A sample of 1000 points from the distribution was provided to us by the authors. Parameter point estimates are in Table D.1 in Appendix D; most, but not all of these values reproduce values given by Sæther *et al.* (2000) in their Table 1.

Sæther *et al.* (2000) estimated the effect of a change in mean winter temperature on the population by changing the value of c (initially set to zero). To compare the effect of a change in mean winter temperature with a change in variability, we change the values of c and σ_c in equation (5.4) separately by 2.5°C, using the point estimates provided in Table D.1. The population was simulated for 50,000 time steps starting with the number of breeding pairs counted in 1978. The last 10,000 population counts were used to produce a distribution. Results show that a change of 2.5°C in mean winter temperature has a $\sim$ 14 times greater impact on the mean log population size than a change of 2.5°C in the standard deviation of mean winter temperature (Figure 5.1). Increasing variability of mean winter temperature has a greater impact on the variance of the distribution of log population size (Figure 5.1).

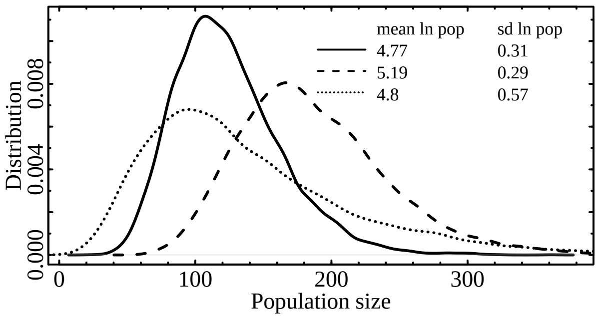

Figure 5.1: Distribution of population size, with no change to mean or variability (solid line), a change in mean (c = 2.5; dashed line) and a change in variability ($\Delta\,\sigma_c$ = 2.5; dotted line). The legend shows the mean values and standard deviations of the log population distributions. The solid and dashed lines are the same as the curves shown in Figure 3A of Sæther *et al.* (2000).

To assess the robustness of the results shown in Figure 5.1, we simulated the population as described above, but using the 1000 points from the posterior distribution. One parameter combination produced non-finite population counts with no change in the environment, and a total of two parameter combinations produced non-finite population counts given a change in mean or standard deviation of winter temperature. These two parameter combinations were left out of the analysis. Figure 5.2 shows the distribution of mean population size for the 998 combinations, given no change in climate, a change in climate mean, and a change in variability. For $\sim$ 3% of these combinations, changes in environmental variability had a greater impact on mean population size than changes in the mean of the environment. Changes in the variability of winter temperature had a greater impact on the standard deviation of log population size for all parameter combinations. These results support the findings of Figure 5.1.

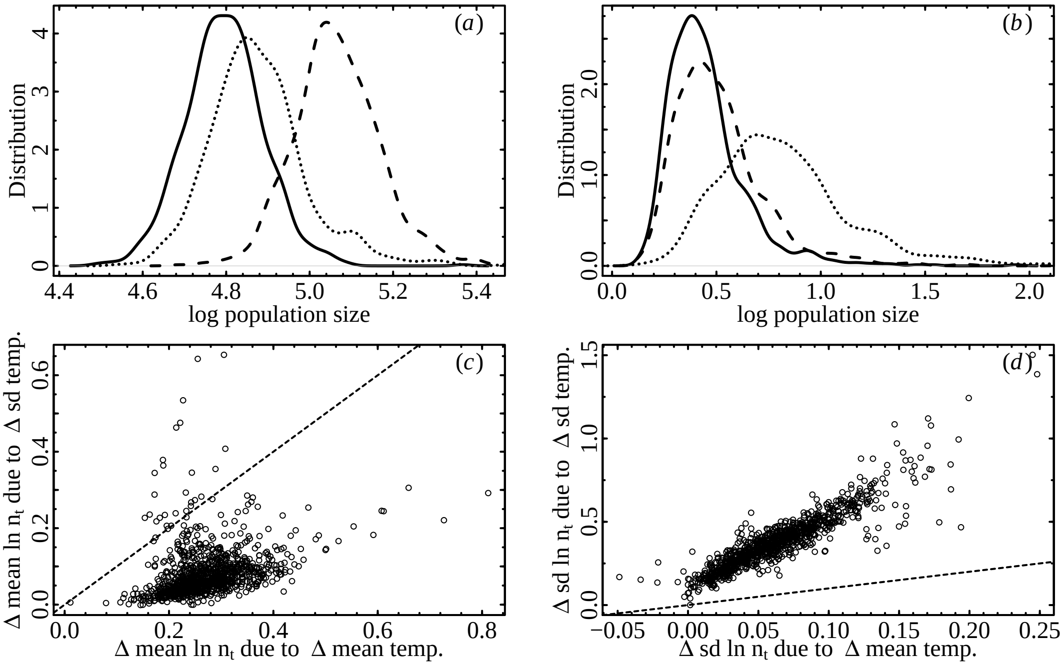

Figure 5.2: The distribution of mean $\ln n_t$ (a) and standard deviation of $\ln n_t$ (b) for the 998 parameter combinations of the posterior distribution, with no change in mean or variability (solid line), a 2.5°C change in mean (dashed line) and a 2.5°C change in variability (dotted line). (c) The change in mean $\ln n_t$ caused by a 2.5°C change in mean winter temperature versus the change in mean $\ln n_t$ caused by a 2.5°C change in the standard deviation of winter temperature. For 28 of the parameter combinations, a 2.5°C change in standard deviation caused a greater impact on mean $\ln n_t$. (d) The change in the standard deviation of $\ln n_t$ caused by a 2.5°C change in mean winter temperature versus that caused by a 2.5°C change in the standard deviation of winter temperature. For all 998 parameter combinations, an increase of 2.5°C in the standard deviation of winter temperature had a greater impact on the standard deviation of $\ln n_t$ than the same change in mean winter temperature. The dashed line in (c) and (d) is the y=x line.

5.2.2 Soay sheep

The Soay sheep (*Ovis aries*) population on the Island of Hirta in the St. Kilda archipelago, Scotland, are a food-limited population free of interspecific competition and predation, and for this reason represent an ideal setting to study the cause of fluctuations in population numbers (Clutton-Brock & Pemberton, 2004). They have been annually censused since 1955, and their dynamics are characterised by quasiperiodic population crashes, a product of the interaction between weather effects and density dependence (Grenfell *et al.*, 1998; Coulson *et al.*, 2001; Stenseth *et al.*, 2004). Several studies have used different approaches to model the population and characterise its dynamics (Grenfell *et al.*, 1998; Coulson *et al.*, 2001; Stenseth *et al.*, 2004; Coulson *et al.*, 2008). The North Atlantic Oscillation (NAO) has often been used as the environmental variable (Coulson *et al.*, 2001; Stenseth *et al.*, 2004; Coulson *et al.*, 2008; Ezard & Coulson, 2010), together with proxies for local weather (Coulson *et al.*, 2001), and sward height (Ezard & Coulson, 2010). Coulson *et al.* (2008) parameterised a two sex model with seven age classes. The purpose of the study was to compare the relative contributions of the environment (NAO), density dependence, and their interaction to the variability explained by the model.

We use the model in Coulson *et al.* (2008) to compare the sensitivity of the population to changes in mean and variability of NAO. Survival and fecundity are functions of density and NAO. Parameter estimates for the effects of density, NAO, and their interaction are given in Table D.2 in Appendix D, reproduced from Coulson *et al.* (2008). The models were linear on the logit scale, so they can be transformed using

$$\frac{1}{1 + 1/\exp(a + b\,x_1 + c\,x_2 + d\,x_3)}, \tag{5.5}$$

where a is the value for the intercept given in Table D.2, b, c, and d are the parameters corresponding to density, NAO, and their interaction respectively, and x_1, x_2, and x_3 are the time series of density, NAO, and their interaction respectively. Recruitment is given by the product of fecundity, litter size (values provided in the caption of Table D.2), and neonatal survival. New recruits have equal chance of being male or female, therefore recruitment is divided by two in the 11 by 11 projection matrices for the two sexes. The initial population size is arbitrarily set at 1000, with equal numbers allocated to each age class.

Coulson *et al.* (2001) simulated NAO by drawing values from a normal distribution with mean and standard deviation equal to the observed values over the study period. Following Coulson *et al.* (2001, 2008), data for station-based winter (December to March) NAO, defined as the difference of normalised sea level pressure between Lisbon, Portugal and Stykkisholmur, Iceland, were downloaded on 02/06/2012 from The National Center for Atmospheric Research website (`https://climatedataguide.ucar.edu/sites/default/files/cas_data_files/asphilli/nao_station_djfm_0.txt`). The data since 1864 were visually inspected for normality. NAO was then modelled as a first-order autoregressive process:

$$x_{t+1} \sim \mathcal{N}(a\,(x_t - c), \sigma_n^2) + c, \tag{5.6}$$

with mean c and standard deviation σ_n equivalent to the observed mean and standard deviation of NAO for the time period 1985–2006 ($c = 1.006$ and $\sigma_n = 2.135$), and $a = 0.15$ being the return time of the process estimated using the time series since 1864. To change the mean and standard deviation of NAO, we increased the values of c and σ_n respectively. We ran the population model for 50,000 time steps, and calculated the mean of the distribution of population size for the last 10,000 time steps. The process was repeated by increasing the mean NAO and separately increasing its standard deviation.

Figure 5.3a shows the mean population size for the last 10,000 time steps for a change in mean and standard deviation of NAO. The effect of a change in mean NAO on mean population size is similar to that caused by a change in standard deviation of NAO. Changes in the variability of NAO have a more substantial impact on the variability of population size (Figure 5.3b), whereas an increase in mean NAO reduces the variability of the population. Coulson *et al.* (2001) found that changing both the mean and variability of NAO affected the strength of the density dependence of the population; the effect of changes in NAO shown here may be caused by the same mechanism.

It is notoriously complicated to predict future trends in mean and variability of NAO (Osborn, 2004). A group of seven GCMs analysed by Osborn (2004) predict a value of NAO for 2050 ranging between ~ -2 and ~ 6. Figure 5.4 shows the population distributions when increasing c and σ_n by two, and confirms the results observed in Figure 5.3.

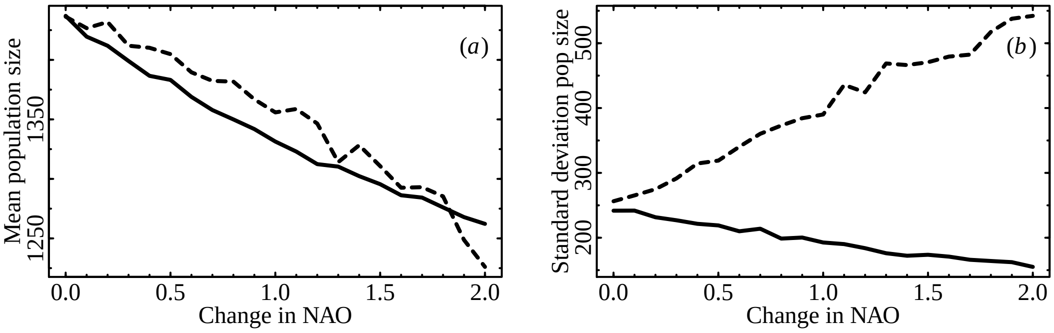

Figure 5.3: The effect of a change in mean NAO (solid line) and a change in the standard deviation of NAO (dashed line) on mean population size (a) and standard deviation of population size (b) of Soay sheep.

5.2.3 Eurasian oystercatchers

The objective of the studies by van de Pol *et al.* was to compare the impact of changes in variability (van de Pol *et al.*, 2010) and autocorrelation (van de Pol *et al.*, 2011) of mean winter temperature to changes in the mean, on a declining population of resident Eurasian oystercatchers (*Haematopus ostralegus*) in the Netherlands. Oystercathers are long-lived, territorial, shore birds, with a demography that exhibits distinct age-structure (van de Pol *et al.*, 2010). They parameterised a density

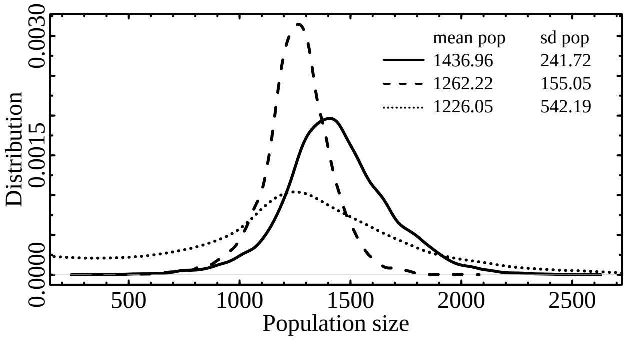

Figure 5.4: Distribution of population size, with no change to mean or variability (solid line), increasing the mean (by two; dashed line) and increasing the variability (also by two; dotted line) of NAO. The legend shows the mean values and standard deviations of the population distributions.

dependent stochastic structured population model (given in equation (2) of van de Pol *et al.*, 2010) which also incorporates movement between breeding habitats of different quality. Fecundity and survival were assumed to be Poisson-distributed and binomial respectively, and movement between habitats was modelled as a function of population density in the two kinds of breeding habitats. The authors estimate how survival, movement, and fecundity vary with winter temperature, identified as the most important environmental variable for this population. Winter temperature was modelled as an independent and identically distributed (iid) lognormal process. They then observed how changes in mean and variability of winter temperature affected these vital rates, and how the changes affected median time to extinction, which they used as a proxy for population fitness. Median time to extinction was defined as the number of time steps it took for 50% of 300,000 simulated populations to go extinct.

Van de Pol *et al.* (2010) found that a 0.1°C change in mean temperature had a 1.5 times greater effect on median time to extinction than a 0.1°C change in standard deviation. Although the oystercatcher population is more sensitive to mean temperature, changes in variability are nevertheless still evidently important. However, when this result is considered together with the projected changes in mean and variability of local winter temperature, the authors conclude that changes in mean temperature are likely to overwhelm the effects of changes in variability. They also conclude that the concavity of the functions linking vital rates and environment largely determines the effect that changes in environmental variability have on the population. In a subsequent study, van de Pol *et al.* (2011) also added changes in the autocorrelation structure of winter temperature to the comparison, coming to the conclusion that these have an even smaller effect on the population than changes in variability.

5.2.4 Red kangaroos

Jonzén *et al.* (2010) studied a population of South Australian red kangaroos (*Macropus rufus*, Desmarest) living in arid and semi-arid environments, to compare the effects of changes in the mean of an environmental variably with the effects of changes in standard deviation. The population of kangaroos live in an arid environment characterised by unpredictable and highly variable rainfall, and are harvested annually for meat and skins. The authors modelled vital rates as functions of rainfall, using a logistic function for survival, and determining probability of reproduction for each age class using logistic regressions. Annual rainfall was sampled from a 123-year-long time series of local rainfall data. With these vital rates, the authors parameterised a density independent stochastic matrix population model with three age classes, and following the methods described in Haridas & Tuljapurkar (2005), calculated the elasticities of $\ln \lambda_s$ to changes in mean and variability of both the vital rates and rainfall.

Changes in the variability of the kangaroo population vital rates had a very weak effect on $\ln \lambda_s$: almost 40 times smaller than the impact caused by changes in mean vital rates. It may be tempting to conclude that the impact of changes in environmental variability are probably of little relevance (see, e.g., Coulson *et al.*, 2011). In fact, the elasticity of $\ln \lambda_s$ to changes in mean rainfall turned out to be only ~ 5 times greater than the elasticity to changes in variability. This was further reduced to a factor of 2.4 if comparing sensitivities instead of elasticities. A change in the variability of rainfall may alter both the mean and the standard deviation of vital rates, and therefore, a low elasticity to changes in vital rate variability does not presuppose that a population is insensitive to environmental variability (Jonzén *et al.*, 2010; Tuljapurkar, 2010).

5.2.5 Emperor penguins

Using data from 1962 onwards on a population of emperor penguins (*Aptenodytes forsteri*) in Terre Adélie, Antarctica, Jenouvrier *et al.* (2009) developed a two-state Markov chain density independent matrix model. Sea-ice concentration, defined as the fraction of area covered by ice, drives the emperor penguin life-cycle, so the two states represented years where sea ice concentration (SIC) was 'normal' and 'warm'. Jenouvrier *et al.* (2010) then added males to the model, and partitioned the annual projection matrix into four seasonal steps. Finally, the effects of SIC on the vital rates was explicitly incorporated into the model in Jenouvrier *et al.* (2012).

Amongst the objectives of the study by Jenouvrier *et al.* (2012) was to compare the impact of changes in mean annual SIC_a (anomalies of SIC relative to the mean annual SIC value from 1979 to 2007) and variability of SIC_a on the $\ln \lambda_s$ of the population. The current mean annual SIC_a is close to its optimum level for the penguin population, as shown by Figure 6(a) in Jenouvrier *et al.* (2012). Both an absence of sea ice, and heavy, persistent sea ice (i.e., higher values of $|SIC_a|$), reduce the $\ln \lambda_s$ of the population (Jenouvrier *et al.*, 2012). They also analysed the impact of doubling the observed variance of SIC_a on $\ln \lambda_s$, and find that while at intermediate values of mean SIC_a, increasing variability reduces $\ln \lambda_s$, at extreme values of SIC_a, variability can in fact benefit the population (Figure 6(a) in Jenouvrier *et al.*, 2012).

Jenouvrier *et al.* (2012) provide the necessary information to compare the relative impacts of changes in mean and variability of SIC_a on the penguin population, but do not make the comparison explicitly. To make the direct comparison, we first digitised Figure 6(a) (Figure 5.5(a)). The observed standard deviation of mean annual SIC_a (provided by Stéphanie Jenouvrier) is 1.4970. Doubling the variance of SIC_a therefore corresponds to an increase of $(\sqrt{2} - 1)\,\mathrm{sd}(SIC_a) \approx 0.62$ in the standard deviation of SIC_a. We calculated the change in $\ln \lambda_s$ due to a ~ 0.6 increase in the variability of SIC_a by taking the difference between the two curves of Figure 5.5(a) at each mean annual SIC_a value. We then estimated the impact of an increase in mean annual SIC_a on the population by calculating the change in $\ln \lambda_s$ given an increase of ~ 0.6 in mean annual SIC_a, at the observed variability (Figure 5.5(b)). The ratios of the changes in $\ln \lambda_s$ due to an increase in mean SIC_a, over the changes in $\ln \lambda_s$ due to an increase in the variability of SIC_a, are shown in Figure 5.5(c). Results show that for intermediate ($|SIC_a| \lesssim 2$) and extreme values of SIC_a ($|SIC_a| \gtrsim 5$), changes in variability of SIC_a have a greater impact on $\ln \lambda_s$ than do changes in mean values of SIC_a.

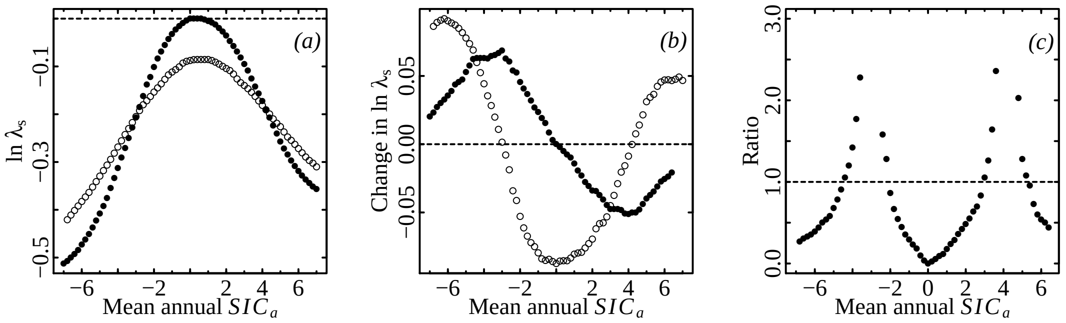

Figure 5.5: (a) Digitised reproduction of Figure 6(a) in Jenouvrier *et al.* (2012), where black points correspond to observed variance, and white points to twice the observed variance. (b) Change in $\ln \lambda_s$ given a 0.6 change in mean SIC_a (black points) and given a 0.6 increase (approximately equivalent to doubling the variance) in the standard deviation of SIC_a (white points). The white points in this panel correspond to the difference between white and black points in panel (a). (c) The ratio of the absolute change in $\ln \lambda_s$ due to an increase in mean SIC_a over the absolute change in $\ln \lambda_s$ due to an increase in variability of SIC_a. The line at Ratio = 1 denotes where the effect due to changes in mean is of the same magnitude as that due to changes in variability of SIC_a.

5.3 Discussion

The main findings are summarised in Table 5.1. Results confirm the general conclusion of Chapters 3 and 4: changes in environmental variability are similarly important for the dynamics of populations when compared to changes in mean conditions, for most populations. Support for this conclusion is strengthened by the fact that all five populations analysed here cover a wide range of taxa, include thriving (e.g., red kangaroos) and declining (e.g., oystercatchers) populations, and use different models and assumptions. In two of the five populations (Soay sheep, emperor penguins), changes in variability were at least as important as changes mean conditions. The ratio of the impact of changes in mean conditions to impact of changes in variability on the population ranged from close to 0 (emperor penguins) to 14 (dippers). However, changes in the variability of the environment had a greater effect on the variability of population size (dippers, Soay sheep), which affects the dynamics of the population (Chapter 4). Therefore, for all studies analysed here, changes in environmental variability had a significant effect on the dynamics of the populations.

Chapters 3 and 4 also made more specific predictions: changes in environmental variability are more likely to affect populations closer to their ideal environment, and changes in mean conditions are expected to affect populations closer to the periphery of their environmental range. The only study that provides an environmental range across which to compare the effects of changes in environmental mean and variability is that by Jenouvrier *et al.* (2012). Results show that close to ideal conditions (i.e., for $|SIC_a| \lesssim 2$), changes in variability have a far greater effect on the emperor penguin population than changes in mean conditions. Changes in mean conditions become progressively more important as $|SIC_a|$ increases. At extreme values of SIC_a, however, changes in variability once again have a greater effect on $\ln \lambda_s$ than changes in mean values of SIC_a. These results closely resemble and support the predictions made by the model in Chapters 3 and 4, except for the ratio at extreme values of SIC_a. This may be due to the fact that the extreme values of SIC_a considered are very unlikely. The five Global Circulation Models (GCMs) analysed by Jenouvrier *et al.* (2012) show a likely decline in future trends of SIC_a, but values remain well within ± 1 range (as shown in Figure 7 of their study).

The results from these studies could also be compared to see whether populations presumed to be living closer to their ideal environment are more affected by changes in variability than those living further away from it. However, no clear pattern emerges. Direct comparisons between these studies is complicated by the idiosyncrasies specific to each population. A wide range of modelling approaches is used, including structured and unstructured models, some incorporating density dependence. These choices entail the use of different proxies for population fitness. For example, $\ln \lambda_s = 0$ for density-dependent populations, making it unsuitable as a measure of fitness. The studies by Sæther *et al.* (2000) and Coulson *et al.* (2008) were furthermore designed and conducted with aims that did not include the comparison of sensitivities of the population to changes in mean and variability.

A greater number of studies could be added to this analysis, if those that use a Markov chain to simulate the environment were to be included. However, there are two separate issues to contend with that complicate re-analysis of these studies. Markov chains require the environment to be split into a discrete number of states. A projection matrix is then parameterised for each state. The probability of staying in the current state or changing to any of the other states is then defined in a transition matrix, which is used to generate a sequence of projection matrices and an estimate of $\ln \lambda_s$. While it is not possible to explicitly change the mean and standard deviation of the environment, it is possible to simulate their effect by altering the vital rates of the projection matrices. For example, in a two-state Markov chain the environment is split into good and bad years. An increase in mean environment would then be analogous to increasing the values of all vital rates in both projection matrices, assuming that increasing the values benefits the population (an exception could be plant populations that can revert to a smaller size class). Likewise, environmental variability could be increased by reducing the vital rates for the projection matrix representing bad years, and increasing the vital rates for the matrix standing for good years (taking the aforementioned caveat into account). The amount by which each vital rate is changed would necessarily be a function of the transition probabilities. The first issue arises from the fact that Markov chains are particularly useful for modelling populations prone to disturbances such as hurricanes (e.g., Tuljapurkar *et al.*, 2003; Horvitz *et al.*, 2005), fires (e.g., Gross *et al.*, 1998; Caswell & Kaye, 2001), and floods (e.g., Smith *et al.*, 2005). In these cases, it would make little biological sense to reduce the vital rates for a population that has just suffered, for instance, a hurricane. However, Markov chains are also used to model continuous environmental variables, such as sea ice concentration (Jenouvrier *et al.*, 2009, 2010; Hunter *et al.*, 2010), NAO, and sward height (Ezard & Coulson, 2010). For these, another issue arises. Taking the same two-state Markov chain as an example, changing the vital rates to simulate an increase in environmental mean and variance ignores the function that connects the vital rate in a good year with that in a bad year (Figure 5.6). Therefore, although the environment is simplified down to a discrete set of states, more detailed information on how each vital rate changes with the environmental variable is necessary. Specifically, information on the slope of the function at the two points shown in Figure 5.6 would be required. Re-analysing studies using Markov chains therefore requires a more substantial effort.

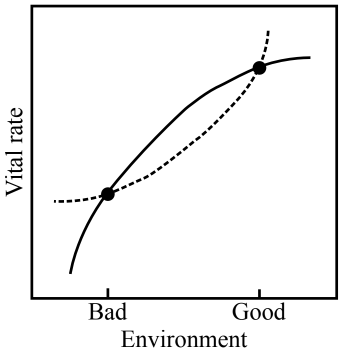

Figure 5.6: Information on how the vital rates vary with the environment is lost when the environment is split into good and bad years in a two-state Markov chain. Altering vital rates to simulate an increase in environmental mean and variability requires information on the gradient of the function linking vital rate to the environment at the points defined as good and bad years. The function could have different shapes (e.g., solid and dotted lines), so ignoring this information would be a mistake.

It should be straightforward to add changes in autocorrelation of the environment to the analysis, in order to compare its effects on populations to those caused by changes in mean and variance of the environment. The models analysed so far use autoregressive processes to simulate the environment, therefore changing the term defining the return time (e.g., a in equation (5.6)) would change the autocorrelation of the environmental variable.

One of the recommendations of Chapters 3 and 4 was to encourage the comparison of populations thought to be living in close-to-ideal conditions with those far from ideal conditions. For example, it would be interesting to replicate the study of van de Pol *et al.* (2010) with an expanding oystercatcher population. The recommendation still holds, because the same population model and assumptions would be used, and a direct comparison would be fair. For a meta-analysis to prove useful for validating the more specific predictions of our theoretical model, more studies need to be added to the analysis.

In Chapter 3 we suggested that more biological detail could be introduced to the model, for instance by adding age-structure. An age-structured model would not only allow us to investigate how survival and fecundity are affected by changes in mean and variability of the environment, but also how age-structure affects the predictions made with the univariate model. Similarly, it would be interesting to investigate how density dependence and its form would alter the predictions made. Adding density dependence, however, would most likely make the model analytically intractable, and would therefore probably need to be done through simulations.

Table 5.1: Summary of results of the meta-analysis. The population fitness parameter column lists what population attributes were investigated. The factor by which changes in mean environmental conditions cause a greater impact on the population than changes in environmental variability is provided. The last column provides information on the state of the population, as well as additional comments on results.

Species	***Pop. fitness param.***	***Factor***	***Approach used***	***Comments***
Dippers	mean $\ln n_t$	14	Density dependent, univariate	Changes in the variability of mean winter temperature had a greater impact on the standard deviation of log population distribution.
Soay sheep	mean n_t	~ 1	Density dependent, age structured	Population suffers quasi-periodic crashes, but mean trend is positive. Changes in the variability of winter NAO had a greater impact on the standard deviation of population distribution.
Eurasian oystercatchers	Mean time-to-extinction	1.5	Density dependent, age structured	Population numbers are declining, movement between territories included in model.
Red kangaroos	$\ln \lambda_s$	2.4	Density independent, age structured	Population is harvested but still manages to grow.
Emperor penguins	$\ln \lambda_s$	-	Density independent, age structured	Only study to include a gradient of environmental conditions. Population barely stable in its ideal environment. Changes in variability of SIC_a have a greater effect on $\ln \lambda_s$ for values of SIC_a closer to the population's ideal environment.

6 An empirical link between the spectral colour of climate and the spectral colour of field populations in the context of climate change

Abstract

The spectral colour of population dynamics and its causes have attracted much interest. The spectral colour of a time series can be determined from its *power spectrum*, which shows what proportion of the total variance in the time series occurs at each frequency. A time series with a *red* spectrum (a negative *spectral exponent*) is dominated by low-frequency oscillations, and a time series with a *blue* spectrum (a positive spectral exponent) is dominated by high-frequency oscillations. Both climate variables and population time series are characterised by red spectra, suggesting that a population's environment might be partly responsible for its spectral colour. Laboratory experiments and models have been used to investigate this potential link. However, no study using field data has directly tested whether populations in redder environments are redder. This study uses the Global Population Dynamics Database together with climate data to test for this effect. We found that the spectral exponent of mean summer temperatures correlates positively and significantly with population spectral exponent. We also found that over the last century, temperature climate variables on most continents have become bluer. Although population time series are not long or abundant enough to judge directly whether their spectral colours are changing, our two results taken together suggest that population spectral colour may be affected by the changing spectral colour of climate variables. Population spectral colour has been linked to extinction; we discuss the potential implications of our results for extinction probability.

N. B.: This chapter has been published as: García-Carreras, B. & Reuman, D. C. (2011). An empirical link between the spectral colour of climate and the spectral colour of field populations in the context of climate change. *The Journal of Animal Ecology*, **80**(5), 1042–1048. The corresponding supplementary information is provided in Appendix E.

6.1 Introduction

The positive autocorrelation typical in animal population dynamics and its causes have stimulated substantial interest over the past 30 years (Roughgarden, 1975; Lawton, 1988; Cohen, 1995; Akçakaya *et al.*, 2003; Schwager *et al.*, 2006; Ruokolainen *et al.*, 2009). Many climatic variables are also positively autocorrelated, suggesting that a population's environment might be partly responsible for the positive autocorrelation seen in its dynamics. However, no study using field data has directly tested whether more positively autocorrelated populations live in more positively autocorrelated environments. Also, insufficient work in the ecological literature has addressed the related question of how the autocorrelation of environmental variables may be affected by climate change and what the population consequences of these changes may be. These questions have practical implications because the level of autocorrelation in population dynamics affects population extinction probabilities as well as temporal patterns of offtake in the case of exploited populations and temporal patterns of economic or disease burden in the case of pest or vector populations (Reuman *et al.*, 2006, 2008).

Empirical data show that annually censused population dynamics are positively autocorrelated, and consequently described by *red power spectra* (Pimm & Redfearn, 1988; Sugihara, 1995; Halley, 1996; Inchausti & Halley, 2001); we provide definitions to make this statement precise. The *power spectrum* is a widely used mathematical technique that takes a time series (population or environmental) as input and returns as output a plot which shows the decomposition of the total variance (or *power*) in the time series into its frequency components (Brillinger, 2001). A *red* time series, by definition, has more variation at low frequencies than at high frequencies. A *blue* time series has more variation at high frequencies and a *white* time series has equal variation at all frequencies in a range. The colour-based terminology used here was coined because red (respectively, blue) light is more dominated by lower (respectively, higher) frequencies than other colours of visible light. Colour can be quantified for a time series by calculating the *spectral exponent*, defined as the slope of a linear regression line drawn through a log-power-versus-log-frequency plot of the spectrum; negative slopes correspond to red time series, and positive slopes to blue time series, with white noise having a spectral exponent equal to or close to zero. Inchausti & Halley (2002) found that the spectral exponents in annually censused animal populations across several clades and trophic levels were negative: population dynamics, as typically measured by ecologists, are red.

Ascribing the spectral colour of populations to a cause or mechanism has proven more complex than describing the pattern. Early work focussed on simple unstructured deterministic population models to see whether intrinsic dynamics could be the cause of population spectral redness. For example, Cohen (1995) investigated several such population models using a single point in parameter space chosen to be in the models' chaotic regime, finding that the dynamics predicted by the selected models tended to be blue. Other authors subsequently found, however, that the same models with other parameters produced red spectra (Blarer & Doebeli, 1996; White *et al.*, 1996a): simple deterministic models can produce dynamics of a range of colours, depending on parameters. Deterministic models alone failed to completely explain the origin of populations' spectral colour, unless accompanied by an argument that real populations are constrained to certain parameter regimes.

Several modifications of the initial deterministic models were examined, all with the potential to redden spectra. These included the introduction of measurement error (Akçakaya *et al.*, 2003), a spatial component (White *et al.*, 1996b), delayed stochastic density dependence (Kaitala & Ranta, 1996), and age structure (Greenman & Benton, 2005). One mechanism that has received much attention is environmental variability (Lawton, 1988; Sugihara, 1995; Kaitala *et al.*, 1997b; Ranta *et al.*, 2000). Climatic variables are also characterised by reddened spectra (Steele & Henderson, 1994; Cyr & Cyr, 2003; Vasseur & Yodzis, 2004). Given populations' reliance on the surrounding environment, it seems likely that their spectral redness can, at least in part, be traced back to the redness of climate.

If environmental colour were to have any influence on population spectral colour, population dynamics should be redder in redder environments (Roughgarden, 1975; Kaitala *et al.*, 1997b). To investigate this link, both laboratory experiments (Petchey, 2000; Laakso *et al.*, 2003b) and theoretical studies (Roughgarden, 1975; May, 1981; Kaitala *et al.*, 1997b; Laakso *et al.*, 2001, 2003a; Greenman & Benton, 2005; Ruokolainen *et al.*, 2007) have been undertaken, tentatively concluding that some of the environmental spectral colour is likely to propagate through to the population spectra, "tinging" the dynamics with a similar colour. Figure 6.1 provides a summary presentation of some prior modelling results demonstrating this effect using the well-known Ricker model (Methods). A similar pattern generally arises in other simple univariate models such as the Hassell and Maynard Smith models (Section E.1). It is important, however, to augment prior modelling (Roughgarden, 1975; May, 1981; Kaitala *et al.*, 1997b; Greenman & Benton, 2005) and experimental (Laakso *et al.*, 2003b) results summarised here with tests based on field data. Although the use of observational field data makes it difficult or impossible to establish a causal relationship between climate and population spectral colour, field data can be used to test for correlations that such a causal relationship would produce. Modelling and experimental studies have explored causation in a context where it is possible to do so whereas observational field studies are now necessary to see to what degree predicted consequences of the causal hypothesis actually pertain in a broad way to real systems.

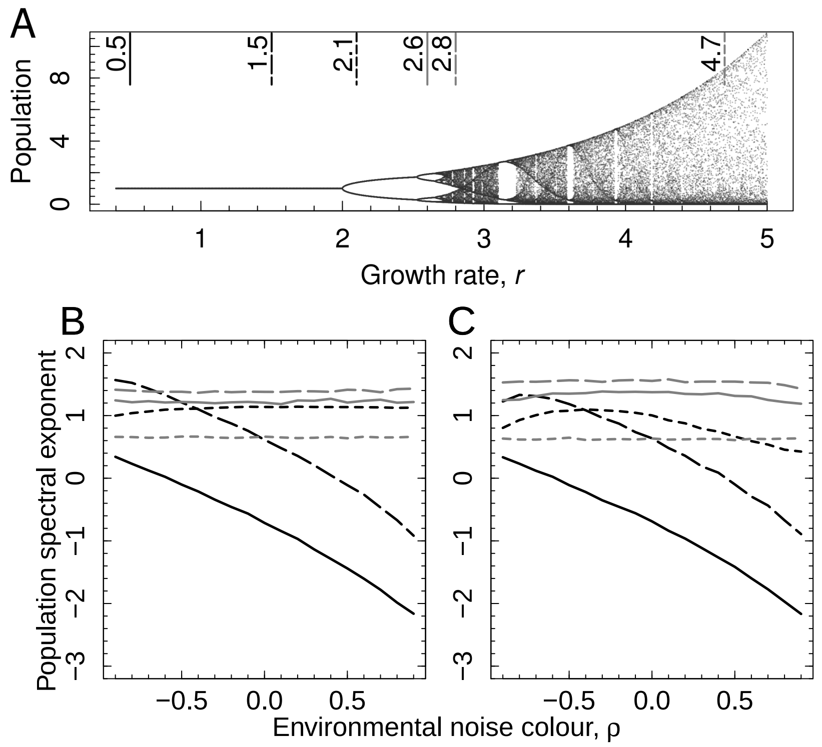

Figure 6.1: The impact of environmental spectral colour on population spectral colour in a stochastic formulation of the Ricker model (Methods). Panel A is the bifurcation plot for the deterministic skeleton of the model, indicating the growth rate (r) values and respective line types used for the following panels. Panel B is with weak environmental noise ($\sigma = 0.01$; see Methods), and panel C is with strong environmental noise ($\sigma = 0.1$). Results show that environmental spectral colour tinges population spectral colour, to an extent that depends on growth rate and the strength of environmental noise.

Environmental noise colour has an influence on population extinction risk, but results so far indicate that this influence can be complex and contingent on the details of population dynamics. Prompted by the positive autocorrelation reported for both climatic variables and populations, Lawton (1988; later supported by Halley, 1996; Pike *et al.*, 2004 and Inchausti & Halley, 2003, the latter using empirical data and the concept of “quasi extinction”, a 90% reduction in population size) argued that red noise should increase the risk of extinction, based on the intuition that populations would then suffer long runs of adverse conditions. In apparent contradiction to this intuition, Ripa & Lundberg (1996) claimed that red noise decreases extinction risk. Subsequent studies (Petchey *et al.*, 1997; Heino, 1998) expressed a more nuanced view.

Theoretical studies have not reached a consensus predominantly due to differences in population model and parameter choice (Ripa & Lundberg, 1996, 2000; Heino, 1998; Ripa & Heino, 1999), environmental noise model (Heino, 1998; Halley & Kunin, 1999; Cuddington & Yodzis, 1999), variance used (Heino *et al.*, 2000; Schwager *et al.*, 2006), and the time scales on which extinctions are scored (Halley & Kunin, 1999; Heino *et al.*, 2000). It is difficult to systematically explore the relationship between colour and extinction risk with models given the variety of modelling choices that must be made. We return to the relationship between spectral colour and extinction risk in the Discussion.

The relationships between the spectral colours of climate and populations and the associated population extinction risk need to be viewed in a context of climate change. Climate patterns throughout the world are changing rapidly, as evidenced by increases in average global temperature and in the variability of climatic conditions (IPCC, 2007). These changes are conceivably shifting the spectral colour of climatic variables, and consequently may be affecting populations' spectra, if climate and population spectra are causally related. We test the hypothesis that the spectral exponents of climate variables have changed over the last century and combine the results with our observations about how population and climate spectral exponents are related to formulate hypotheses about how population spectral exponents may be influenced by climate change.

6.2 Methods

6.2.1 Data sources

Two data sets of climate variables were used, respectively, for the purposes of analysing changes in climate spectral exponent over time and for comparison with population time series: a large collection of direct measurements taken from weather stations; and a global-coverage, spatially gridded data set derived from measurements by interpolation. These data sets have, respectively, the complementary strengths of greater reliability and coverage that make them suitable to be used for the intended purposes. Weather station data were downloaded from the Global Historical Climatology Network (GHCN; Peterson & Vose, 1997). The GHCN provides data from about 7280 stations worldwide, although different stations were active for different periods. Spatially gridded data were downloaded from the Climatic Research Unit (CRU TS 2.1 data set). CRU data have global terrestrial coverage at 0.5° by 0.5° resolution and monthly temporal resolution from 1901 to 2002 (Mitchell & Jones, 2005). The interpolation procedure used for the CRU data is described by New *et al.* (2000).

CRU data span a century and are spatially comprehensive, enabling comparison between population time series and interpolated climate data from the same location. However, the reliability of the interpolated data depends on location and time, being related to the number and proximity of nearby weather stations. A density index of nearby stations for each grid cell at each time is provided with the CRU data set. CRU data were validated against the GHCN data (see Section E.2) to obtain a threshold value for the station density index above which the CRU data were found to be sufficiently reliable. Only data with reliability above this threshold value were used for comparison with population data, so populations in a time or place with CRU data reliability below the threshold were not used.

The Global Population Dynamics Database (GPDD; NERC Centre for Population Biology & Imperial College, 1999) currently holds nearly 5000 animal and plant population time series and is freely accessible. It has been used in several population dynamics studies, some of which investigated population spectral colour (Kendall *et al.*, 1998; Inchausti & Halley, 2001; Halley & Inchausti, 2002; Inchausti & Halley, 2003). GPDD data were filtered to remove time series not suitable for our analysis. The filtering process, described in detail in Section E.3, kept only annual time series with at least 30 continuous data points that were also accompanied by metadata with the geographic coordinates of the location. Other filtering constraints were also applied. 147 time series remained after filtering (see Section E.3.1 for a complete list of time series used).

6.2.2 Preprocessing of weather data

The GPDD data used is annual, whereas the CRU and GHCN data used consist of mean monthly temperatures (i.e., time series with a sampling frequency of 12 per year). In order for the two to have the same temporal resolution, the CRU and GHCN data were preprocessed to derive several variables, all with a sampling frequency of one per year. *Mean annual temperatures* were obtained by taking the mean of the 12 mean monthly temperature values (January to December). All but one of the populations left over from the filtering process were located in the Northern hemisphere, so seasons were defined accordingly, with winter being December to February, spring being March to May, and so on. *Mean summer temperature* is the mean of the three monthly temperature values corresponding to summer. Similarly, the other seasons are defined as the means of their respective months. *Mean seasonal temperature* refers to all four time series, collectively.

6.2.3 General methods

The wide prior use of the spectral exponent facilitates direct comparisons of our results with earlier studies. All time series were linearly detrended and the spectrum was then estimated using an unsmoothed periodogram (`spec.pgram` function in the *R* programming language). Before detrending and computing spectra, population numbers, p, were transformed by $\log_{10}(p+1)$. Climate variables were detrended but not transformed. All computations and graphics were done in the *R* computing environment, version 2.10.0 (2009-10-26; R Development Core Team, 2009).

6.2.4 Testing for correlation between climate and population spectral exponents

Using the CRU data, the spectral exponents of mean seasonal and mean annual temperatures were calculated for the same time period and location (rounded to 0.5°) as each of the 147 GPDD population time series. The null hypothesis that the correlation between climate and population spectral exponents was zero was then tested by computing a Pearson correlation coefficient and P value, taking spatial autocorrelation into account as described below.

6.2.5 Testing for change in climate spectral exponent

The GHCN data were filtered to include time series that covered the 1911–1990 period. These years were chosen because they gave a good compromise between length of time period and number of weather stations active throughout that period. Using the most recent years available (until 2002 in the version of the GHCN data set used for this study) would have greatly reduced the number of weather stations available (New *et al.*, 2000). For each half of the time series (1911–1950 and 1951–1990) a maximum proportion of missing values of 0.15 was allowed. Because it can accommodate missing data, for this spectral analysis the Lomb periodogram (Scargle, 1982) was used to calculate spectra. Spectral exponents for both halves of the time series (1911–1950 and 1951–1990) were calculated for mean annual and mean seasonal temperatures. The null hypothesis that the spectral exponents of the two halves were the same was tested using a t-test, taking spatial autocorrelation into account as described below. This hypothesis was tested for the whole world and for continental regions separately (see Section E.4 for region definitions). Although we used both Lomb periodograms and ordinary periodograms in this study, the two methods were used in different analyses and results were kept separate.

6.2.6 Correcting for spatial autocorrelation

The focus of this study is the analysis of temporal variations in climate and populations. Climate and population phenomena have a spatial structure, however, that needs to be accounted for to avoid inflation of Type I error rates (Legendre & Legendre, 1998; see Section E.5). The software package SAM (Spatial Analysis in Macroecology; Rangel *et al.*, 2006) was used to calculate effective numbers of degrees of freedom, with which the appropriate reference distributions could then be found for the t-tests mentioned above, and the corrected value of P computed for the correlations between climate and population spectral exponents. We followed the method of Dutilleul (1993a). This standard approach does not depend on any *a priori* assumption on the functional form of spatial autocorrelation, as might be the case when using, for example, generalised least squares methods (e.g. exponential, Gaussian, or spherical assumptions; see Dormann *et al.*, 2007).

6.2.7 Setup of models

We use a stochastic formulation of the Ricker model to help illustrate and explain background information and interpret empirical results. The model is $p_{t+1} = p_t \exp(r(1 - p_t/K) + x_t)$, where K is carrying capacity ($K = 1$ was used), r is growth rate, and x_t is the environmental noise modelled as an autoregressive order 1 (AR1) process. The spectral colour of x_t is determined by ρ, its lag-1 autocorrelation ($-1 < \rho < 1$, $\rho > 0$ for red noise, $\rho < 0$ for blue noise). The strength of environmental noise is σ, the standard deviation of the process.

We used a threshold autoregressive model of Grenfell *et al.* (1998) to help interpret results. The model is defined as $x_{t+1} = a_0 + b_0 x_t + \varepsilon_0$ for $x_t \leq C$ and $x_{t+1} = a_1 + \varepsilon_1$ for $x_t > C$, where x_t is log population density. The model is diagrammatically depicted in Grenfell *et al.* (1998). Here C is a carrying capacity above which winter weather, ε_1, may cause a substantial crash or a modest increase in very good years. Below C, growth is exponential, with noise that depends on summer weather, ε_0. Each noise time series ε_i is autoregressive order 1 with standard deviation σ_i ($\sigma_1 > \sigma_0$) and colour ρ_i, where ρ_i ranges from -0.9 (very blue noise) to 0.9 (very red noise). Parameter values a_i, b_0, and σ_i used were those given in Grenfell *et al.* (1998), except C was slightly changed from 7.01 to 7.23 to better illustrate the phenomenon of interest, although the original value produced qualitatively similar results.

6.3 Results

Mean summer and annual temperatures had spectral exponents significantly correlated with population spectral exponents (Table 6.1), even after accounting for spatial autocorrelation, confirming the hypothesis that redder populations live in redder climates. The correlation coefficients r for separate species groups were generally similar to overall r values and were always positive for mean summer and annual temperatures.

Table 6.1: Correlations between the spectral exponents of animal populations and the spectral exponents of mean temperature, for seasonal and annual averages. P is the P-value corrected for spatial autocorrelation. $N_{total} = 147$, N for *Aves* is 56, for *Crustacea* 12, for *Mammalia* 47, and for *Osteichthyes* 23. The P-values for the clade-specific regressions were not significant because of the reduced statistical power that comes from a reduced data set, although r values show that clade-specific patterns were consistent with overall trends.

	r	P	*Aves r*	*Crustacea r*	*Mammalia r*	*Osteichthyes r*
Winter	-0.055	0.659	-0.040	0.508	-0.230	0.062
Spring	0.060	0.590	0.226	0.538	-0.065	0.123
Summer	0.312	0.021	0.294	0.406	0.306	0.207
Autumn	-0.179	0.146	-0.179	-0.105	-0.160	-0.250
Annual	0.135	0.049	0.191	0.206	0.299	0.202

The change in spectral exponent from 1911–1950 to 1951–1990 was generally statistically significant for most climate variables and geographical regions: most spectral exponents became less red-shifted (see Figure 6.2 for mean summer temperatures, Figure 6.3 for other examples, and Section E.6 for all climate variables examined). There is a conspicuous exception to the trend: Asia was redder in 1951-1990 than it was in 1911-1950 for all climate variables except for mean autumn temperatures. The spectral exponents for all continents were still typically red, however, in both the first and second halves of the time series examined. Mean summer temperatures are of particular interest because their spectral exponents correlated most strongly with population spectral exponents. For mean summer temperatures, Asia and Australasia became redder, and other regions became conspicuously bluer (Figure 6.2).

Distributions of the spectral exponents of population and climate variables appeared symmetric and unimodal, and quantile-quantile plots indicated they were not markedly different from normal. These results help justify the use of t-tests and Pearson correlations.

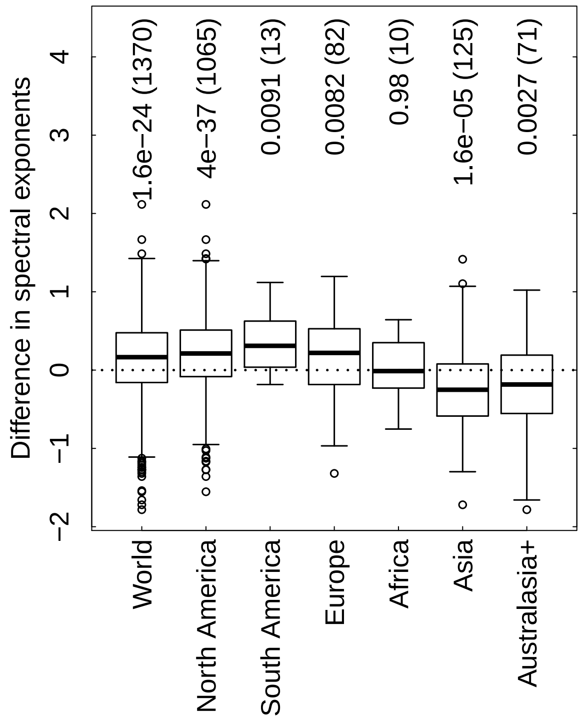

Figure 6.2: Change in the spectral exponents of mean summer temperature time series from 1911-1950 to 1951-1990. P values (t-test corrected for spatial autocorrelation, N in parentheses) are listed above each box-whisker plot. A positive (respectively negative) difference in spectral exponent denotes a bluer (respectively redder) spectrum during 1951-1990 compared to 1911-1950.

6.4 Discussion

Our results show that the spectral exponents of population time series correlated positively and significantly with the spectral exponents of the mean summer temperatures the populations experienced. The correlation is weak, but this is expected because we analysed a wide range of species, and each could be affected predominantly by different factors only partly related to those considered; a variety of measurement errors will also have weakened the correlation. The fact that a relationship can be detected at all in spite of these heterogeneities is a valuable result that merits analyses in future research using additional data sets.

We also found that mean seasonal and annual temperatures have become bluer over the past century on all continents, except Asia and, for some climate variables, Australasia and North America. This indicates that high frequencies are generally becoming increasingly important relative to low frequencies in the climate variables we examined.

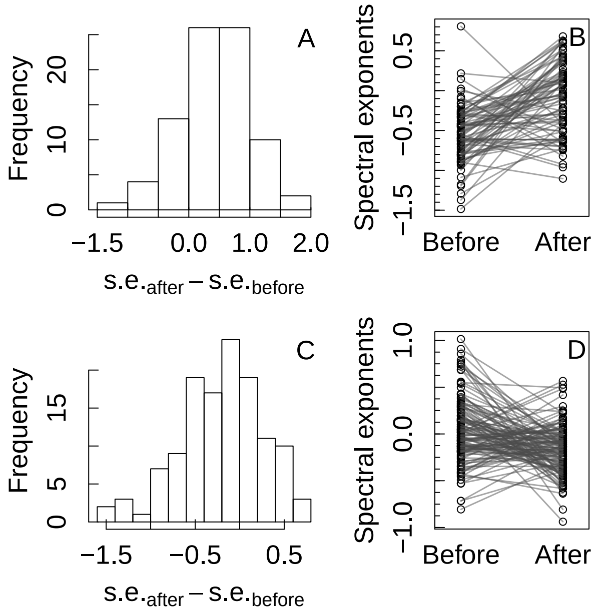

Figure 6.3: Other examples of changes in climate spectral exponents (s.e.). The change in the spectral exponents to 1951-1990 (‘after’) from 1911-1950 (‘before’) for annual mean temperature in Europe (A, B) and winter mean temperature in Asia (C, D) as histograms (A, C) and as paired values (B, D).

The combination of our two results suggests the possibility that population spectra are in the process of becoming bluer as a consequence of ongoing climate change. Although this conclusion is indirect because population time series are not abundant or long enough to directly examine how their spectral exponents are changing, it is important because it represents a broad possible impact of climate change on population dynamics.

6.4.1 Why summer?

Why does summer mean temperature correlate most significantly of the variables we examined? Many of the populations were at high latitudes, with severe winter weather, suggesting that spectral exponents of winter climatic variables should perhaps correlate more strongly with population spectral exponents than summer climate spectral exponents. We argue here that this expectation is flawed, and we present a possible hypothetical explanation for the importance of summer.

In populations for which bad winter weather causes crashes at high densities, interannual autocorrelation in winter weather is not transmitted to population autocorrelation because a crash caused by the first bad winter makes subsequent bad winters have little effect. In contrast, summer weather maps more directly onto successive years of population growth if it takes multiple years for a population to reach carrying capacity and summer weather affects population growth. This reasoning and the assumptions implicit in it are explained in more detail in Section E.7.

The hypothesis presented here is supported by a simple model of Grenfell *et al.* (1998) which quantitatively captures the mechanisms (see Methods for the model definition). Model output (Figure 6.4) indicates that the impact of summer noise colour on population spectral colour can indeed be substantially greater than the impact of winter noise colour when growth is slow and affected by summer weather and crashes are rapid and brought about by bad winter weather and high population density. The model thereby supports our explanation of empirical results.

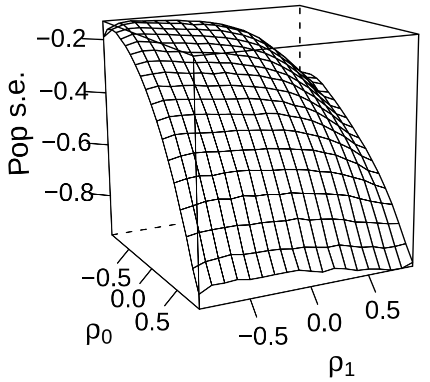

Figure 6.4: The effect of winter and summer environmental spectral colour on population spectral colour according to the model of Grenfell *et al.* (1998) (Methods), for which the repercussions of environmental autocorrelation in the two seasons on population spectral exponent can be separately analysed. Model population spectral colour was much more strongly affected by summer spectral colour (ρ_0) than by winter spectral colour (ρ_1). *s.e.* = spectral exponent.

6.4.2 Extinction risk

The impacts that climate and population spectral colours have on extinction risk are complex and have not been settled, as testified by the lack of consensus in the prior theoretical work summarised in the Introduction. Nevertheless, it is important to discuss the link between our results and the large extinction risk literature because extinction risk is one major reason for studying population and climate spectral colour. For this reason, we discuss the link within the context of a family of univariate population models for which the relationship between spectral colour and extinction risk is well understood. For the Ricker model (Figure 6.5) and other unstructured population models (Section E.8) it has been observed that for red-shifted, slow-growing populations, reddening of environmental noise increases extinction risk, whereas for blue-shifted, fast-growing populations, reddening of environmental noise decreases extinction risk (Cuddington & Yodzis, 1999; Heino *et al.*, 2000; Schwager *et al.*, 2006). In particular, for populations which are already red-shifted, becoming less red-shifted is associated with decreased extinction risk. Since most populations typically monitored by ecologists are red-shifted (Inchausti & Halley, 2002), and since we have shown that spectra of some environmental variables are getting bluer and this is correlated with bluer population spectra, our results suggest that the observed shifts may broadly contribute to decreased extinction risk. This conclusion is in the context of the univariate population models considered here; the same patterns may not hold for stage-structured, spatially structured models, or models with other elaborations. Also, numerous other factors contribute to extinction risk, including aspects of environmental signals such as their mean and variance, and direct human factors such as habitat destruction and population exploitation. Future research quantifying the relative contributions of these and other factors to total extinction risk under different scenarios of population dynamics would be useful.

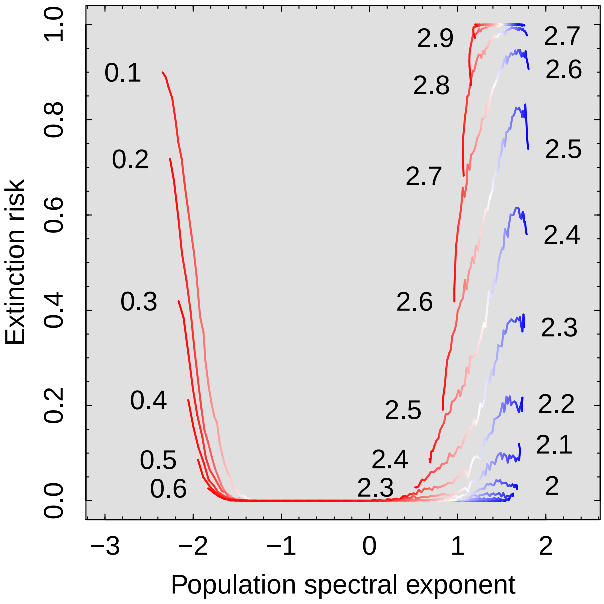

Figure 6.5: The relationship between noise and population spectral colour and extinction risk in the stochastic Ricker model of Figure 6.1 (Methods). The results suggest that for red-shifted, slow-growing populations, reddening of environmental noise increases extinction risk; in contrast, for blue-shifted, fast growing populations, the opposite is true. Each individual line is labelled by the fixed growth rate (r) value used for all points on the line; line colour corresponds to environmental noise colour (the value of ρ used; see Methods). For $0.7 < r < 1.9$, extinction risk was ≤ 0.0165 for all environmental noise colours, hence lines for these growth rate values are not visible in the plot. The results presented in this Figure are present in the literature in fragmented form (Cuddington & Yodzis, 1999; Heino *et al.*, 2000; Schwager *et al.*, 2006).

7 Conclusion

The aim of this thesis was to investigate how different statistical descriptions of currently ongoing climate change may affect the dynamics of populations and their risk of extinction, and how their effects compare.

In Chapter 3, we developed a simple population model explicitly linked to an environmental process, and used it to compare the sensitivity of the population long-term stochastic growth rate to changes in the mean and the variability of the environment. Results showed that changes in the variability of the environment can be more important for populations than changes in mean conditions. The main gradient along which the relative contributions of changes in environmental mean and variability vary was the population's distance from its ideal environment. Changes in mean conditions are likely to have a greater impact than changes in variability on populations far from their ideal environment, such as populations near species range boundaries and potentially of conservation concern. Pests and disease vectors living near range centres and close to their ideal environment are more likely to be affected by changes in variability. US weather station data was also analysed to compare the observed changes in mean and variability of biologically relevant environmental variables. The observed changes in means of all temperature variables were generally larger than the changes in standard deviations, although not markedly so. The observed changes in variability may benefit pests and disease vectors.

The population model of Chapter 3 was extended in Chapter 4 to provide an estimate of extinction risk and its sensitivity to changes in the mean and the variability of the environment. The conclusion was that even when considering extinction risk as the population fitness parameter, an increase in environmental variability can still have a greater impact on populations than an increase in mean conditions. Like in Chapter 3, the main gradient along which the relative contributions of changes in environmental mean and variability varied was the population's distance from its ideal environment. Changes in mean environment are more likely to affect populations characterised by slow life histories and larger body sizes, living close to their ideal environment, but yet risking extinction. A change in environmental variability, on the other hand, could have a greater impact on populations with a high maximum intrinsic growth rate but that live far from ideal conditions, and are more likely to be composed by populations of small body size and fast life histories.

In Chapter 5, we re-analysed some existing population models to obtain sensitivities of populations to changes in mean and variability of climate, and thereby provide more points against which to compare the model of Chapters 3 and 4. We found that the empirical studies re-analysed support the general conclusion that changes in variability affect the dynamics of populations, and can be as important as changes in mean environmental conditions. Changes in variability were found to have a more substantial impact on the variability of population dynamics. The only study that provided an environmental range across which to compare the relative effects of changes in mean and variability of the environment closely resembled results from Chapter 3.

In Chapter 6 we explored possible correlations between the spectral colour of environmental variables and the spectral colour of population dynamics of a taxonomically heterogeneous group of populations. We found that the spectral exponent of mean summer temperatures correlates positively and significantly with population spectral exponent. We also suggest a plausible hypothesis for the observed results, quantitatively supported by a simple exploratory model, that provides a mechanism that explains the correlation found. Using weather station data, changes in the spectral colour of temperature variables over the last century were also analysed. Over the last century the spectral colour of temperature climate variables on most continents has become bluer, suggesting that a broad possible impact of climate change on population dynamics may be under way.

7.1 Recommendations for future work

Possibilities for further work have been discussed in individual chapters, but the main recommendations are summarised here.

7.1.1 Extending the theoretical population model & simulations

The theoretical model of Chapters 3 and 4 could be extended to introduce more biological detail. As mentioned in Chapter 3, a possible development may be the introduction of age or stage structure. An age-structured model would make it possible to study the differing impacts of climate change on fecundity and survival rates, as well as effects that may only emerge when some age structure is present, such as, for example, changes in the autocorrelation structure of the environment. The introduction of age structure could conceivably affect the net impact of an environmental change on the population fitness, when compared to the univariate model of Chapters 3 and 4. The change in impact on a population after introducing age structure could also provide useful insight into how to further interpret the meta-analysis of Chapter 5, where univariate and age-structured models are compared. Haridas & Tuljapurkar (2005) could be used as a starting point to analyse an age-structured model, and in this case Tuljapurkar's (1982; 1990) approximation would be required to estimate $\ln \lambda_s$. If a general model proves too complicated to usefully analyse, an intermediate step may be a two by two matrix model with juveniles and adults.

Chapter 4 focussed on populations of conservation concern by using extinction risk as a proxy for population fitness. The diffusion approximation of Lande & Orzack (1988) provides an extinction estimate by calculating the probability that a population goes below a threshold. The approximation can be modified to investigate population booms, by estimating the probability that population size increases beyond a large threshold. This modified approximation would be useful to focus on the second type of population identified in Chapter 3: pests and disease vectors.

7.1.2 Further analyses of empirical data

Field studies & extending the meta-analysis of Chapter 5 Chapters 3 and 4 discussed the need for empirical data to validate the results obtained from the theoretical population model. There are currently few studies that explicitly compare the sensitivity of some population fitness parameter to changes in mean and variability of the environment. There are none that compare more than one population across an environmental gradient. We therefore strongly encourage field work that encompasses multiple populations with different levels of adaptation to their environment (thereby including struggling and successful populations). The meta-analysis of Chapter 5 provided some support for our theoretical model, although no clear pattern arose when comparing results across the different studies due to the differences in study systems and modelling approaches. The addition of a greater number of studies may help to draw conclusions from comparisons across the different studies. Studies driven by Markov chains could be added if the necessary information on how vital rates are affected by the environment were available. Depending on how the environment is modelled in each study, changes in autocorrelation of the environment could also be added to the comparison. For example, if the environment is modelled as an autoregressive process, it is possible to change the autocorrelation of the environment and measure its impact on a population.

Variability & power at low and high frequencies - The change in spectral exponent of an environmental time series provides no information on how the absolute variance at low and high frequencies has changed (Figure 7.1). Both changed variance and changed spectral exponent may affect population extinction probability. A complementary analysis could be undertaken where the total power (or variance) and how it changes is analysed. In addition to the total power, the total power at low and high frequencies could be analysed separately (in both environmental and population time series, and exploring the relationship between these). Considering all these results in concert would help illuminate the expected effects of changing environmental signals on population extinction probability in a multifaceted way that goes beyond prior work.

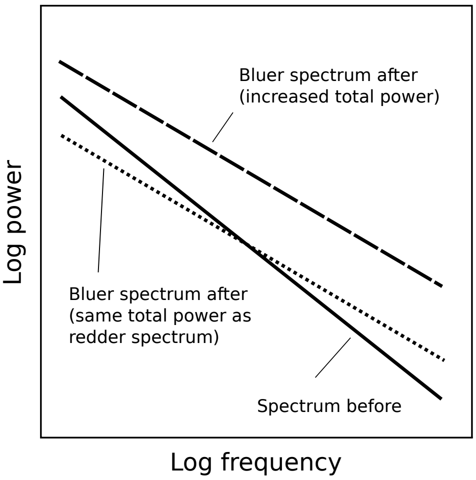

Figure 7.1: The change in spectral exponent gives no indication as to the change in total variance. The same spectral exponent can both mean that low frequency variance has been reduced and high frequency variance increased (keeping the total amount of variance constant) or that the high frequency explains more of the total variance (increasing total variance).

Spectral colour - The results of Chapter 6 merit further analyses in future research. It would be particularly useful to perform a similar analysis on a dataset of a taxonomically more constrained group to test the robustness of the correlation found using the GPDD. Such a database would likely be more homogeneous, and therefore eliminated a source of noise associated with using taxonomically diverse species. It would also enable us to test more biologically probing hypotheses. For example, were there a correlation to be found between the spectral colours of climate and populations,

- does the correlation depend on geographic location (e.g., is the correlation different for populations living at high latitudes compared to those living at low latitudes)?
- do different taxonomic groups respond differently to environmental fluctuations (e.g., *Passeriformes* versus non-passerines in birds)?

- does the correlation depend on life-history (for example migratory versus non-migratory populations) or phenotypic (e.g., body size) traits?

7.2 Concluding remarks

Changes in the variability of the environment were found to significantly affect population dynamics. The results presented in this thesis show that it is important to understand how different statistical descriptions of changes in the environment affect population dynamics and contribute to the observed impact of climate change on animal populations. The balance in the current research effort should be readdressed to incorporate further analysis on how changes in variability and autocorrelation of the environment contribute to changes in population fitness.

Appendices

Appendix A

Overview of methods

The main statistical tool we use in Chapter 6 is called the power spectrum. Its purpose is to reveal the frequencies of oscillations that predominate in a time series, and to provide information on their relative importance. The input for this kind of analysis is a time series, and the output is a plot that shows frequency on the horizontal axis and "power" on the vertical axis, where power indicates the amount of variation occurring in a time series at each frequency. For example, Figure A.1 shows a monthly average temperature time series from Montreal for the period 1950 to 2000, along with the respective power spectrum. The peak that dominates the power spectrum corresponds to the seasonal component of temperature fluctuations for Montreal. Figure A.2 provides a series of examples that further illustrate the information the power spectrum provides.

A large number of statistical methods have been developed to estimate the power spectra from time series data (Brillinger, 2001), but these will not be reviewed here. A suite of commonly used methods use a "periodogram" combined with various degrees of smoothing to estimate the power spectrum. Henceforth, the term "spectrum" will be used to denote a periodogram. The term "frequency domain analysis" refers to analysis of the periodic or oscillatory elements of a time series, by for example estimating and analysing the spectrum, whereas "time domain analysis" refers to the direct analysis of time series without estimating the spectrum.

Time series and their corresponding spectra are often described by colours; the terminology is intended to convey information about whether lower or higher frequencies predominate. 'Red' indicates that variation at lower frequencies is more powerful (Figure A.2 c, h), 'blue' noise is dominated by higher frequencies (Figure A.2 e, j) and 'white' noise or spectra are characterised by equal contributions of lower and higher frequencies (Figure A.2 d, i). The colour-based terminology was coined because red (respectively, blue) light is dominated by lower (respectively, higher) frequencies than other colours of visible light. The colour of a time series can be qualitatively appreciated from its spectrum, but there are also several methods that

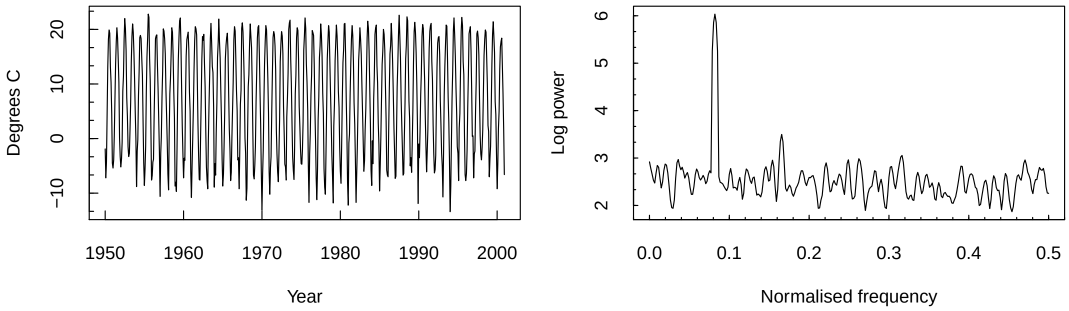

(a) Time series

(b) Power spectrum

Figure A.1: (a) Time series of mean monthly temperature between 1950 and 2000 for Montreal, Canada, and (b) its respective power spectrum. The peak in the power spectrum corresponds to the dominant seasonal component of temperature fluctuations characteristic of higher latitude locations such as Montreal.

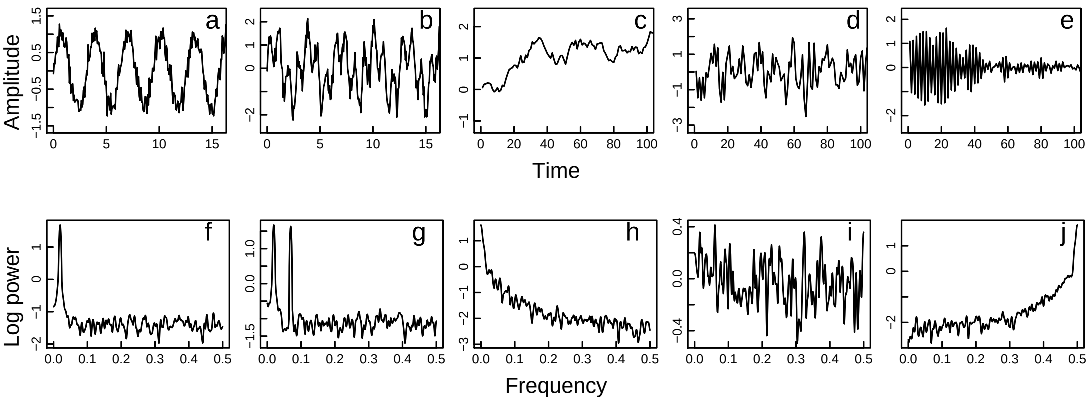

Figure A.2: Examples of time series (a-e) and their corresponding power spectra (f-j), illustrating the capacity of the power spectrum method to decompose variation in time series according to the frequencies at which the variation occurs. Panel (a) is a sine wave of frequency 2 rad/s with a small amount of added noise, hence the variation in (a) is mostly at frequency 2 rad/s. This is revealed by the peak in the power spectrum in (f) at frequency 2 rad/s. Panel (b) is the sum of two sine waves of frequencies 2 and 5 rad/s, again with a small amount of white noise, hence the variation in (b) is mostly at those frequencies. This is revealed by the peaks in the power spectrum in (g) at 2 and 5 rad/s. Panel (c) depicts highly autocorrelated noise, for which most variation occurs at low frequencies. This is revealed by the corresponding power spectrum in (h). Panel (d) has white noise, which has equal components of variation at all frequencies, as indicated by the flat spectrum in (j). Panel (e) has negatively autocorrelated noise, for which most variation occurs at high frequencies, as revealed in (j).

quantify this measure. The most common, the spectral exponent, refers to the slope of a linear regression line drawn through a log-log plot of the spectrum (e.g. Figure A.3). The slope indicates whether it is the lower or the higher frequencies that are relatively more important in the signal being analysed: negative slopes correspond to greater dominance of low-frequency variation (red noise), and positive slopes to greater dominance of high-frequency variation (blue noise). White noise has a spectral exponent close to 0. The spectral exponent helps indicate the relative contributions of lower and higher frequencies to the variance of a signal. However, the spectral exponent does not capture the detailed structure of the spectrum: the spectrum can be of different forms whilst having the same spectral exponent (see Figure A.4).

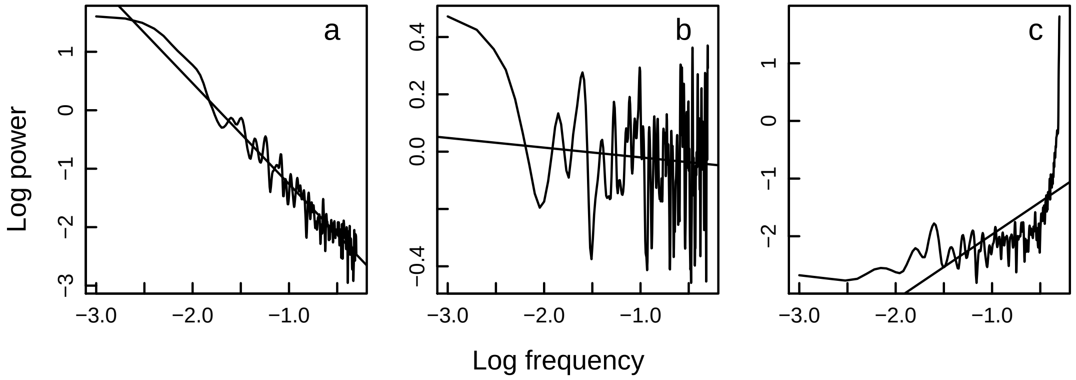

Figure A.3: The spectra are the log-log plots of those shown in Figure A.2 (h-j). The straight solid lines are their respective regression lines. (a) is highly autocorrelated noise, for which the regression line has a negative slope; (b) is white noise, hence its regression line has a slope close to zero; and (c) is negatively autocorrelated noise, for which the regression line has a positive slope.

A commonly cited form is the so-called $1/f^{\beta}$ family of noises. In this formulation, f refers to frequency, so $1/f^{\beta}$ noise is a specific form of the spectrum that is mathematically described by its name. When log transforming the equation power $= 1/f^{\beta}$, you get a linear relationship between log(power) and log(f) with slope β. In this family of noises, consequently, $-\beta$ corresponds to the spectral exponent (Mandelbrot, 1982; Halley, 1996).

Colours are often used to refer specifically to the value of β within the context of $1/f^{\beta}$ noise. Confusingly, however, the colour terminology used in the literature to describe spectra with this form follow conventions that are not completely consistent with the colour terminology above. In the context of $1/f^{\beta}$ noise, $\beta \sim 1$ is called “pink” noise, $\beta \sim 2$ is called “brown” (also termed ‘random walk’ or ‘Brownian motion’ noise), and $\beta \sim 3$ is called “black” noise. All these, by the prior terminology, would be different degrees of “red”. For clarity, we will only use the terms “pink”, “brown”, or “black” in

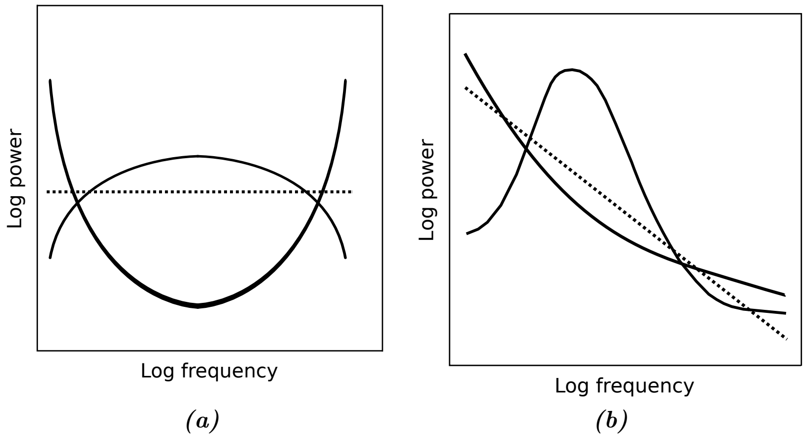

Figure A.4: Two diagrammatic examples of spectra, each with two spectra with different structure yielding the same spectral exponent (depicted by the slope of the regression line, shown as dotted lines). (a) Two example spectra drawn on log-log scales, both of which would have the same spectral exponent and would therefore be defined as being white; and (b) two example spectra, both of which would give a negative spectral exponent and would therefore be defined as being red.

reference to power spectra specifically of the $1/f^{\beta}$ form. The terms "red" and "blue" noise will be used in their qualitative sense as described previously, not corresponding to any specific value of the spectral exponent or to any particular functional form of the power spectrum.

Time series with spectra of the form $1/f^{\beta}$ with $\beta > 0$ are characterised by a variance that increases continuously as the length of a block of the time series used to measure the variance increases. There is another type of noise, called autoregressive (AR) noise, that on the other hand has a variance that increases initially for short lengths of time series, but then stabilises. AR noise is, in its simplest form, defined as $p_{t+1} = \varphi p_t + \varepsilon_t$, where ε_t is normally distributed with zero mean and standard deviation σ, and φ is a parameter with $|\varphi| < 1$. The variance for both brown ($\beta = 2$) and highly autocorrelated AR noise is shown in Figure A.5. The brown noise in this case was produced using $p_{t+1} = p_t + \varepsilon_t$. AR noise is often used in studies as it is easy to produce.

Spectral exponents, as mentioned above, are perhaps the most common and simplest way to describe the relative importance of different frequencies in a time series. There are alternatives too. White *et al.* (1996a), for instance, also used a periodogram, but rather than using the slope of a regression as an indication of the colour, they integrated the spectrum separately over lower and higher frequencies and used the ratio of total power at lower frequencies to total power at upper frequencies. Ripa

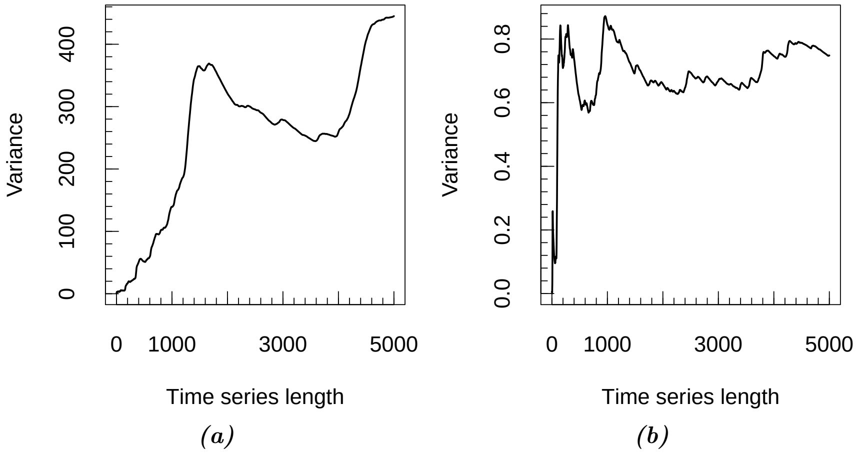

Figure A.5: Variance per time series length for (a) brown noise; and (b) AR noise. The variance for brown noise increases indefinitely with the length of the time series used to calculate it. On the other hand, the variance for AR noise quickly reaches a maximum.

& Lundberg (1996) and Petchey *et al.* (1997) used the autocorrelation function to characterise colour. The Hurst exponent is a statistic related to the spectral exponent (Clegg, 2006). There are several techniques that can be used to estimate it. One way is by computing the spectral exponent and converting it to the Hurst exponent H (H is related to the spectral exponent β (of the $1/f^{\beta}$ family) by the formula $\beta = 2H + 1$; Clegg, 2006). Another is to estimate the so-called rescaled range, a measure of how the apparent variability of a time series changes with the length of the time period considered (Ariño & Pimm, 1995). More specifically, it involves dividing the range by the standard deviation for time series chunks of increasing length. The logarithm of the rescaled range is then plotted against the logarithm of the number of data points, and the slope of the resulting line is H. Detrended fluctuation analysis (DFA; Koscielny-Bunde *et al.*, 1996, 1998; Blender & Fraedrich, 2003) is also similar to the aforementioned Hurst exponent, except that DFA can also be applied to non-stationary signals. The scaling exponent α is analogous to H, and is tied to the spectral exponent by $\beta = 2\alpha - 1$. Singular-spectrum analysis (SSA; Yiou *et al.*, 1996; Rodó *et al.*, 2002), is based on principle component analysis, and provides a decomposition of the signal into a trend, oscillatory components, and noise (Rodó *et al.*, 2002). Some studies have also used the maximum entropy method (e.g. Rodó *et al.*, 2002). This method consists of obtaining the power spectrum by determining the most random process (i.e. with fewest assumptions), with the same autocorrelation coefficients as the original signal (Yiou *et al.*, 1996). Wavelets have also been increasingly used for frequency domain analysis (Lau & Weng, 1995; Torrence & Compo, 1998; Datsenko *et al.*, 2004; Corbineau *et al.*, 2008). They are a statistically rigorous and generalised form of a windowed Fourier transform, i.e., estimating the spectrum of numerous subsets (or 'windows') of the signal and characterising how the spectrum changes with location of the window in the longer time series. Wavelets can indicate, given sufficient data, not only the frequency-decomposition of variance in a time series, but how this changes from the beginning of the signal to the end (Lau & Weng, 1995). Wavelet decompositions can detect transient or changing components of system dynamics. The quality of the wavelet decomposition depends on a frequency versus time resolution trade-off, and the method performs poorly with time series that are too short.

Appendix B

Are changes in the mean or variability of climate signals more important for long-term stochastic growth rate?

B.1 Transforming the environmental variable

Let $\tilde{w}_t$ be the original, untransformed environmental variable, assuming without loss of generality it is normally distributed (it can be transformed to make it so). Let

$$w_t = \alpha\,\tilde{w}_t + \beta$$

where $\alpha = 1/\mathrm{sd}(\tilde{w}_t)$ and $\beta = -\mathrm{E}(\tilde{w}_t)/\mathrm{sd}(\tilde{w}_t)$.

B.2 Derivation of $\ln \lambda_s$

Let $g(w_t) = p(w_t) - c$. Then,

$$\ln \lambda_s = \int_{-\infty}^{\infty} g(w_t)\,\varphi_{\mu,\sigma}(w_t)\,\mathrm{d}w_t + c \tag{B.1}$$

$$= a_1 \int_{-\infty}^{b} h(-w_t + b)\,\varphi_{\mu,\sigma}(w_t)\,\mathrm{d}w_t + a_2 \int_{b}^{\infty} h(w_t - b)\,\varphi_{\mu,\sigma}(w_t)\,\mathrm{d}w_t + c. \tag{B.2}$$

Therefore $\ln \lambda_s$ is a function of a_1, a_2, b, c, and α, i.e. the parameters that define the log response function.

B.3 Derivation of $\partial \ln \lambda_s / \partial \mu$

Take the partial derivative of $\ln \lambda_s$ with respect to μ:

$$\frac{\partial \ln \lambda_s}{\partial \mu} = \int_{-\infty}^{\infty} p(w_t)\, \frac{\partial}{\partial \mu}\, \varphi_{\mu,\sigma}(w_t)\, \mathrm{d}w_t, \tag{B.3}$$

$$\frac{\partial}{\partial \mu}\varphi_{\mu,\sigma}(w_t) = \frac{\partial}{\partial \mu}\left[\frac{1}{\sigma\,\sqrt{2\,\pi}}\, \exp\!\left(\frac{-(w_t-\mu)^2}{2\,\sigma^2}\right)\right] \tag{B.4}$$

$$= \left(\frac{w_t-\mu}{\sigma^2}\right)\varphi_{\mu,\sigma}(w_t). \tag{B.5}$$

So

$$\frac{\partial \ln \lambda_s}{\partial \mu} = \int_{-\infty}^{\infty} p(w_t)\left(\frac{w_t-\mu}{\sigma^2}\right)\varphi_{\mu,\sigma}(w_t)\, \mathrm{d}w_t, \tag{B.6}$$

and

$$\left.\frac{\partial \ln \lambda_s}{\partial \mu}\right|_{\substack{\mu=0\\ \sigma=1}} = \int_{-\infty}^{\infty} g(w_t)\, w_t\, \varphi_{0,1}(w_t)\, \mathrm{d}w_t + c \int_{-\infty}^{\infty} w_t\, \varphi_{0,1}(w_t)\, \mathrm{d}w_t. \tag{B.7}$$

We need two lemmas to proceed.

Lemma B.3.1

$$\int_0^{\infty} x^n\, e^{-\beta\, x^2}\, \mathrm{d}x = \frac{\Gamma(\gamma)}{2\,\beta^{\gamma}},$$

where $\Gamma(z)$ *is the Gamma function (Abramowitz & Stegun, 1964, pg. 255),* $\gamma = \frac{n+1}{2}$*,* $\mathrm{Re}\,\beta > 0$*, and* $\mathrm{Re}\, n > 0$*.*

Proof See Section 3.326 in pg. 337 of Gradshteyn & Ryzhik (2007). □

Lemma B.3.2

$$\int_{-\infty}^{\infty} x^n\, \varphi_{0,1}(x)\, \mathrm{d}x = \begin{cases} \dfrac{\Gamma\left(\frac{n+1}{2}\right) 2^{\frac{n}{2}}}{\sqrt{\pi}} & \textit{if } n \geq 0 \textit{ is an even integer} \\ 0 & \textit{if } n \geq 0 \textit{ is an odd integer.} \end{cases}$$

Proof

$$\int_{-\infty}^{\infty} x^n \, \varphi_{0,1}(x) \, \mathrm{d}x = \frac{1}{\sqrt{2\,\pi}} \int_{-\infty}^{\infty} x^n \, \exp\!\left(-\frac{x^2}{2}\right) \mathrm{d}x \tag{B.8}$$

$$= \begin{cases} \dfrac{2}{\sqrt{2\,\pi}} \displaystyle\int_{0}^{\infty} x^n \, \exp\!\left(-\frac{x^2}{2}\right) \mathrm{d}x & \text{if } n \text{ is even,} \\ 0 & \text{if } n \text{ is odd,} \end{cases} \tag{B.9}$$

$$= \begin{cases} \dfrac{2}{\sqrt{2\,\pi}} \, \dfrac{\Gamma\left(\frac{n+1}{2}\right)}{2\left(\frac{1}{2}\right)^{\frac{n+1}{2}}} & \text{if } n \text{ is even,} \\ 0 & \text{if } n \text{ is odd,} \end{cases} \tag{B.10}$$

$$= \begin{cases} \dfrac{\Gamma\left(\frac{n+1}{2}\right) 2^{\frac{n}{2}}}{\sqrt{\pi}} & \text{if } n \text{ is even,} \\ 0 & \text{if } n \text{ is odd.} \end{cases} \tag{B.11}$$

□

Given lemma B.3.2, the second term of equation (B.7) is equal to zero, so

$$\left.\frac{\partial \ln \lambda_s}{\partial \mu}\right|_{\substack{\mu=0\\ \sigma=1}} = a_2 \left[f_s \int_{-\infty}^{b} h(-w_t + b) \, w_t \, \varphi_{0,1}(w_t) \, \mathrm{d}w_t + \int_{b}^{\infty} h(w_t - b) \, w_t \, \varphi_{0,1}(w_t) \, \mathrm{d}w_t \right]. \tag{B.12}$$

The sensitivity of $\ln \lambda_s$ to changes in μ therefore depends on a_2, f_s, b, and α.

B.4 Derivation of $\partial \ln \lambda_s / \partial \sigma$

Take the partial derivative of $\ln \lambda_s$ with respect to σ:

$$\frac{\partial \ln \lambda_s}{\partial \sigma} = \int_{-\infty}^{\infty} p(w_t) \, \frac{\partial}{\partial \sigma} \, \varphi_{\mu,\sigma}(w_t) \, \mathrm{d}w_t, \tag{B.13}$$

$$\frac{\partial}{\partial\sigma}\varphi_{\mu,\sigma}(w_t) = \frac{\partial}{\partial\sigma}\left[\frac{1}{\sigma\sqrt{2\,\pi}}\,\exp\!\left(\frac{-(w_t-\mu)^2}{2\,\sigma^2}\right)\right] \tag{B.14}$$

$$= \frac{-1}{\sigma^2\sqrt{2\,\pi}}\,\exp\!\left(\frac{-(w_t-\mu)^2}{2\,\sigma^2}\right) + \frac{1}{\sigma\sqrt{2\,\pi}}\,\exp\!\left(\frac{-(w_t-\mu)^2}{2\,\sigma^2}\right)\left(\frac{(w_t-\mu)^2}{\sigma^3}\right) \tag{B.15}$$

$$= -\frac{1}{\sigma}\,\varphi_{\mu,\sigma}(w_t) + \frac{(w_t-\mu)^2}{\sigma^3}\,\varphi_{\mu,\sigma}(w_t). \tag{B.16}$$

Therefore

$$\frac{\partial\ln\lambda_s}{\partial\sigma} = \int_{-\infty}^{\infty} p(w_t)\left[-\frac{1}{\sigma}\,\varphi_{\mu,\sigma}(w_t) + \frac{(w_t-\mu)^2}{\sigma^3}\,\varphi_{\mu,\sigma}(w_t)\right]\mathrm{d}w_t, \tag{B.17}$$

and

$$\left.\frac{\partial\ln\lambda_s}{\partial\sigma}\right|_{\substack{\mu=0\\ \sigma=1}} = \int_{-\infty}^{\infty}(g(w_t)+c)\,(w_t^2-1)\,\varphi_{0,1}(w_t)\,\mathrm{d}w_t \tag{B.18}$$

$$= \int_{-\infty}^{\infty} g(w_t)\,(w_t^2-1)\,\varphi_{0,1}(w_t)\,\mathrm{d}w_t + c\int_{-\infty}^{\infty} w_t^2\,\varphi_{0,1}(w_t)\,\mathrm{d}w_t - c. \tag{B.19}$$

Given lemma (B.3.2),

$$\left.\frac{\partial\ln\lambda_s}{\partial\sigma}\right|_{\substack{\mu=0\\ \sigma=1}} = \int_{-\infty}^{\infty} g(w_t)\,(w_t^2-1)\,\varphi_{0,1}(w_t)\,\mathrm{d}w_t + c\,\frac{2\,\Gamma\left(\frac{3}{2}\right)}{\sqrt{\pi}} - c. \tag{B.20}$$

But $2\,\Gamma(3/2)/\sqrt{\pi} = 1$, so

$$\left.\frac{\partial\ln\lambda_s}{\partial\sigma}\right|_{\substack{\mu=0\\ \sigma=1}} = a_2\left[f_s\int_{-\infty}^{b} h(-w_t+b)\,(w_t^2-1)\,\varphi_{0,1}(w_t)\,\mathrm{d}w_t + \int_{b}^{\infty} h(w_t-b)\,(w_t^2-1)\,\varphi_{0,1}(w_t)\,\mathrm{d}w_t\right]. \tag{B.21}$$

Therefore, the sensitivity of $\ln\lambda_s$ to changes in σ depends on a_2, f_s, b, and α. Because the variance of the environment is the square of the standard deviation of the environment, sensitivities of $\ln\lambda_s$ to changes in the variance of the environment can be computed straightforwardly from the results above using the chain rule. We use sensitivities to changes in standard deviation because they have the same units as sensitivities to changes in the mean of the environment, and this is necessary for comparison of the sensitivities.

B.5 Analysis of climate data

The United States Historical Climatology Network database (USHCN; Menne *et al.*, 2009; National Climatic Data Center, National Oceanic and Atmospheric Administration, 2011) consists of monthly values of precipitation, and minimum, maximum and average temperature from 1221 weather stations from the conterminous United States. The data had been corrected to account for various historical changes in station location, instrumentation, and observing practice; and temperatures (but not precipitation) had been adjusted for time-of-observation bias (due to the 24-hour observation period beginning and ending at times other than local midnight at different stations; Vose *et al.*, 2003). Data had been tested for homogeneity by testing for changepoints using a 'pairwise' homogenisation algorithm, as described in Menne & Williams Jr (2009). Estimates for missing data had been calculated using a weighted average of values from highly correlated neighbouring values (Menne *et al.*, 2009), providing time series that are complete. All corrections had been performed by climate researchers prior to our use of the database and were described in the data documentation.

The weather data in the USHCN consist of monthly values. These data were preprocessed to derive several variables, all with a sampling frequency of one per year. We chose example aggregations that are likely to be biologically meaningful to populations living in temperate latitudes. *Mean summer temperatures* were obtained by taking the mean of the three mean monthly temperature values corresponding to summer (June-August). *Minimum winter temperature* is the minimum monthly temperature registered during the three winter months (December-February) and *maximum summer temperature* is the maximum monthly temperature during summer. Finally, *total spring precipitation* is the total precipitation during the three spring months (March-May).

B.6 Special case with $\alpha = 2$ and $a_1 = a_2 = a$

Let $h(w_t) = w_t^2$ and $a_1 = a_2 = a$. Then,

$$\ln\lambda_s = a\int_{-\infty}^{\infty}(w_t-b)^2\,\varphi_{0,1}(w_t)\,\mathrm{d}w_t + c \tag{B.22}$$

$$= a\int_{-\infty}^{\infty}w_t^2\,\varphi_{0,1}(w_t)\,\mathrm{d}w_t - 2\,a\,b\int_{-\infty}^{\infty}w_t\,\varphi_{0,1}(w_t)\,\mathrm{d}w_t + a\,b^2 + c. \tag{B.23}$$

By lemma B.3.2,

$$\ln\lambda_s = a\,\frac{2\Gamma\left(\frac{3}{2}\right)}{\sqrt{\pi}} + a\,b^2 + c \tag{B.24}$$

$$= a\,(b^2+1) + c. \tag{B.25}$$

Turning to the sensitivity with respect to μ,

$$\left.\frac{\partial\ln\lambda_s}{\partial\mu}\right|_{\substack{\mu=0\\ \sigma=1}} = a\int_{-\infty}^{\infty}(w_t-b)^2\,w_t\,\varphi_{0,1}(w_t)\,\mathrm{d}w_t \tag{B.26}$$

$$= a\int_{-\infty}^{\infty}w_t^3\,\varphi_{0,1}(w_t)\,\mathrm{d}w_t - 2\,a\,b\int_{-\infty}^{\infty}w_t^2\,\varphi_{0,1}(w_t)\,\mathrm{d}w_t$$

$$+ a\,b^2\int_{-\infty}^{\infty}w_t\,\varphi_{0,1}(w_t)\,\mathrm{d}w_t \tag{B.27}$$

$$= -2\,a\,b\,\frac{2\,\Gamma\left(\frac{3}{2}\right)}{\sqrt{\pi}} = -2\,a\,b. \tag{B.28}$$

The sensitivity of $\ln\lambda_s$ to changes in σ is

$$\left.\frac{\partial\ln\lambda_s}{\partial\sigma}\right|_{\substack{\mu=0\\ \sigma=1}} = a\int_{-\infty}^{\infty}(w_t-b)^2\,(w_t^2-1)\,\varphi_{0,1}(w_t)\,\mathrm{d}w_t \tag{B.29}$$

$$= a\int_{-\infty}^{\infty}\left(w_t^4 - 2\,b\,w_t^3 - w_t^2 + b^2\,w_t^2 + 2\,b\,w_t - b^2\right)\varphi_{0,1}(w_t)\,\mathrm{d}w_t. \tag{B.30}$$

But by lemma B.3.2,

$$\left.\frac{\partial \ln \lambda_s}{\partial \sigma}\right|_{\substack{\mu=0\\ \sigma=1}} = a \int_{-\infty}^{\infty} \left(w_t^4 + (b^2-1)\, w_t^2\right) \varphi_{0,1}(w_t)\,\mathrm{d}w_t - a\, b^2 \tag{B.31}$$

$$= a \int_{-\infty}^{\infty} w_t^4\, \varphi_{0,1}(w_t)\,\mathrm{d}w_t + a\,(b^2-1) \int_{-\infty}^{\infty} w_t^2\, \varphi_{0,1}(w_t)\,\mathrm{d}w_t - a\, b^2 \tag{B.32}$$

$$= a\,\frac{4\,\Gamma\left(\frac{5}{2}\right)}{\sqrt{\pi}} + a\,(b^2-1) - a\,b^2 = 2\,a. \tag{B.33}$$

The ratio of sensitivities is

$$\frac{\left.\dfrac{\partial \ln \lambda_s}{\partial \mu}\right|_{\substack{\mu=0\\ \sigma=1}}}{\left.\dfrac{\partial \ln \lambda_s}{\partial \sigma}\right|_{\substack{\mu=0\\ \sigma=1}}} = \frac{-2\,a\,b}{2\,a} = -b. \tag{B.34}$$

B.7 Additional climate data analysis results

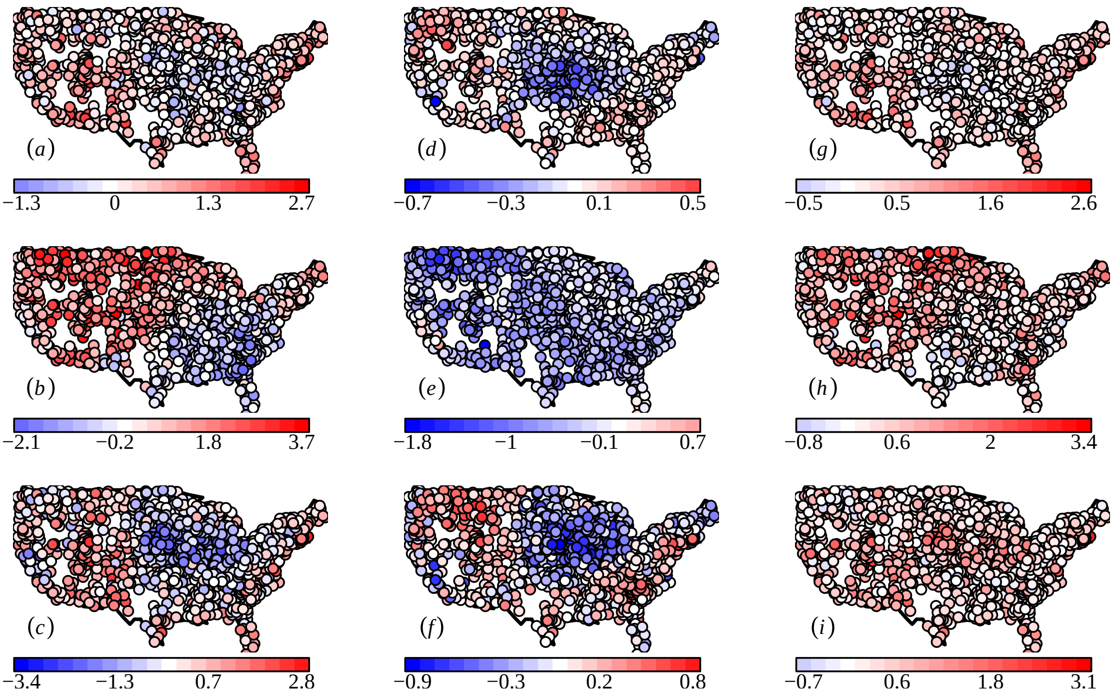

Figure B.1: Mean (a-c) and standard deviation (d-f) values for 1976-2010 minus values for 1911-1945, and absolute values of changes in mean minus absolute values of changes in standard deviation (g-i), for summer mean temperature (a, d, g), winter minimum temperature (b, e, h), summer maximum temperature (c, f, i). White corresponds to no change.

B.8 Semelparous populations

Our results apply not only to unstructured populations, but also to semelparous populations. Consider a semelparous population with k age classes with a transition matrix

$$\mathbf{\Lambda}_t = \begin{bmatrix} 0 & \cdots & g(t) \\ s_1(t) & \cdots & 0 \\ \cdots & s_{k-1}(t) & 0 \end{bmatrix},$$

where the $s(t)$ are the survival rates for each age class and $g(t)$ is the fertility rate for the final, reproductive age class. The product of k matrices like the one above yields a diagonal matrix model equivalent to our model (Tuljapurkar, 1990).

Appendix C

Are changes in the mean or variability of climate signals more important for extinction risk?

C.1 Derivation of σ_r^2

The log variance is

$$\sigma_r^2 = \mathrm{Var}(\ln\lambda_t) = \mathrm{E}\big[p(w_t)^2\big] - [\mathrm{E}(p(w_t))]^2 \tag{C.1}$$

$$= \int_{-\infty}^{\infty} p(w_t)^2\,\varphi_{\mu,\sigma}(w_t)\,\mathrm{d}w_t - (\ln\lambda_s)^2. \tag{C.2}$$

Let $g(w_t) = p(w_t) - c$. Then,

$$\sigma_r^2 = \int_{-\infty}^{\infty} (g(w_t)+c)^2\,\varphi_{\mu,\sigma}(w_t)\,\mathrm{d}w_t - (\ln\lambda_s)^2 \tag{C.3}$$

$$= \int_{-\infty}^{\infty} g(w_t)^2\,\varphi_{\mu,\sigma}(w_t)\,\mathrm{d}w_t + 2\,c\int_{-\infty}^{\infty} g(w_t)\,\varphi_{\mu,\sigma}(w_t)\,\mathrm{d}w_t + c^2 - (\ln\lambda_s)^2 \tag{C.4}$$

$$\begin{aligned}= a_1^2\int_{-\infty}^{b} h(-w_t+b)^2\,\varphi_{\mu,\sigma}(w_t)\,\mathrm{d}w_t + a_2^2\int_{b}^{\infty} h(w_t-b)^2\,\varphi_{\mu,\sigma}(w_t)\,\mathrm{d}w_t \\ + 2\,c\,a_1\int_{-\infty}^{b} h(-w_t+b)\,\varphi_{\mu,\sigma}(w_t)\,\mathrm{d}w_t + 2\,c\,a_2\int_{b}^{\infty} h(w_t-b)\,\varphi_{\mu,\sigma}(w_t)\,\mathrm{d}w_t \\ + c^2 - (\ln\lambda_s)^2\end{aligned} \tag{C.5}$$

$$= a_1^2 \int_{-\infty}^{b} h(-w_t + b)^2 \, \varphi_{\mu,\sigma}(w_t) \, \mathrm{d}w_t + a_2^2 \int_{b}^{\infty} h(w_t - b)^2 \, \varphi_{\mu,\sigma}(w_t) \, \mathrm{d}w_t$$

$$- (\ln \lambda_s - c)^2. \tag{C.6}$$

Therefore σ_r^2 is a function of a_1, a_2, b, and α, i.e. the parameters that define the log response function, but is independent of c.

C.2 Transforming the environmental variable

Let $\tilde{w}_t$ be the original, untransformed environmental variable, assuming without loss of generality it is normally distributed (it can be transformed to make it so). Let

$$w_t = \alpha \, \tilde{w}_t + \beta$$

where $\alpha = 1/\mathrm{sd}(\tilde{w}_t)$ and $\beta = -\mathrm{E}(\tilde{w}_t)/\mathrm{sd}(\tilde{w}_t)$.

C.3 Derivation of $\partial\sigma_r^2/\partial\mu$

Take the partial derivative of σ_r^2 with respect to μ:

$$\frac{\partial \sigma_r^2}{\partial \mu} = \int_{-\infty}^{\infty} p(w_t)^2 \, \frac{\partial}{\partial \mu} \, \varphi_{\mu,\sigma}(w_t) \, \mathrm{d}w_t$$

$$- \left(2 \int_{-\infty}^{\infty} p(w_t) \, \varphi_{\mu,\sigma}(w_t) \, \mathrm{d}w_t \right) \left(\int_{-\infty}^{\infty} p(w_t) \, \frac{\partial}{\partial \mu} \, \varphi_{\mu,\sigma}(w_t) \mathrm{d}w_t \right), \tag{C.7}$$

$$\frac{\partial}{\partial \mu} \varphi_{\mu,\sigma}(w_t) = \frac{\partial}{\partial \mu} \left[\frac{1}{\sigma \sqrt{2\,\pi}} \, \exp\!\left(\frac{-(w_t - \mu)^2}{2\,\sigma^2} \right) \right] = \left(\frac{w_t - \mu}{\sigma^2} \right) \varphi_{\mu,\sigma}(w_t). \tag{C.8}$$

So

$$\frac{\partial \sigma_r^2}{\partial \mu} = \frac{1}{\sigma^2} \int_{-\infty}^{\infty} p(w_t)^2 \, (w_t - \mu) \, \varphi_{\mu,\sigma}(w_t) \, \mathrm{d}w_t$$

$$- 2 \left(\int_{-\infty}^{\infty} p(w_t) \, \varphi_{\mu,\sigma}(w_t) \, \mathrm{d}w_t \right) \left(\frac{1}{\sigma^2} \int_{-\infty}^{\infty} p(w_t) \, (w_t - \mu) \, \varphi_{\mu,\sigma}(w_t) \mathrm{d}w_t \right), \tag{C.9}$$

and

$$\left.\frac{\partial \sigma_r^2}{\partial \mu}\right|_{\substack{\mu=0\\ \sigma=1}} = \int_{-\infty}^{\infty} (g(w_t)+c)^2\, w_t\, \varphi_{0,1}(w_t)\, \mathrm{d}w_t - 2\, \ln \lambda_s \left(\left.\frac{\partial \ln \lambda_s}{\partial \mu}\right|_{\substack{\mu=0\\ \sigma=1}} \right) \tag{C.10}$$

$$\begin{aligned} &= \int_{-\infty}^{\infty} g(w_t)^2\, w_t\, \varphi_{0,1}(w_t)\, \mathrm{d}w_t + 2\, c \int_{-\infty}^{\infty} g(w_t)\, w_t\, \varphi_{0,1}(w_t)\, \mathrm{d}w_t \\ &\quad + c^2 \int_{-\infty}^{\infty} w_t\, \varphi_{0,1}(w_t)\, \mathrm{d}w_t - 2\, \ln \lambda_s \left(\left.\frac{\partial \ln \lambda_s}{\partial \mu}\right|_{\substack{\mu=0\\ \sigma=1}} \right). \end{aligned} \tag{C.11}$$

We need two lemmas to proceed.

Lemma C.3.1

$$\int_0^{\infty} x^n\, e^{-\beta\, x^2}\, \mathrm{d}x = \frac{\Gamma(\gamma)}{2\, \beta^{\gamma}},$$

where $\Gamma(z)$ *is the Gamma function (Abramowitz & Stegun, 1964, pg. 255),* $\gamma = \frac{n+1}{2}$, $\operatorname{Re}\beta > 0$, *and* $\operatorname{Re} n > 0$.

Proof See Gradshteyn & Ryzhik (2007; 3.326, pg. 337). ☐

Lemma C.3.2

$$\int_{-\infty}^{\infty} x^n\, \varphi_{0,1}(x)\, \mathrm{d}x = \begin{cases} \dfrac{\Gamma\left(\frac{n+1}{2}\right) 2^{\frac{n}{2}}}{\sqrt{\pi}} & \textit{if } n \ge 0 \textit{ is an even integer} \\ 0 & \textit{if } n \ge 0 \textit{ is an odd integer.} \end{cases}$$

Proof

$$\int_{-\infty}^{\infty} x^n\, \varphi_{0,1}(x)\, \mathrm{d}x = \frac{1}{\sqrt{2\,\pi}} \int_{-\infty}^{\infty} x^n\, \exp\!\left(-\frac{x^2}{2}\right) \mathrm{d}x \tag{C.12}$$

$$= \begin{cases} \dfrac{2}{\sqrt{2\,\pi}} \displaystyle\int_0^{\infty} x^n\, \exp\!\left(-\frac{x^2}{2}\right) \mathrm{d}x & \text{if } n \text{ is even,} \\ 0 & \text{if } n \text{ is odd,} \end{cases} \tag{C.13}$$

$$= \begin{cases} \dfrac{2}{\sqrt{2\,\pi}}\, \dfrac{\Gamma\left(\frac{n+1}{2}\right)}{2\left(\frac{1}{2}\right)^{\frac{n+1}{2}}} & \text{if } n \text{ is even,} \\ 0 & \text{if } n \text{ is odd,} \end{cases} \tag{C.14}$$

$$= \begin{cases} \dfrac{\Gamma\left(\frac{n+1}{2}\right) 2^{\frac{n}{2}}}{\sqrt{\pi}} & \text{if } n \text{ is even,} \\ 0 & \text{if } n \text{ is odd.} \end{cases} \tag{C.15}$$

□

Given lemma C.3.2,

$$\begin{aligned} \left.\frac{\partial \sigma_r^2}{\partial \mu}\right|_{\substack{\mu=0\\ \sigma=1}} &= a_1^2 \int_{-\infty}^{b} h(-w_t+b)^2\, w_t\, \varphi_{0,1}(w_t)\, \mathrm{d}w_t + a_2^2 \int_{b}^{\infty} h(w_t-b)^2\, w_t\, \varphi_{0,1}(w_t)\, \mathrm{d}w_t \\ &\quad + 2\, c\, a_1 \int_{-\infty}^{b} h(-w_t+b)\, w_t\, \varphi_{0,1}(w_t)\, \mathrm{d}w_t \\ &\quad + 2\, c\, a_2 \int_{b}^{\infty} h(w_t-b)\, w_t\, \varphi_{0,1}(w_t)\, \mathrm{d}w_t - 2\, \ln\lambda_s \left(\left.\frac{\partial \ln \lambda_s}{\partial \mu}\right|_{\substack{\mu=0\\ \sigma=1}} \right) \end{aligned} \tag{C.16}$$

$$\begin{aligned} &= a_1^2 \int_{-\infty}^{b} h(-w_t+b)^2\, w_t\, \varphi_{0,1}(w_t)\, \mathrm{d}w_t \\ &\quad + a_2^2 \int_{b}^{\infty} h(w_t-b)^2\, w_t\, \varphi_{0,1}(w_t)\, \mathrm{d}w_t - 2 \left(\left.\frac{\partial \ln \lambda_s}{\partial \mu}\right|_{\substack{\mu=0\\ \sigma=1}} \right) (\ln\lambda_s - c). \end{aligned} \tag{C.17}$$

The sensitivity of σ_r^2 to changes in μ therefore depends on a_2, f_s, b, and α, but is independent of c.

C.4 Derivation of $\partial\sigma_r^2/\partial\sigma$

Take the partial derivative of σ_r^2 with respect to σ:

$$\begin{aligned} \frac{\partial \sigma_r^2}{\partial \sigma} &= \int_{-\infty}^{\infty} p(w_t)^2\, \frac{\partial}{\partial \sigma}\, \varphi_{\mu,\sigma}(w_t)\, \mathrm{d}w_t \\ &\quad - \left(2 \int_{-\infty}^{\infty} p(w_t)\, \varphi_{\mu,\sigma}(w_t)\, \mathrm{d}w_t \right) \left(\int_{-\infty}^{\infty} p(w_t)\, \frac{\partial}{\partial \sigma}\, \varphi_{\mu,\sigma}(w_t) \mathrm{d}w_t \right), \end{aligned} \tag{C.18}$$

$$\frac{\partial}{\partial \sigma}\varphi_{\mu,\sigma}(w_t) = \frac{\partial}{\partial \sigma}\left[\frac{1}{\sigma\sqrt{2\pi}}\,\exp\!\left(\frac{-(w_t-\mu)^2}{2\,\sigma^2}\right)\right] \tag{C.19}$$

$$= \frac{-1}{\sigma^2\sqrt{2\pi}}\,\exp\!\left(\frac{-(w_t-\mu)^2}{2\,\sigma^2}\right) + \frac{1}{\sigma\sqrt{2\pi}}\,\exp\!\left(\frac{-(w_t-\mu)^2}{2\,\sigma^2}\right)\left(\frac{(w_t-\mu)^2}{\sigma^3}\right) \tag{C.20}$$

$$= -\frac{1}{\sigma}\,\varphi_{\mu,\sigma}(w_t) + \frac{(w_t-\mu)^2}{\sigma^3}\,\varphi_{\mu,\sigma}(w_t). \tag{C.21}$$

Therefore

$$\left.\frac{\partial \sigma_r^2}{\partial \sigma}\right|_{\substack{\mu=0\\ \sigma=1}} = \int_{-\infty}^{\infty} p(w_t)^2\,(w_t^2-1)\,\varphi_{0,1}(w_t)\,\mathrm{d}w_t - 2\left(\int_{-\infty}^{\infty} p(w_t)\,\varphi_{0,1}(w_t)\,\mathrm{d}w_t\right)\left(\int_{-\infty}^{\infty} p(w_t)\,(w_t^2-1)\,\varphi_{0,1}(w_t)\,\mathrm{d}w_t\right) \tag{C.22}$$

$$= \int_{-\infty}^{\infty} p(w_t)^2\,(w_t^2-1)\,\varphi_{0,1}(w_t)\,\mathrm{d}w_t - 2\ln\lambda_s\left(\left.\frac{\partial \ln\lambda_s}{\partial \sigma}\right|_{\substack{\mu=0\\ \sigma=1}}\right) \tag{C.23}$$

$$= \int_{-\infty}^{\infty} g(w_t)^2\,(w_t^2-1)\,\varphi_{0,1}(w_t)\,\mathrm{d}w_t + 2\,c\int_{-\infty}^{\infty} g(w_t)\,(w_t^2-1)\,\varphi_{0,1}(w_t)\,\mathrm{d}w_t + c^2\int_{-\infty}^{\infty}(w_t^2-1)\,\varphi_{0,1}(w_t)\,\mathrm{d}w_t - 2\ln\lambda_s\left(\left.\frac{\partial \ln\lambda_s}{\partial \sigma}\right|_{\substack{\mu=0\\ \sigma=1}}\right). \tag{C.24}$$

Given lemma (C.3.2),

$$\left.\frac{\partial \sigma_r^2}{\partial \sigma}\right|_{\substack{\mu=0\\ \sigma=1}} = a_1^2\int_{-\infty}^{b} h(-w_t+b)^2\,(w_t^2-1)\,\varphi_{0,1}(w_t)\,\mathrm{d}w_t + a_2^2\int_{-b}^{\infty} h(w_t-b)^2\,(w_t^2-1)\,\varphi_{0,1}(w_t)\,\mathrm{d}w_t - 2\left(\left.\frac{\partial \ln\lambda_s}{\partial \sigma}\right|_{\substack{\mu=0\\ \sigma=1}}\right)(\ln\lambda_s - c). \tag{C.25}$$

Therefore, the sensitivity of σ_r^2 to changes in σ depends on a_2, f_s, b, and α, but is independent of c. Because the variance of the environment is the square of the standard deviation of the environment, sensitivities of σ_r^2 to changes in the variance of the environment can be computed straightforwardly from the results above using the chain rule. We use sensitivities to changes in standard deviation because they have the same units as sensitivities to changes in the mean of the environment, and this is necessary for comparison of the sensitivities.

C.5 Sensitivity of G to changes in $\ln \lambda_s$ and σ_r^2

The sensitivities of G are

$$\left.\frac{\partial G(t|x_0)}{\partial \ln \lambda_s}\right|_{\substack{\mu=0\\ \sigma=1}} = \frac{-2\,x_0}{\sigma_r^2}\,\exp\!\left(-\frac{2\,\ln\lambda_s\,x_0}{\sigma_r^2}\right)\Phi\left[\frac{-x_0+\ln\lambda_s\,t}{\sqrt{\sigma_r^2\,t}}\right], \tag{C.26}$$

and

$$\left.\frac{\partial G(t|x_0)}{\partial \sigma_r^2}\right|_{\substack{\mu=0\\ \sigma=1}} = \frac{x_0}{\sqrt{2\,\pi\,t}\,\sigma_r^3}\,\exp\!\left(-\frac{(x_0+\ln\lambda_s\,t)^2}{2\,\sigma_r^2\,t}\right)$$

$$+\frac{2\,\ln\lambda_s\,x_0}{\sigma_r^4}\,\exp\!\left(-\frac{2\,\ln\lambda_s\,x_0}{\sigma_r^2}\right)\Phi\left[\frac{-x_0+\ln\lambda_s\,t}{\sqrt{\sigma_r^2\,t}}\right]. \tag{C.27}$$

As noted by Dennis *et al.* (1991), the calculation of $G(t|x_0)$ (and its sensitivities) can lead to numerical underflow and overflow. Specific values of $\ln\lambda_s$, σ^2, x_0, and t, can lead to the product of a very large number $\exp(\cdot)$ and a very small number $\Phi[\cdot]$. To avoid this problem, the values of $G(t|x_0)$ and its sensitivities were computed on the logarithmic scale.

C.6 Additional results for $\partial G/\partial\mu$ and $\partial G/\partial\sigma$

In the following figures, the panels correspond to (a) $\partial G/\partial\mu$, (b) $\partial G/\partial\sigma$, (c) the sign of the sensitivity shown in panel (a), (d) the relative importance of the sensitivity to changes in μ, i.e. $|\partial G/\partial\mu|/(|\partial G/\partial\mu| + |\partial G/\partial\sigma|)$, (e) the sign of the sensitivity shown in panel (b). The red contour lines are $G(t = 5) = 0.9$, and blue contour lines are for $G(t = 10) = 0.1, 0.9$. The green areas correspond to populations with $G(t = 100) \leq 0.1$ that are therefore relatively safe from extinction.

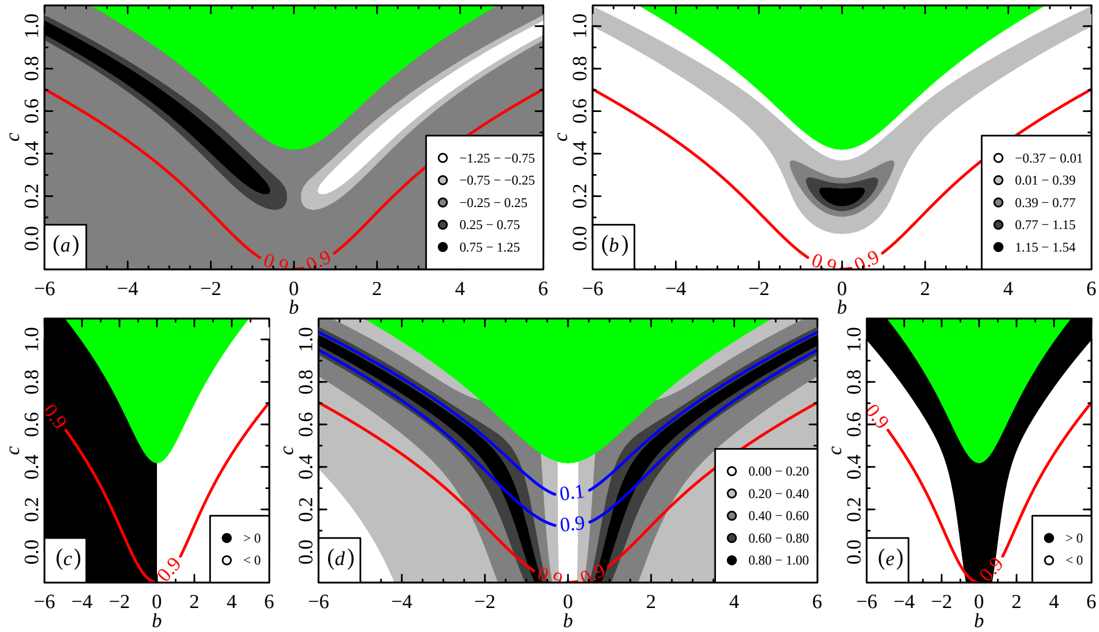

Figure C.1: $\alpha = 0.5$, $f_s = 1$, $a_2 = -0.5$, $t = 10$.

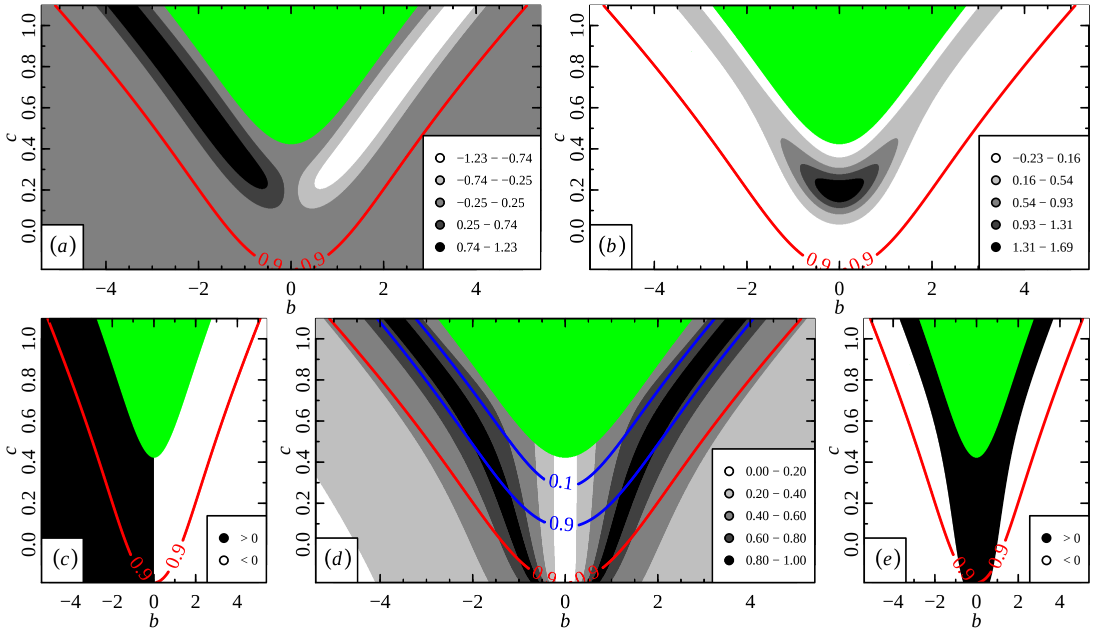

Figure C.2: $\alpha = 0.75,\ f_s = 1,\ a_2 = -0.5,\ t = 10.$

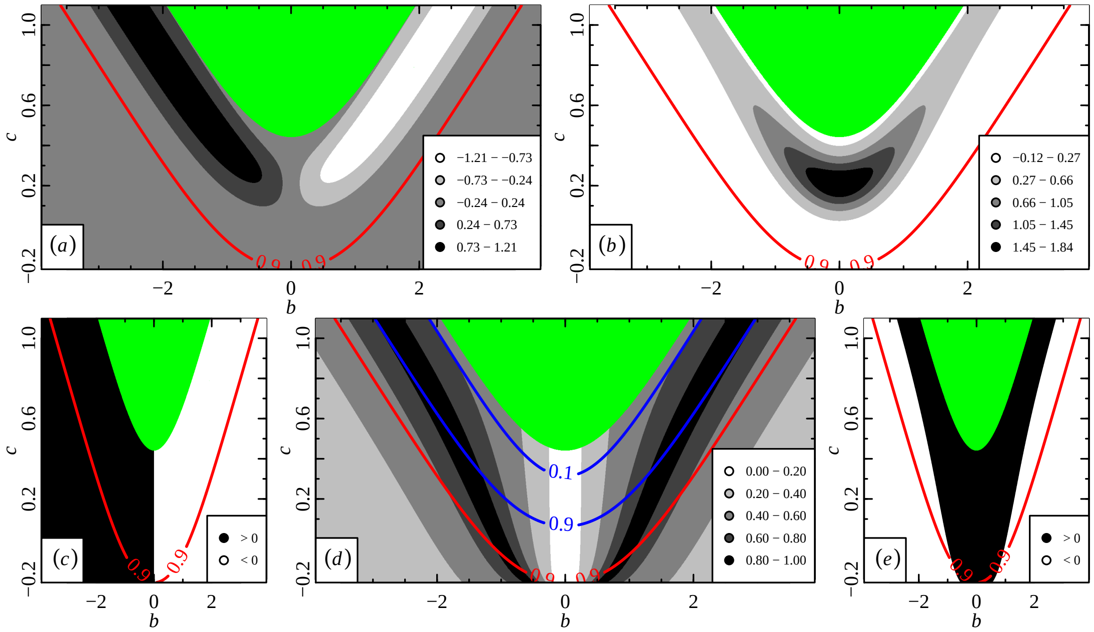

Figure C.3: $\alpha = 1,\ f_s = 1,\ a_2 = -0.5,\ t = 10.$

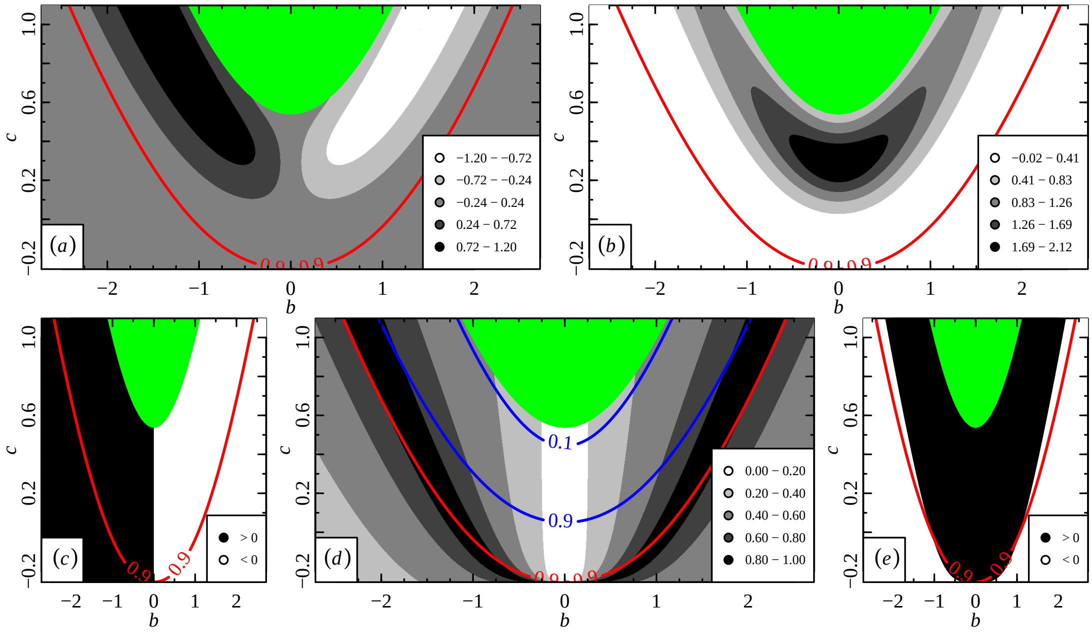

Figure C.4: $\alpha = 1.5,\ f_s = 1,\ a_2 = -0.5,\ t = 10.$

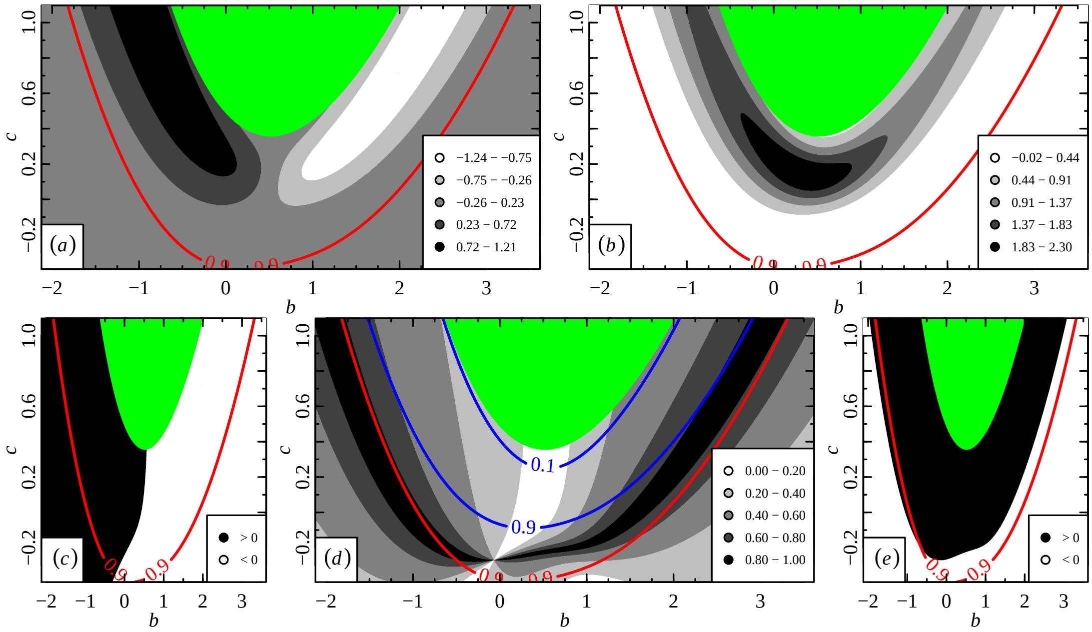

Figure C.5: $\alpha = 2,\ f_s = 1/3,\ a_2 = -0.5,\ t = 10.$

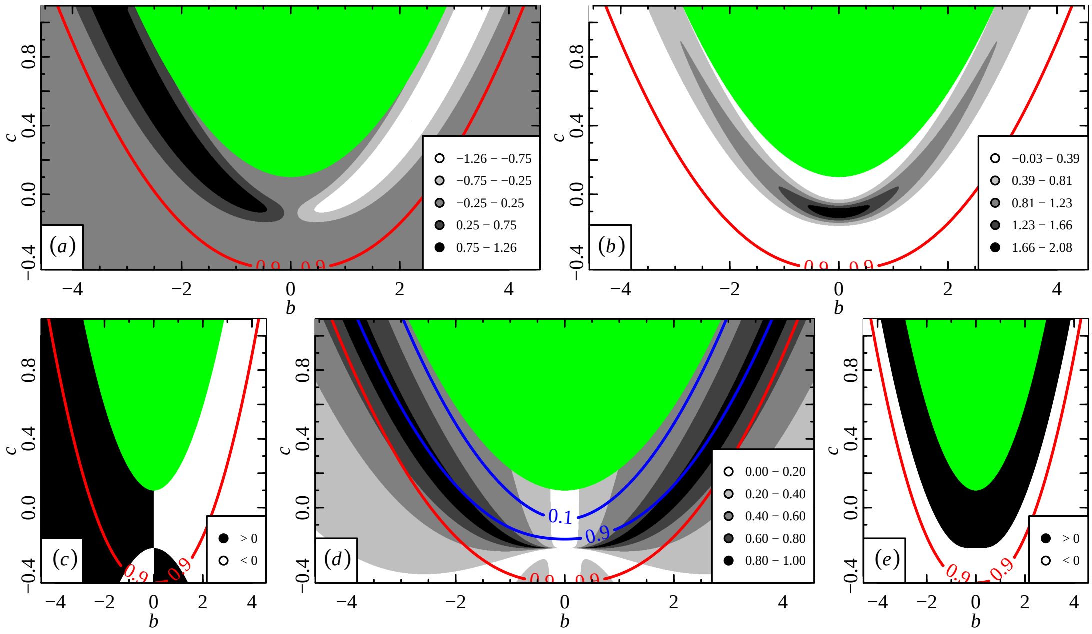

Figure C.6: $\alpha = 2,\ f_s = 1,\ a_2 = -0.1,\ t = 10.$

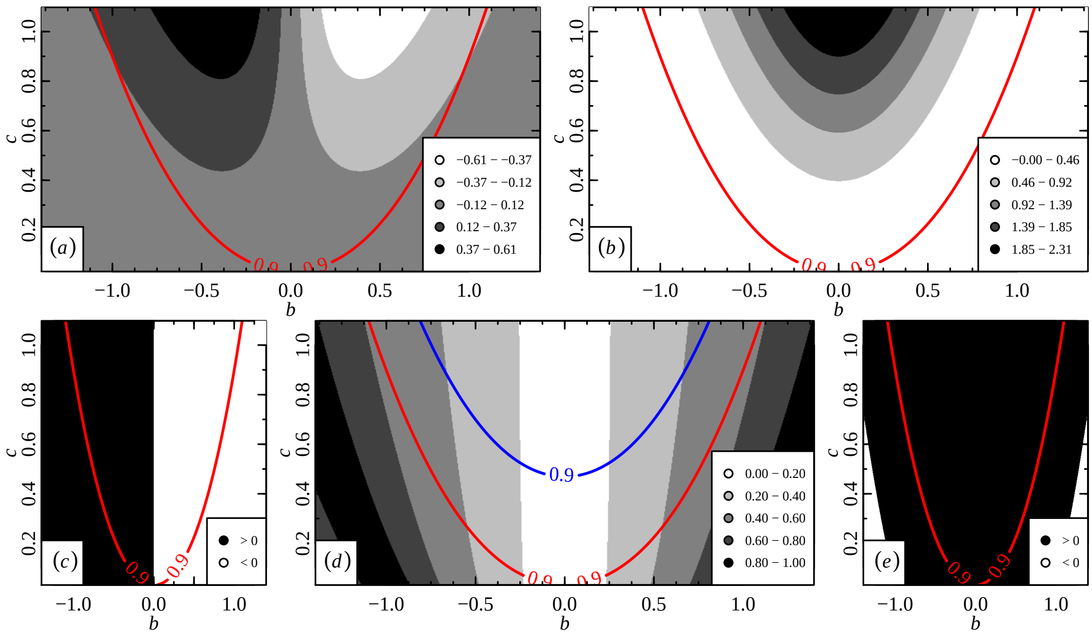

Figure C.7: $\alpha = 2,\ f_s = 1,\ a_2 = -1,\ t = 10.$

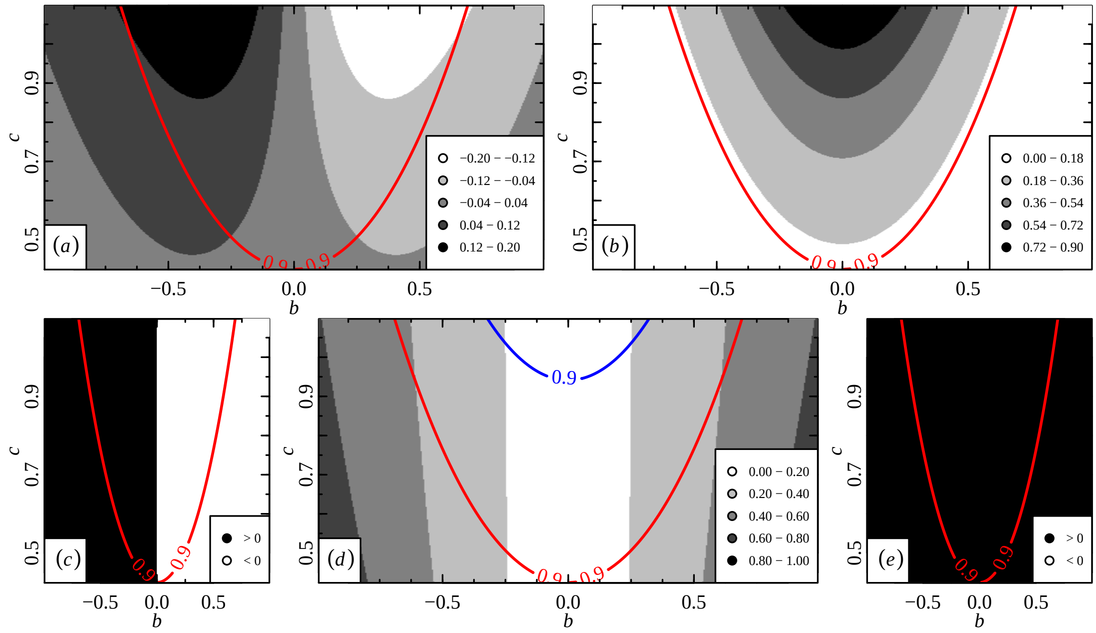

Figure C.8: $\alpha = 2,\ f_s = 1,\ a_2 = -1.5,\ t = 10.$

C.7 Additional results for $\partial G/\partial \ln \lambda_s$ and $\partial G/\partial \sigma_r^2$

In the following figures, the panels correspond to (a) $\partial G/\partial \ln \lambda_s$, (b) $\partial G/\partial \sigma_r^2$, (c) the sign of the sensitivity shown in panel (a), (d) the relative importance of the sensitivity to changes in $\ln \lambda_s$, i.e. $|\partial G/\partial \ln \lambda_s|/(|\partial G/\partial \ln \lambda_s| + |\partial G/\partial \sigma_r^2|)$, (e) the sign of the sensitivity shown in panel (b). The red contour lines are $G(t = 5) = 0.9$, and blue contour lines are for $G(t = 10) = 0.1, 0.9$. The green areas correspond to populations with $G(t = 100) \leq 0.1$ that are therefore relatively safe from extinction.

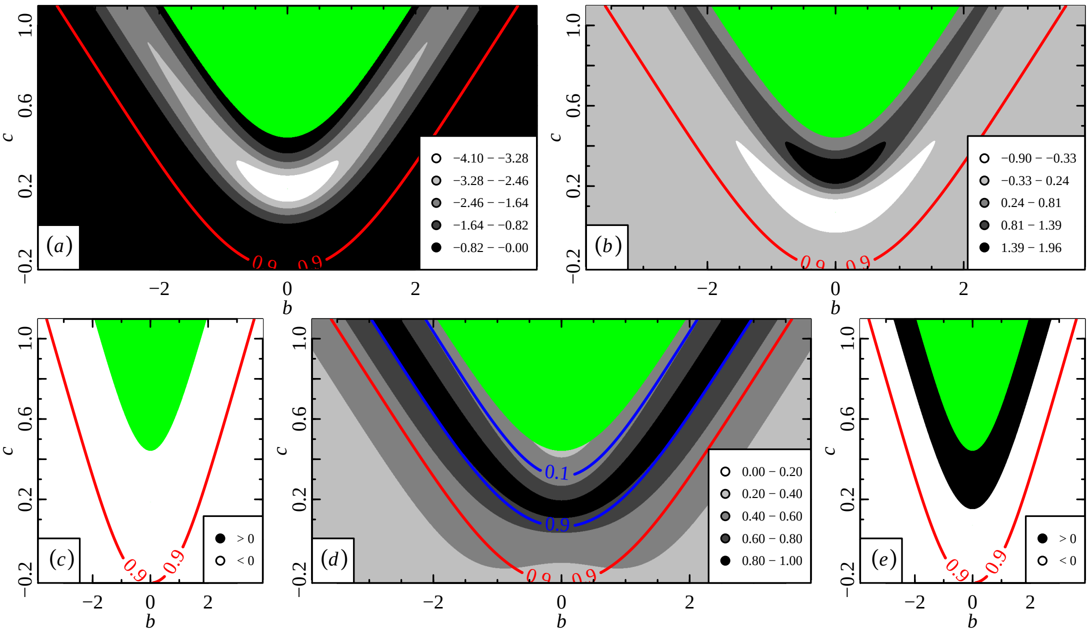

Figure C.9: $\alpha = 1$, $f_s = 1$, $a_2 = -0.5$, $t = 10$.

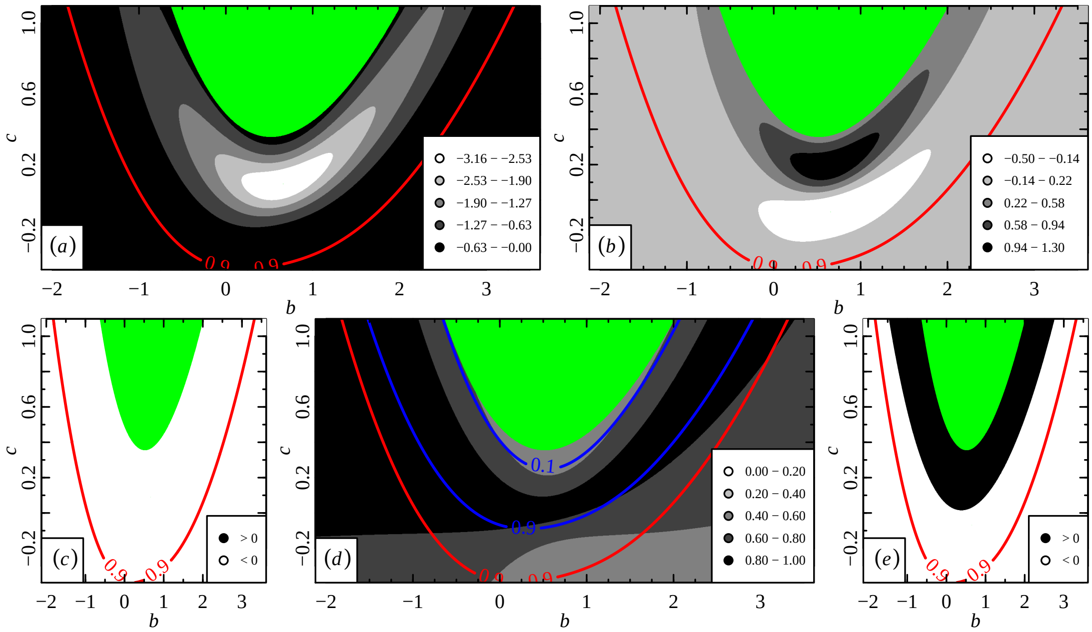

Figure C.10: $\alpha = 2$, $f_s = 1/3$, $a_2 = -0.5$, $t = 10$.

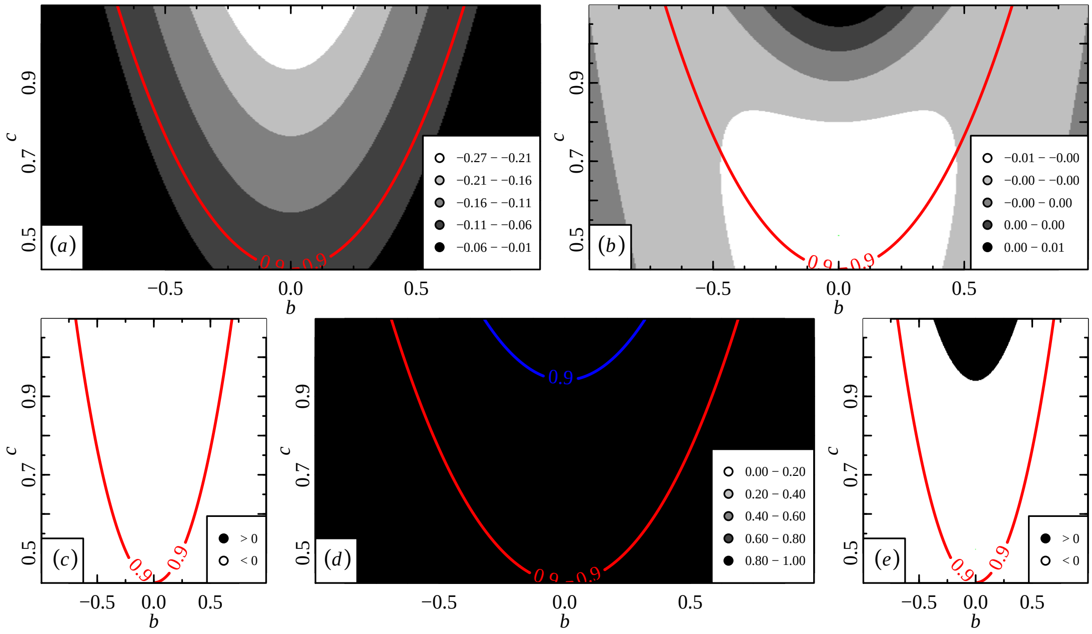

Figure C.11: $\alpha = 2$, $f_s = 1$, $a_2 = -1.5$, $t = 10$.

Appendix D

Are changes in the mean or variability of climate more important for populations?

D.1 Tables of parameters

Table D.1: Posterior mean values and standard deviations reported in Sæther *et al.* (2000), except for the values for a and σ^2_λ, which were provided by Jarle Tufto (personal communication).

Parameter	***Estimate***	$\pm$ ***sd***
r	-0.0860	0.186
α	0.0042	0.0014
β	0.15	0.03
σ^2_e	0.21	0.06
σ^2_d	0.268	0.018
μ_0	3.8979	0.101
μ_1	0.1100	
σ^2_c	4.0701	0.97
σ^2_λ	0.1882	0.84
a	0.0042	0.0015

Table D.2: Parameter estimates for the effects of density, the NAO, and their interaction from statistical models of survival, fecundity, and lamb neonatal survival rates for individual Soay sheep in different demographic classes. All models are linear on the logit scale. Population density was transformed prior to model fitting such that population density = (actual population density − 1202.86)/100. The NAO was transformed such that NAO = (actual NAO − 1.73)/10. The average litter sizes of breeding females aged 1 to 10 years were, respectively 1, 1.06, 1.11, 1.17, 1.23, 1.26, 1.27, 1.25, 1.2 and 1.14 lambs. No individuals $>$ 10 years old produced twins. The table is reproduced from Coulson *et al.* (2008).

Class & parameter	***Intercept***	***Density***	***NAO***	***Interaction***
Survival				
Female lambs	0.5403	-0.3078	-1.6086	-0.6602
Female yearlings	2.2797	-0.1924	-2.4922	-0.5816
Female 2–6 years	2.7725	-0.1702	-1.975	-0.5041
Female $>$ 6 years	1.6199	-0.2409	-1.2312	-1.316
Male lambs	-0.2068	-0.3053	-3.5837	-0.4202
Male 1–6 years	3.4038	-0.5066	-14.7928	1.6893
Male $>$ 6 years	-0.4812	0	0	0
Fecundity				
Female lambs	-0.915	-0.376	-2.069	0
Female yearlings	0.815	-0.1017	-2.085	0
Female 2–6 years	1.3869	-0.0797	0	0
Female 7–9 years	1.106	-1.09	-2.052	-0.812
Female $>$ 9 years	-1.099	0	0	0
Neonatal survival				
Lambs	-0.654	-0.3436	-2.313	0
Yearlings	1.293	-0.2318	-3.55	0
2–9 years	2.084	-0.0614	-1.433	-0.562
$>$ 9 years	0.887	0	0	0

Appendix E

An empirical link between the spectral colour of climate and the spectral colour of field populations in the context of climate change

E.1 Effect of environmental noise on two univariate population models

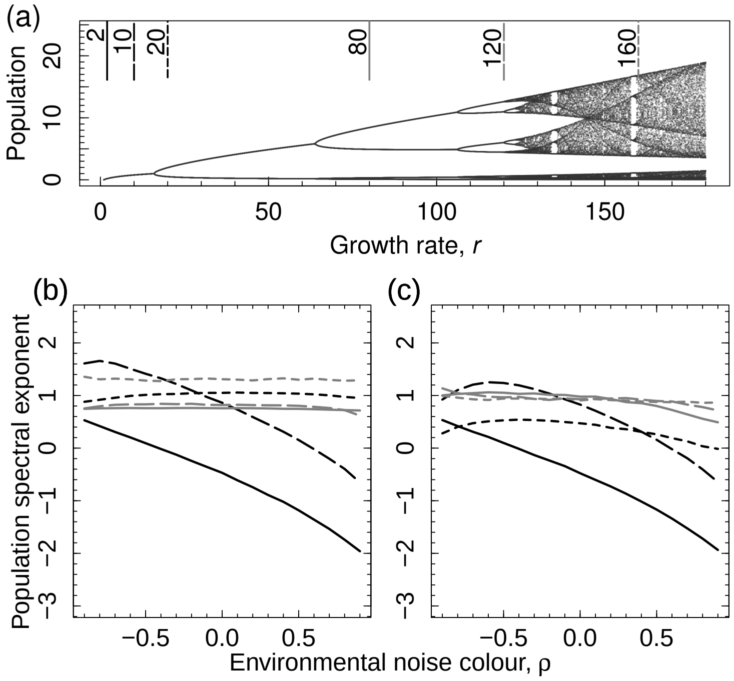

Figure E.1: The impact of environmental spectral colour on population spectral colour in a stochastic formulation of the Hassell model (Hassell, 1975). The model is $p_{t+1} = rp_t(1 + p_t)^{-b}\exp(x_t)$. Here b describes competition for resources, ranging from 'scramble' ($b \to \infty$) to 'contest' ($b \to 1$). In this example $b = 4$. The growth rate is r, and x_t is the same as in Figure 1 in the main text. A starting population $p_0 = 1$ was used for all simulations. Panel a is the bifurcation plot for the deterministic skeleton of the model, indicating the growth rate (r) values and respective line types used for the following panels. Panel b is with weak environmental noise ($\sigma = 0.01$; see Methods in the main text), and panel c is with strong environmental noise ($\sigma = 0.1$). Results show that environmental spectral colour generally tinges the population spectral colour, to an extent that depends on r and σ.

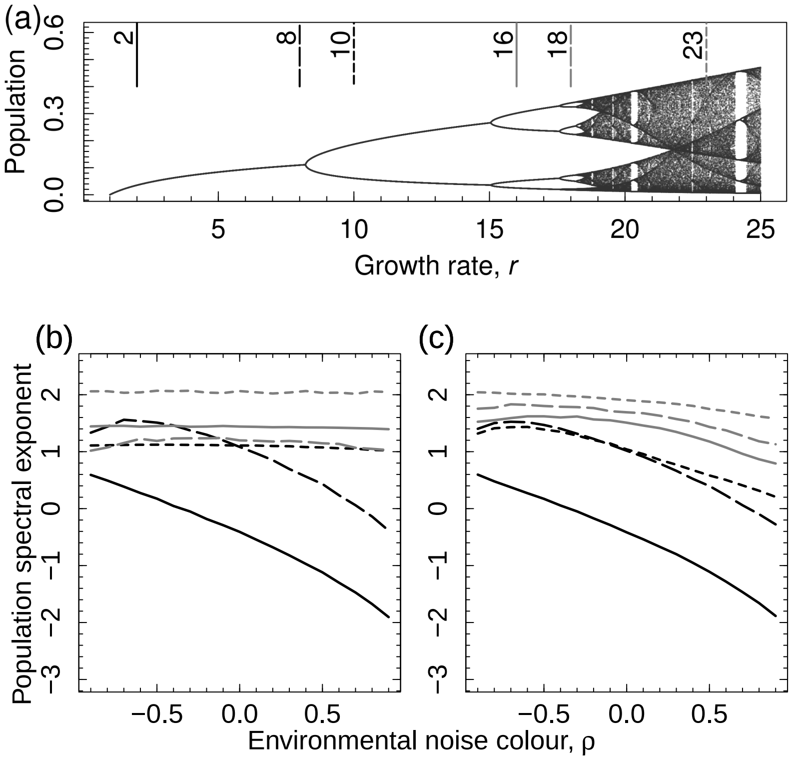

Figure E.2: See caption for Fig. E.1, but with $b = 20$.

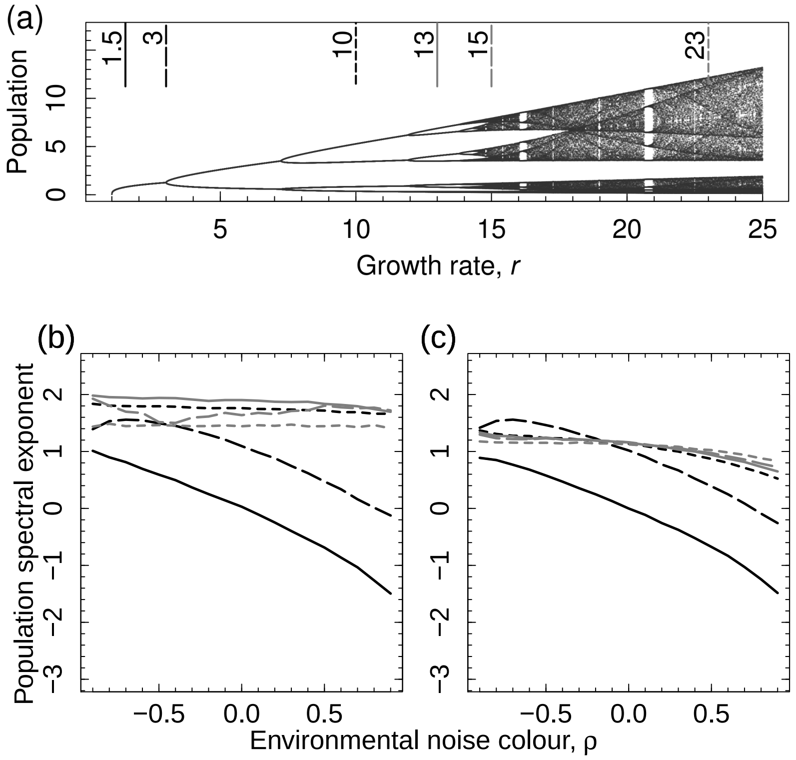

Figure E.3: The impact of environmental spectral colour on population spectral colour in a stochastic formulation of the Maynard Smith model (May & Oster, 1976). The model is $p_{t+1} = rp_t/(1 + p_t^b)\exp(x_t)$. Here b describes the type and intensity of density dependence. In this example $b = 3$. The growth rate is r, and x_t is as in Figure 1 in the main text. A starting population $p_0 = 1$ was used for all simulations. Panel a is the bifurcation plot for the deterministic skeleton of the model, indicating the growth rate (r) values and respective line types used for the following panel. Panel b is with weak environmental noise ($\sigma = 0.01$; see Methods in the main text), and panel c is with strong environmental noise ($\sigma = 0.1$). Results show that environmental spectral colour generally tinges the population spectral colour, to an extent that depends on r and σ.

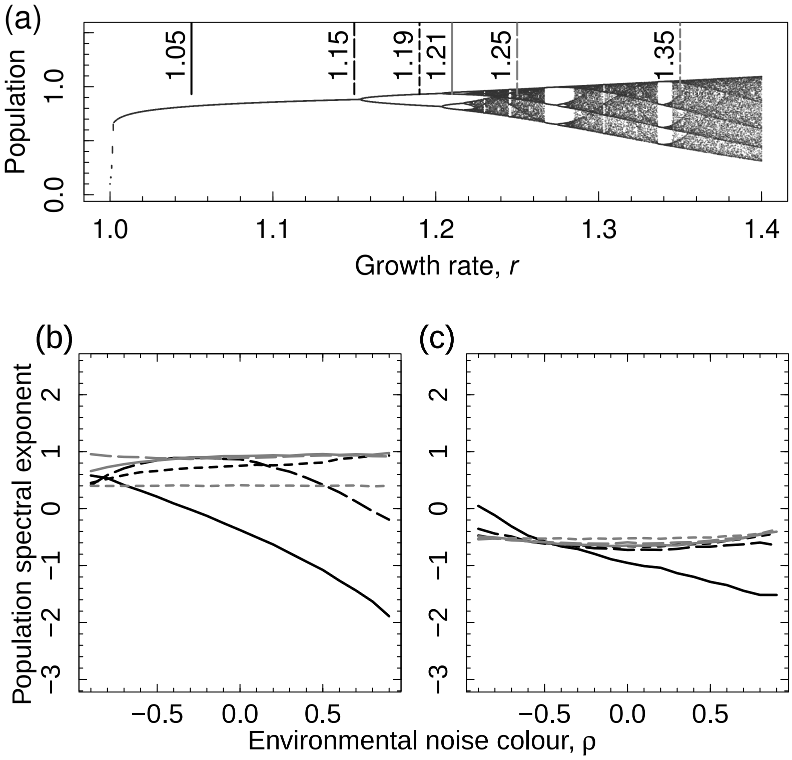

Figure E.4: See caption for Figure E.3, but with $b = 15$.

E.2 Validation of the CRU data set with GHCN data

Mitchell & Jones (2005) and New *et al.* (2000) explain the quality control and homogenisation process passed by the raw data that underlies the CRU data set. The CRU gridded data was optimised for homogeneity in space rather than time; the main objective was to provide spatially complete grids (Mitchell, 2004). We therefore have examined how reliable the database really is for our analyses, which have a temporal as well as a spatial component. In areas with high concentrations of weather stations contributing to the interpolation scheme, the CRU data is likely to follow the raw weather station data quite closely, and is likely to be reliable for our purposes. The spatio-temporal station density index is provided with the CRU data.

We calculated correlations between GHCN time series and corresponding time series from the CRU data set (same location and time span), and related the correlations to the number of weather stations contributing in the CRU data to that location at that time, as computed by the mean CRU density index in the location over the time. Results show that correlation is generally high (Figure E.5). We assumed, based on these results, that grid cells and time periods with more than 50 weather stations on average contributing to the time series were reliable for our intended use: nearly all locations with CRU mean density index above 50 were correlated with weather station data with $R > 0.9$ (Figure E.5).

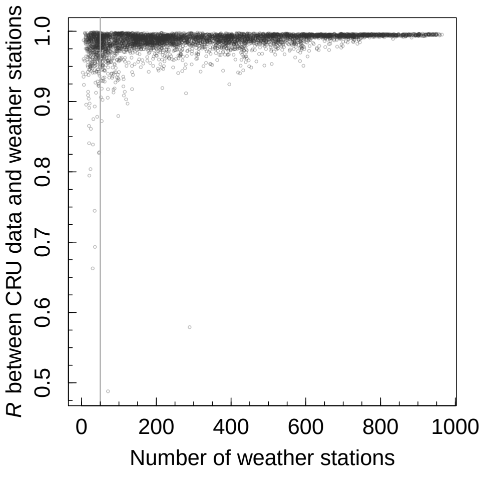

Figure E.5: Value of R, the Pearson correlation coefficient, between weather station and gridded data, plotted against the mean number of weather stations contributing to the interpolation for the relevant grid cell. The horizontal grey line, drawn at 50 contributing weather stations, indicates the quality index used in the filtering of the GPDD (Section E.3).

E.3 GPDD filtering process and filtered list of species

The GPDD authors included as many population dynamics studies as were available, leading to some heterogeneities that need to be accounted for by filtering prior to our analysis (Brook *et al.*, 2006):

- Study lengths vary from months to over a century.
- Sampling frequencies include the range from daily to annual; the sampling interval of some time series is listed as one generation of the focal species, with no specification of generation time.
- Many time series include zero abundance measures; without further information these may reflect local extinction, emigration, or inadequate sampling methods or effort.
- Many abundance measures are transformations of population size, including logarithms and power relationships.
- Sampling methodologies are diverse, sometimes subjective, and difficult to classify.
- Geographical location metadata are occasionally missing. Furthermore, some location data apply to centroids of large study areas, such as countries or states, and other time series have location data that refer to the single location of census. The specificity of the location data is not given.

These shortcomings were first addressed by automatically removing populations that did not satisfy the following conditions:

- A sampling frequency of one year.
- Entries for both latitude and longitude were present and non-zero. Though 0°N, 0°W is a valid location on the globe, it is in the ocean. Time series that are georeferenced with this location were likely to be in error.
- Time series had at least 30 continuous data points (with none missing).
- Time series had a proportion of zeroes to data points of maximum 0.2.
- The study took place in a location that is above the minimum required CRU "quality index", i.e. CRU station density index of 50 or higher (Section E.2).

The GPDD was then further filtered manually by:

- Checking the locations of populations on maps and comparing with centroids of political regions, to remove populations that appeared to have been given centroid or approximate coordinates.
- Fully marine species of the *Osteichthyes* class (censused in coastal regions) were removed. *Osteichthyes* were retained only if they inhabit freshwater during some

life stage.

- The largest contributing references to the filtered database were checked from the original source. Data from Novak *et al.* (1987) were removed because the authors stated that "...the data cannot simply be taken to indicate ... population levels ...". Reasons included inaccurate or imprecise location metadata and a large variety of assumptions on potential correspondence between population density and animals trapped.
- Three populations were removed because despite the fact that logarithmic units were indicated in the database, the numbers provided were still large (> 100), corresponding to impossibly large linear-scale populations that must have been in error.
- Some time series were found to have a constant population value throughout. Since we analyse population fluctuations, these were not useful and were removed.

E.3.1 List of filtered GPDD populations

Following is a list of the details of the filtered time series used in the analysis of the GPDD.

Table E.1: The GPDD populations left after completing the filtering process. The species name is that provided by the GPDD database.

Species	***Class***	***Lat.***	***Long.***	***Time period***
Alauda arvensis	Aves	51	-5	1946-1979
Anas platyrhynchos	Aves	50	-98	1955-2002
Anas platyrhynchos	Aves	50	-98	1955-1992
Ardea cinerea	Aves	52	-1	1928-1970
Ardea sp1	Aves	53	-1	1928-1970
Bucephala albeola	Aves	50	-98	1955-1992
Cardinalis cardinalis	Aves	40	-88	1939-1976
Certhia americana	Aves	40	-88	1937-1976
Ciconia ciconia	Aves	48	7	1945-1986
Coccyzus americanus	Aves	40	-88	1939-1976
Colaptes auratus	Aves	40	-88	1939-1976
Colinus virginianus	Aves	42	-110	1945-1990
Contopus virens	Aves	40	-88	1939-1976
Corvus corone	Aves	51	-5	1946-1979
Cyanocitta cristata	Aves	40	-88	1937-1976
Grus americana	Aves	27	-97	1939-1986
Grus americana	Aves	27	-97	1938-1989
Haematopus ostralegus	Aves	51	-5	1946-1979
Junco hyemalis	Aves	40	-88	1937-1976
Lagopus lagopus scoticus	Aves	56	-4	1901-1978
Lagopus lagopus scoticus	Aves	56	-4	1901-1978
Lagopus lagopus scoticus	Aves	56	-4	1901-1944
Lagopus lagopus scoticus	Aves	56	-4	1901-1943
Lagopus lagopus scoticus	Aves	56	-4	1901-1947
Lagopus lagopus scoticus	Aves	56	-4	1901-1942
Luscinia megahrynchos	Aves	51	-2	1927-1960
Melanerpes carolinus	Aves	40	-88	1939-1976
Melanerpes carolinus	Aves	40	-88	1937-1976
Myiarchus crinitus	Aves	40	-88	1940-1976
Oxyura jamaicensis	Aves	50	-98	1955-1992

Continued on next page...

Table E.1 – *Continued*

Species	***Class***	***Lat.***	***Long.***	***Time period***
Parus bicolor	Aves	40	-88	1937-1969
Parus caeruleus	Aves	51	1	1947-1983
Parus major	Aves	51	1	1947-1978
Passerina cyanea	Aves	40	-88	1939-1976
Perdix perdix	Aves	52	1	1901-1933
Perdix perdix	Aves	54	-1	1901-1933
Perdix perdix	Aves	52	1	1901-1932
Perdix perdix	Aves	51	0	1901-1932
Perdix perdix	Aves	52	1	1901-1933
Phalacrocorax aristotelis	Aves	55	-1	1949-1978
Phylloscopus collybita	Aves	51	-2	1928-1960
Phylloscopus trochilus	Aves	51	-2	1928-1960
Picoides pubescens	Aves	40	-88	1939-1976
Picoides pubescens	Aves	40	-88	1937-1976
Picoides villosus	Aves	40	-88	1939-1976
Picoides villosus	Aves	40	-88	1937-1976
Pterocles namaqua	Aves	-28	24	1950-1992
Rissa tridactyla	Aves	54	-1	1949-1984
Scolopax rusticola	Aves	51	0	1901-1932
Sitta carolinensis	Aves	40	-88	1937-1976
Spizella arborea	Aves	40	-88	1937-1976
Sturnus vulgaris	Aves	51	-5	1946-1979
Sturnus vulgaris	Aves	40	-88	1940-1976
Tetrao tetrix	Aves	60	25	1901-1933
Troglodytes aedon	Aves	40	-88	1939-1976
Vanellus vanellus	Aves	51	-5	1946-1979
Mya arenaria	Bivalvia	36	-122	1916-1947
Tivela stultorum.	Bivalvia	36	-122	1916-1947
Cancer magister	Crustacea	38	-123	1950-1992
Cancer magister	Crustacea	39	-123	1950-1992
Cancer magister	Crustacea	40	-124	1950-1992
Cancer magister	Crustacea	42	-124	1950-1992
Cancer magister	Crustacea	43	-124	1950-1992
Cancer magister	Crustacea	44	-123	1950-1992
Cancer magister	Crustacea	45	-123	1950-1992
Cancer magister	Crustacea	46	-123	1950-1992

Continued on next page...

Table E.1 – *Continued*

Species	***Class***	***Lat.***	***Long.***	***Time period***
Cancer magister	Crustacea	46	-124	1950-1992
Cancer magister	Crustacea	42	-124	1950-1992
Cancer magister	Crustacea	38	-122	1945-1977
Panulirus interruptus	Crustacea	36	-122	1916-1978
Haliotis rufescens	Gastropoda	36	-122	1935-1964
Blissus leucopterus	Insecta	39	-89	1901-1940
Lymantria dispar	Insecta	43	20	1954-1986
Lymantria monacha	Insecta	51	11	1901-1941
Panaxia dominula-dominula	Insecta	51	-1	1939-1978
Panaxia dominula-medionigra	Insecta	51	-1	1939-1978
Panolis flammea	Insecta	52	11	1901-1940
Alopex lagopus	Mammalia	64	28	1958-1989
Arvicola terrestris	Mammalia	46	6	1938-1991
Arvicola terrestris	Mammalia	46	6	1940-1980
Arvicola terrestris	Mammalia	46	7	1951-1992
Arvicola terrestris	Mammalia	46	7	1944-1992
Canis latrans	Mammalia	55	-104	1914-1957
Canis latrans	Mammalia	55	-98	1919-1957
Canis latrans	Mammalia	55	-105	1919-1957
Canis lupus	Mammalia	52	24	1946-1993
Canis lupus	Mammalia	52	24	1946-1993
Clethrionomys glareolus	Mammalia	55	36	1956-1986
Clethrionomys rufocanus	Mammalia	43	143	1962-1992
Clethrionomys rufocanus	Mammalia	43	143	1962-1992
Clethrionomys rufocanus	Mammalia	69	21	1949-1994
Lepus europaeus	Mammalia	54	-1	1901-1932
Lepus europaeus	Mammalia	52	1	1901-1932
Lepus europaeus	Mammalia	51	0	1902-1932
Lepus europaeus	Mammalia	52	-1	1944-1980
Lepus europaeus	Mammalia	52	-1	1944-1977
Lepus europaeus	Mammalia	57	10	1902-1946
Lepus timidus	Mammalia	60	25	1901-1934
Lynx lynx	Mammalia	64	27	1901-1961
Martes americana	Mammalia	45	-78	1961-1992
Martes pennanti	Mammalia	55	-98	1924-1957
Mustela vison	Mammalia	55	-104	1914-1957

Continued on next page...

Table E.1 – *Continued*

Species	***Class***	***Lat.***	***Long.***	***Time period***
Mustela vison	Mammalia	55	-98	1924-1957
Ondatra zibethicus	Mammalia	52	-88	1919-1957
Ondatra zibethicus	Mammalia	55	-104	1914-1957
Ondatra zibethicus	Mammalia	55	-98	1924-1957
Ondatra zibethicus	Mammalia	50	-107	1920-1959
Ondatra zibethicus	Mammalia	54	-107	1916-1959
Ondatra zibethicus	Mammalia	57	-107	1916-1959
Oryctolagus cuniculus	Mammalia	52	1	1901-1933
Oryctolagus cuniculus	Mammalia	52	1	1901-1932
Oryctolagus cuniculus	Mammalia	51	0	1902-1932
Oryctolagus cuniculus	Mammalia	52	-1	1944-1980
Oryctolagus cuniculus	Mammalia	52	-1	1944-1977
Phoca groenlandica	Mammalia	49	-53	1901-1942
Vulpes	Mammalia	55	-125	1919-1957
Vulpes	Mammalia	55	-115	1919-1957
Vulpes	Mammalia	55	-104	1914-1957
Vulpes	Mammalia	55	-98	1919-1957
Vulpes	Mammalia	52	-88	1919-1957
Vulpes	Mammalia	47	-67	1924-1957
Vulpes	Mammalia	45	-63	1919-1957
Vulpes	Mammalia	50	-80	1920-1951
Vulpes	Mammalia	55	-105	1920-1951
Esox lucius	Osteichthyes	54	-3	1944-1981
Esox lucius	Osteichthyes	54	-2	1944-1981
Oncorhynchus gorbuscha	Osteichthyes	45	-121	1938-1994
Oncorhynchus gorbuscha	Osteichthyes	56	-134	1934-1966
Oncorhynchus gorbuscha	Osteichthyes	58	-135	1960-1995
Oncorhynchus gorbuscha	Osteichthyes	56	-133	1960-1995
Oncorhynchus keta	Osteichthyes	50	-126	1955-1987
Oncorhynchus nerka	Osteichthyes	54	-129	1908-1964
Oncorhynchus nerka	Osteichthyes	50	-119	1948-1993
Oncorhynchus nerka	Osteichthyes	50	-122	1948-1993
Oncorhynchus nerka	Osteichthyes	52	-123	1948-1993
Oncorhynchus nerka	Osteichthyes	52	-123	1948-1993
Oncorhynchus nerka	Osteichthyes	52	-123	1949-1988
Oncorhynchus nerka	Osteichthyes	52	-121	1948-1993

Continued on next page...

Table E.1 – *Continued*

Species	***Class***	***Lat.***	***Long.***	***Time period***
Oncorhynchus nerka	Osteichthyes	53	-123	1949-1994
Oncorhynchus nerka	Osteichthyes	52	-121	1948-1993
Oncorhynchus nerka	Osteichthyes	54	-130	1943-1985
Oncorhynchus nerka	Osteichthyes	54	-130	1908-1952
Oncorhynchus nerka	Osteichthyes	51	-127	1951-1995
Oncorhynchus nerka	Osteichthyes	54	-124	1948-1994
Oncorhynchus nerka	Osteichthyes	53	-123	1948-1994
Oncorhynchus nerka	Osteichthyes	49	-121	1948-1992
Salmo salar	Osteichthyes	60	10	1901-1986

E.4 Additional methods

For the stochastic Ricker model simulations presented in Figure 1 in Chapter 6 and described in Methods, a starting population $p_0 = K$ was used for all simulations. For each combination of parameters, 100 time series of length 500 were generated and power spectra were computed based on the last 250 time steps of each simulation. Spectral exponents were computed using the mean power spectra (mean of each frequency over the 100 simulations) and these were plotted against ρ separately for each combination of parameters.

The model developed by Grenfell *et al.* (1998) and used to produce Figure 4 in Chapter 6 was run 2000 times for 1000 time steps for each combination of ρ_0 and ρ_1; the spectral exponent of x_t was calculated for each run and averaged across runs.

For the simulations used to produce Figure 5 in the main text, for each ρ with $-0.9 < \rho < 0.9$ and r with $0.1 < r < 3$, and for $\sigma = 0.3$ and $K = 1$, 2000 population time series of length 512 were simulated starting from $p_0 = K$. Population spectral exponents were computed for the latter 256 time steps of each simulation and averaged. Any population falling below $0.01\,K$ was considered to have gone extinct; the proportion of populations that went below this threshold for each combination of parameters quantified extinction risk for those parameters.

The power spectrum can be used to estimate α for $1/f^{\alpha}$ noise (Halley, 1996; Halley & Kunin, 1999). In that context it is used with an assumed statistical model, so it is important to test the assumptions of the model (i.e. whether noise was actually $1/f^{\alpha}$ noise, which can be assessed by testing if the log-power-versus-log-frequency plot is reasonably characterised by the linear regression). In the present study, however, the spectral exponent provides an index of the relative importance of low and high frequencies only; its use relies on no statistical model or assumptions about the form of the spectrum.

Table E.2: Definition of the geographical regions used.

Region	Latitude	Longitude
North America	> 10°N	50° to 170°W
South America	< 10°N	34° to 82°W
Africa	< 34°N	50°E to 20°W
Europe	> 34°N	60°E to 25°W
Asia	> 10°N	> 60°E
Australasia+	< 10°N	> 90°E

E.5 Spatial autocorrelation

So far, only temporal autocorrelation has been discussed and considered. Similarly, variables can also have a spatial context (Dale & Fortin, 2009). In much the same way that the temperature today is likely to be similar to that of yesterday, the temperature in two nearby locations is bound to be more similar (if positively autocorrelated) than expected for randomly associated observations (Legendre & Fortin, 1989; Legendre, 1993). The structure can largely be attributed to the physical processes that form the environment. Biological systems are also not distributed uniformly or at random (Legendre, 1993), but are spatially autocorrelated, although in this case it is more complicated to discern to what extent it is spatial dependence (induced by spatially autocorrelated variables such as the environment) or actual spatial autocorrelation in the variable of interest (Dale & Fortin, 2009). In any case, the heterogeneity in biological systems is functional, and therefore dictated by, for example, habitat, mates and food availability, and predator-prey interactions. Through these, environmental heterogeneity may influence the response in biological systems (albeit at a range of scales) by affecting their distribution (Legendre & Legendre, 1998).

The lack of independence among observations in autocorrelated processes impairs our ability to perform standard statistical tests of hypotheses (Legendre & Fortin, 1989; Legendre, 1993; Legendre & Legendre, 1998). In a spatially structured variable, each new observation does not provide a full degree of freedom, given that these can at least in part be predicted by the values of neighbouring sites, but rather a fraction which is inversely proportional to the degree of autocorrelation in the data (Cliff & Ord, 1975; Fortin & Dale, 2005). It is therefore difficult to decide what the appropriate null reference distribution for the test should be. On the other hand, if a classical statistical test were performed without taking spatial autocorrelation into account, the effect for positively autocorrelated processes would be an artificial inflation of the number of degrees of freedom, and consequently the probability of a Type I error would be larger than the assumed α value (Legendre *et al.*, 1990).

The simplest way to tackle the issue of spatial autocorrelation in statistical testing is to remove the spatial dependency among observations (Dutilleul, 1993b). For example, one could reduce the resolution of the data (by using a subset or by averaging) in order to eliminate autocorrelation, or otherwise by using filtering techniques (such as detrending) (Student, 1914; Cliff & Ord, 1981). These solutions are far from ideal given that data is lost in the process, and is something that fields such as ecology, with relative scarcity of data, cannot afford. A more complex approach involves modifying the tests in order to take the spatial structure into account.

Several techniques have been proposed for a range of tests (Cliff & Ord, 1973, 1981; Fortin & Dale, 2005). The methods that have perhaps received more attention, however, are those that propose to estimate a modified number of degrees of freedom (Clifford *et al.*, 1989; Dutilleul, 1993a). Randomization procedures can also be used to generate a reference distribution, although these entail the challenge of developing a permutation scheme that maintains the spatial structure in the data (Legendre *et al.*, 1990; Manly, 2007).

As mentioned above, spatial autocorrelation effectively reduces the effective sample size. The degree of autocorrelation could therefore be used to determine how much smaller the sample size is than the number of observations (Clifford *et al.*, 1989; Dutilleul, 1993a). With the geographically effective sample size, it is then possible to find a reference distribution and standard parametric tests can then be used. Several implementations of these methods are available (e.g. Legendre (2000)). One is SAM (Spatial Analysis in Macroecology), developed by Rangel *et al.* (2006), which estimates the effective sample size derived from spatial correlograms by using either the method described in Clifford *et al.* (1989), or its generalisation as formulated by Dutilleul (1993a).

E.6 Results for all climate variables

Figure E.6: Change in the spectral exponents of GHCN temperature time series from 1911-1950 to 1951-1990, for (a) mean annual temperatures, and (b)-(e) mean winter, spring, summer, and autumn temperatures respectively. Panel (d) for mean summer temperature is exactly the same as Figure 2 in the main text, and is reproduced here to ease comparison with the other panels. P values (t-test corrected for spatial autocorrelation, N in parentheses) are listed above each box-whisker plot. A positive (respectively negative) difference in spectral exponent denotes a bluer (respectively redder) spectrum during 1951-1990 compared to 1911-1950.

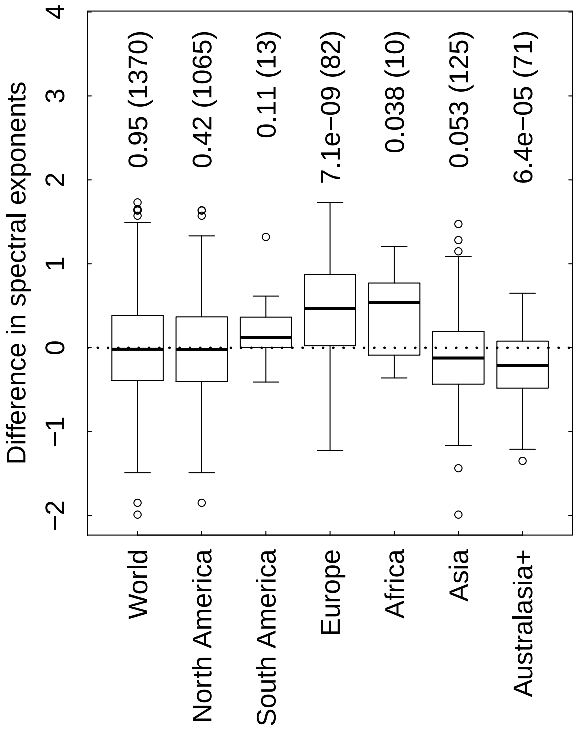

(a) Mean annual temperature

Figure E.6

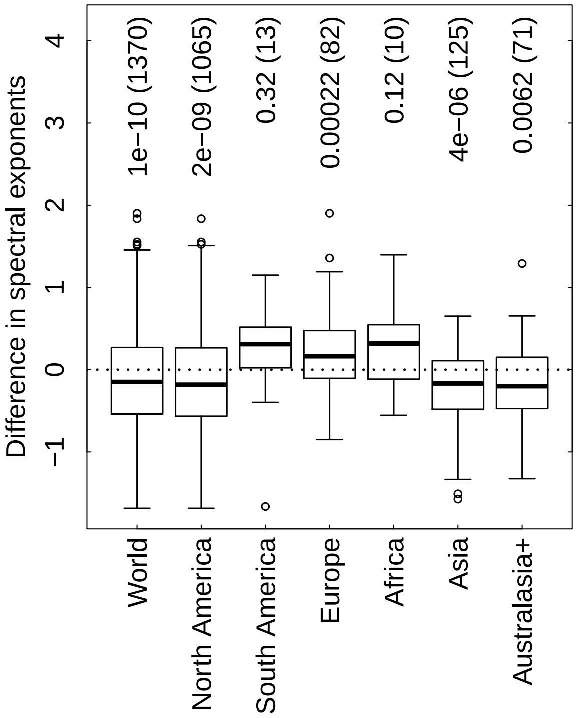

(b) Mean winter temperature

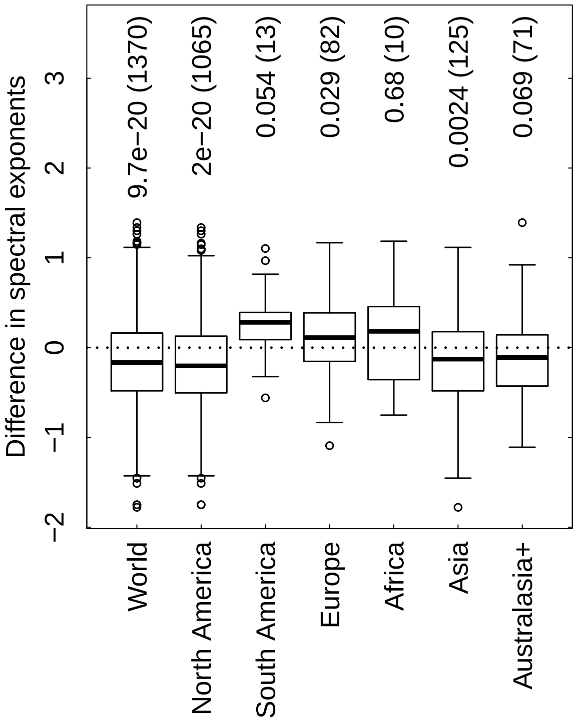

(c) Mean spring temperature

Figure E.6

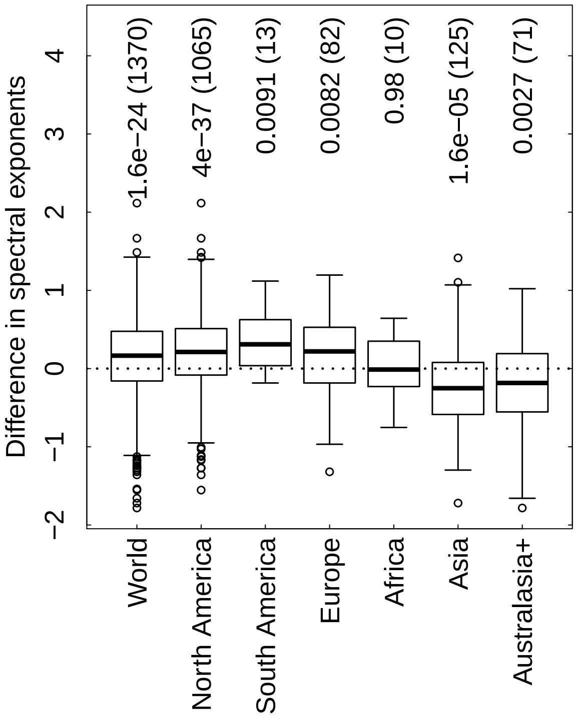

(d) Mean summer temperature

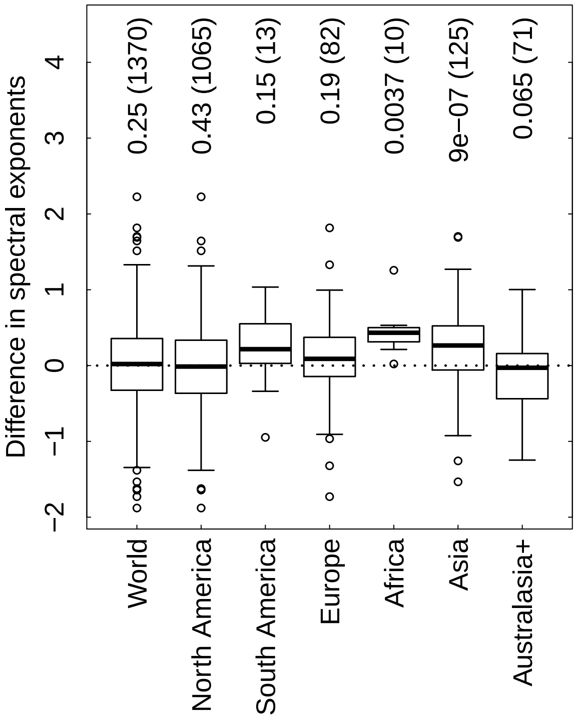

(e) Mean autumn temperature

Figure E.6

E.7 Why summer?

We present a conceptual model which suggests a general mechanism whereby autocorrelation in summer climatic variables will propagate through to population autocorrelation more than autocorrelation in winter climatic variables. We then consider a previously studied mathematical model of a particular population that serves as a concrete specific example of the general conceptual model. The model presented here is the same as the one presented in the "Why Summer?" section of the Discussion, but a more detailed exposition is provided here.

The conceptual model applies to the class of populations for which three assumptions are reasonable. First, we assume that a population takes more than one year to grow to carrying capacity following a crash. In contrast to the slow growth phase, populations can crash quickly, falling to below carrying capacity in a single year. Second, we assume that crashes occur only once a population has reached or is close to carrying capacity, and are due to an interaction between density dependence and bad winter weather. Density-dependent effects alone and poor winter weather alone are assumed less likely to cause crashes than their combination, such that winter weather has no or limited effect on dynamics during a population's growth phase. Finally, we assume that summer environmental conditions are responsible for year-to-year variation during the growth phase. For many populations, reproduction occurs in spring or summer, so it is reasonable to assume that population growth depends on the conditions that pertain when recruits are youngest and most vulnerable. These assumptions seem more or less reasonable for the primarily temperate and generally large-bodied species that dominate our dataset. The assumptions are presented diagrammatically in Figure E.7.

The conceptual model helps us understand intuitively how climate autocorrelation in summer months more effectively propagates through to population autocorrelation than climate autocorrelation in winter months. A sequence of bad winters leads a population that is at or above carrying capacity to a crash in population numbers in the first year, bringing the population below carrying capacity so that the second and subsequent bad winters have little effect and winter autocorrelation cannot be transmitted to the population time series. In contrast, since growth from low numbers to carrying capacity can take more than one year, multiple good (respectively bad) summers all have the potential to affect the population, producing population autocorrelation.

To illustrate the conceptual model quantitatively, we used the model of Grenfell *et al.* (1998) described in Methods. The model meets the assumptions of the conceptual model in Figure E.7. The model of Grenfell *et al.* (1998) is characterised by two distinct regimes: one describing populations at or above carrying capacity, and the other pertaining to populations below carrying capacity. These two regimes are affected by winter and summer seasons respectively, which allows us to introduce noise for both winter and summer months separately; the repercussions of autocorrelation in the two seasons on the resulting spectral exponent of the modelled population can be separately analysed. Model output (Figure 4 in the main text) indicates that the impact of summer noise colour on population spectral colour can be substantially greater than the impact of winter noise colour, as expected according to the conceptual model and in parallel with our empirical results.

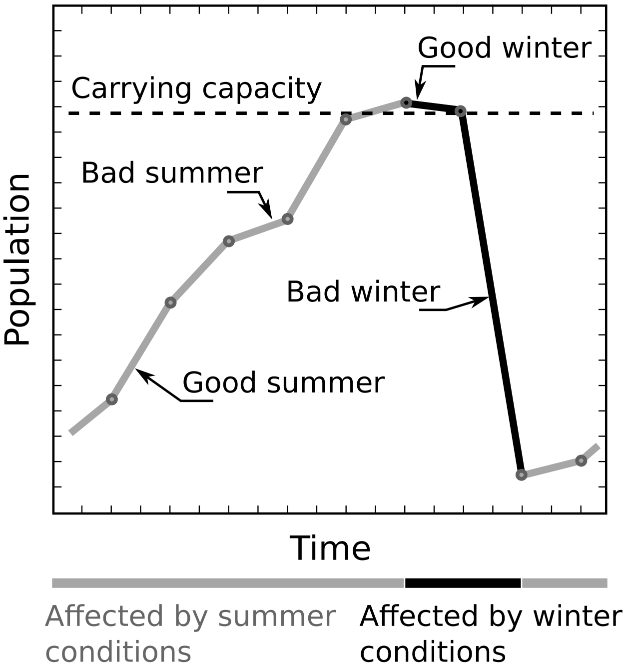

Figure E.7: Diagram explaining the main assumptions of the conceptual model proposed in the text: (i) crashes in population numbers are generally faster than the growth regime; (ii) crashes occur once the population is near or above carrying capacity and depend on winter weather, but winter weather has little effect below carrying capacity; and (iii) growth is mediated primarily by summer conditions.

E.8 Extinction risk in other univariate models

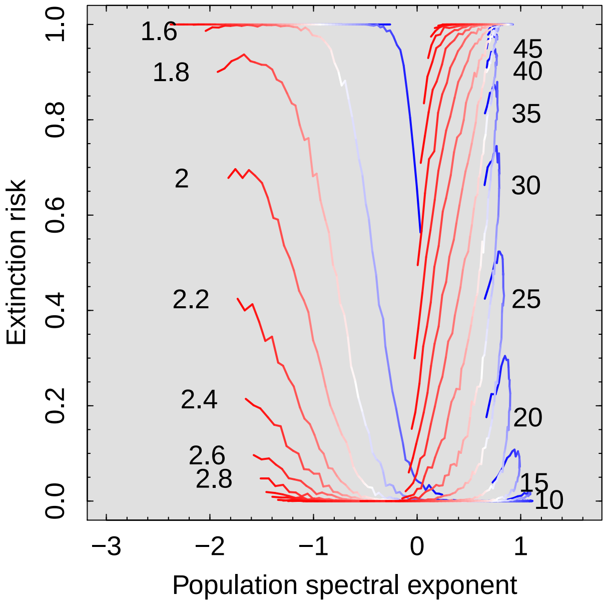

Figure E.8: The relationship between noise and population spectral colour and extinction risk in the stochastic formulation of the Hassell model of Figure E.1 (with $b = 4$). The same procedure used to obtain Figure 5 in the main text was followed (Methods and Section E.4), but with $1 < r < 50$. In this case, any population falling below $0.05\,K$ was considered to have gone extinct. The results are similar to those of Figure 5 in the main text. The reddening of environmental noise increases extinction risk for red-shifted, slow-growing populations; in contrast, for blue-shifted, fast growing populations, the opposite is generally true. Each individual line is labelled by the fixed r value used for all points on the line; line colour corresponds to the value of ρ used.

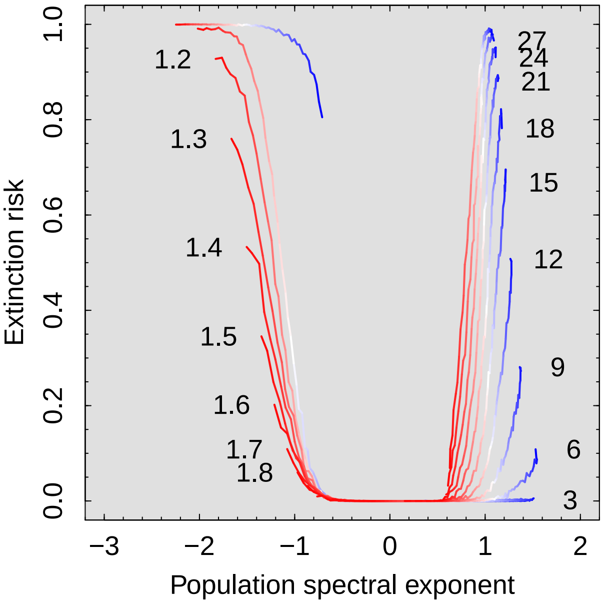

Figure E.9: The relationship between noise and population spectral colour and extinction risk in the stochastic formulation of the Maynard Smith model of Figure E.3 (with $b = 3$). The same procedure used to obtain Figure 5 in the main text was followed (Methods and Section E.4), but with $1 < r < 30$. In this case, any population falling below $0.05\,K$ was considered to have gone extinct. The results are similar to those of Figure 5 in the main text. The reddening of environmental noise increases extinction risk for red-shifted, slow-growing populations; in contrast, for blue-shifted, fast growing populations, the opposite is true. Each individual line is labelled by the fixed r value used for all points on the line; line colour corresponds to the value of ρ used.

References

Abramowitz, M. & Stegun, I. A., eds. (1964). *Handbook of Mathematical Functions with Formulas, Graphs, and Mathematical Tables.* Dover publications.

Aebischer, N. J., Coulson, J. C., & Colebrook, J. M. (1990). Parallel long-term trends across four marine trophic levels and weather. *Nature*, **347**, 753–755.

Akçakaya, H. R., Halley, J. M., & Inchausti, P. (2003). Population-level mechanisms for reddened spectra in ecological time series. *The Journal of Animal Ecology*, **72**, 698–702.

Altwegg, R., Roulin, A., Kestenholz, M., & Jenni, L. (2006). Demographic effects of extreme winter weather in the barn owl. *Oecologia*, **149**, 44–51.

Anderson, B., Akakaya, H., Arajo, M., Fordham, D., Martinez-Meyer, E., Thuiller, W., & Brook, B. (2009). Dynamics of range margins for metapopulations under climate change. *Proceedings of the Royal Society of London. Series B: Biological Sciences*, **276**(1661), 1415–1420.

Ariño, A. & Pimm, S. L. (1995). On the nature of population extremes. *Evolutionary Ecology*, **9**, 429–443.

Atkinson, D. & Sibly, R. M. (1997). Why are organisms usually bigger in colder environments? Making sense of a life history puzzle. *Trends in Ecology & Evolution*, **12**(6), 235–239.

Beever, E. A., Brussard, P. F., & Berger, J. (2003). Patterns of apparent extirpation among isolated populations of pikas (*Ochotona princeps*) in the Great Basin. *Journal of Mammalogy*, **84**(1), 37–54.

Begon, M., Harper, J. L., & Townsend, C. R. (1996). *Ecology: Individuals, Populations and Communities.* Oxford, UK: Blackwell Science Ltd.

Blarer, A. & Doebeli, M. (1996). In the red zone. *Nature*, **380**(6575), 589.

Blender, R. & Fraedrich, K. (2003). Long time memory in global warming simulations. *Geophysical Research Letters*, **30**(14), 1769.

BLUEWEISS, L., FOX, H., KUDZMA, V., NAKASHIMA, D., PETERS, R., & SAMS, S. (1978). Relationships between body size and some life history parameters. *Oecologia*, **37**, 257–272.

BOER, G. J. (2010). Changes in interannual variability and decadal potential predictability under global warming. *Journal of Climate*, **22**, 3098–3109.

BOYCE, M. S., HARIDAS, C. V., LEE, C. T., & THE NCEAS STOCHASTIC DEMOGRAPHY WORKING GROUP (2006). Demography in an increasingly variable world. *Trends in Ecology & Evolution*, **21**(3), 141–148.

BOYLES, J. G., SEEBACHER, F., SMIT, B., & MCKECHNIE, A. E. (2011). Adaptive thermoregulation in endotherms may alter responses to climate change. *Integrative & Comparative Biology*, **51**(5), 676–690.

BRILLINGER, D. R. (2001). *Time Series: Data Analysis and Theory.* Classics in Applied Mathematics. Philadelphia, USA: Society for Industrial and Applied Mathematics.

BROOK, B. W., TRAILL, L. W., & BRADSHAW, C. J. A. (2006). Minimum viable population sizes and global extinction risk are unrelated. *Ecology Letters*, **9**, 375–382.

BUNDE, A., EICHNER, J. F., HAVLIN, S., KOSCIELNY-BUNDE, E., SCHELLNHUBER, H. J., & VYUSHIN, D. (2004). Comment on "Scaling of atmosphere and ocean temperature correlations in observations and climate models". *Physical Review Letters*, **92**(3), 108501.

CASWELL, H. (2001). *Matrix Population Models: Construction, Analysis, and Interpretation.* Sunderland, MA: Sinauer Associates, Inc.

CASWELL, H. & KAYE, T. N. (2001). Stochastic demography and conservation of an endangered perennial plant (*Lomatium bradshawii*) in a dynamic fire regime. *Advances in Ecological Research*, **32**, 1–51.

CHAVES, L. F., MORRISON, A. C., KITRON, U. D., & SCOTT, T. W. (2011). Non-linear impacts of climatic variability on the density-dependent regulation of an insect vector of disease. *Global Change Biology.*

CHAVEZ, F. P., RYAN, J., LLUCH-COTA, S. E., & ÑIQUEN, C. M. (2003). From anchovies to sardines and back: Multidecadal change in the Pacific Ocean. *Science*, **299**(5604), 217–221.

CLEGG, R. G. (2006). A practical guide to measuring the Hurst parameter. *International Journal of Simulation: Systems, Science & Technology*, **7**(2), 3.

CLIFF, A. D. & ORD, J. K. (1973). *Spatial Autocorrelation.* Pion Ltd.

CLIFF, A. D. & ORD, J. K. (1975). The comparison of means when samples consist of spatially autocorrelated observations. *Environment and Planning A*, **7**, 725–734.

CLIFF, A. D. & ORD, J. K. (1981). *Spatial Processes: Models & Applications.* Pion Ltd.

CLIFFORD, P., RICHARDSON, S., & HÉMON, D. (1989). Assessing the significance of the correlation between two spatial processes. *Biometrics*, **45**, 123–134.

CLUTTON-BROCK, T. & PEMBERTON, J., eds. (2004). *Soay Sheep: Dynamics and Selection in an Island Population.* Cambridge University Press.

COHEN, J. E. (1995). Unexpected dominance of high frequencies in chaotic nonlinear population models. *Nature*, **378**, 610–612.

CORBINEAU, A., ROUYER, T., CAZELLES, B., FROMENTIN, J.-M., FONTENEAU, A., & MÉNARD, F. (2008). Time series analysis of tuna and swordfish catches and climate variability in the Indian Ocean (1968-2003). *Aquatic Living Resources*, **21**, 277–285.

COULSON, T., CATCHPOLE, E. A., ALBON, S. D., MORGAN, B. J. T., PEMBERTON, J. M., CLUTTON-BROCK, T. H., CRAWLEY, M. J., & GRENFELL, B. T. (2001). Age, sex, density, winter weather, and population crashes in Soay sheep. *Science*, **292**(5521), 1528.

COULSON, T., EZARD, T. H. G., PELLETIER, F., TAVECCHIA, G., STENSETH, N. C., CHILDS, D. Z., PILKINGTON, J. G., PEMBERTON, J. M., KRUUK, L. E. B., CLUTTON-BROCK, T., & CRAWLEY, M. J. (2008). Estimating the functional form for the density dependence from life history data. *Ecology*, **89**(6), 1661–1674.

COULSON, T., MACNULTY, D. R., STAHLER, D. R., VONHOLDT, B., WAYNE, R. K., & SMITH, D. W. (2011). Modeling effects of environmental change on wolf population dynamics, trait evolution, and life history. *Science*, **334**(6060), 1275–1278.

CUDDINGTON, K. M. & YODZIS, P. (1999). Black noise and population persistence. *Proceedings of the Royal Society of London. Series B: Biological Sciences*, **266**, 969–973.

CYR, H. (1997). Does inter-annual variability in population density increase with time? *Oikos*, **79**, 549–558.

Cyr, H. & Cyr, I. (2003). Temporal scaling of temperature variability from land to oceans. *Evolutionary Ecology Research*, **5**, 1183–1197.

Dale, M. R. T. & Fortin, M. J. (2009). Spatial autocorrelation and statistical tests: some solutions. *Journal of Agricultural, Biological, and Environmental Statistics*, **14**(2), 188–206.

Datsenko, N. M., Monin, A. S., Berestov, A. A., Ivashchenko, N. N., & Sonechkin, D. M. (2004). Global climate oscillations over the last 150 years. In *Doklady Rossijskoj Akademii Nauk*, volume 399. 253–256.

Dell, A. I., Pawar, S., & Savage, V. M. (2011). Systematic variation in the temperature dependence of physiological and ecological traits. *Proceedings of the National Academy of Sciences of the United States of America*, **108**(26), 10591–10596.

Dennis, B., Munholland, P. L., & Scott, J. M. (1991). Estimation of growth and extinction parameters for endangered species. *Ecological Monographs*, **61**(2), 115–143.

Deutsch, C. A., Tewksbury, J. J., Huey, R. B., Sheldon, K. S., Ghalambor, C. K., Haak, D. C., & Martin, P. R. (2008). Impacts of climate warming on terrestrial ectotherms across latitude. *Proceedings of the National Academy of Sciences of the United States of America*, **105**(18), 6668–6672.

Dormann, C. F., McPherson, J. M., Araújo, M. B., Bivand, R., Bolliger, J., Carl, G., Davies, R. G., Hirzel, A., Jetz, W., Kissling, W. D., Kühn, I., Ohlemüller, R., Peres-Neto, P. R., Reineking, B., Schröder, B., Schurr, F. M., & Wilson, R. (2007). Methods to account for spatial autocorrelation in the analysis of species distributional data: a review. *Ecography*, **30**, 609–628.

Drake, J. M. (2005). Population effects of increased climate variation. *Proceedings of the Royal Society of London. Series B: Biological Sciences*, **272**(1574), 1823.

Dutilleul, P. (1993a). Modifying the t test for assessing the correlation between two spatial processes. *Biometrics*, **49**, 305–314.

Dutilleul, P. (1993b). Spatial heterogeneity and the design of ecological field experiments. *Ecology*, **74**(6), 1646–1658.

Eichner, J. F., Koscielny-Bunde, E., Bunde, A., Havlin, S., & Schellnhuber, H.-J. (2003). Power-law persistence and trends in the atmosphere: A detailed study of long temperature records. *Physical Review E: Statistical, Nonlinear, and Soft Matter Physics*, **68**(4), 046133.

Ezard, T. H. G. & Coulson, T. (2010). How sensitive are elasticities of long-run stochastic growth to how environmental variability is modelled? *Ecological Modelling*, **221**(2), 191–200.

Ezard, T. H. G., Gaillard, J.-M., Crawley, M. J., & Coulson, T. (2008). Habitat Dependence and Correlations between Elasticities of Long-Term Growth Rates. *The American Naturalist*, **172**(3), 424–430.

Fieberg, J. & Ellner, S. P. (2000). When is it meaningful to estimate an extinction probability? *Ecology*, **81**(7), 2040–2047.

Forster, J., Hirst, A. G., & Woodward, G. (2011). Growth and development rates have different thermal responses. *The American Naturalist*, **178**(5), 668–678.

Fortin, M. J. & Dale, M. R. T. (2005). *Spatial Analysis*. Cambridge University Press.

Fraedrich, K. & Blender, R. (2003). Scaling of atmosphere and ocean temperature correlations in observations and climate models. *Physical Review Letters*, **90**(10), 108501.

Frazier, M. R., Huey, R. B., & Berrigan, D. (2006). Thermodynamics constrains the evolution of insect population growth rates: "warmer is better". *The American Naturalist*, **168**(4), 512–520.

Gao, M., Li, Z., & Dai, H. (2007). Effects on spectral color of a spatially-structured population: Environmental noise, dispersal, spatial heterogeneity. *Ecological Modelling*, **201**(3-4), 326–330.

García-Carreras, B. & Reuman, D. C. (2011). An empirical link between the spectral colour of climate and the spectral colour of field populations in the context of climate change. *The Journal of Animal Ecology*, **80**(5), 1042–1048.

Gradshteyn, I. S. & Ryzhik, I. M. (2007). *Table of Integrals, Series, and Products*. Oxford: Academic Press, seventh edition.

Greenman, J. V. & Benton, T. G. (2005). The frequency spectrum of structured discrete time population models: its properties and their ecological implications. *Oikos*, **110**(2), 369–389.

Grenfell, B. T., Wilson, K., Finkenstädt, B. F., Coulson, T. N., Murray, S., Albon, S. D., Pemberton, J. M., Clutton-Brock, T. H., & Crawley, M. J. (1998). Noise and determinism in synchronized sheep dynamics. *Nature*, **394**(6694), 674–676.

GROSS, K., LOCKWOOD III, J. R., FROST, C. C., & MORRIS, W. F. (1998). Modeling controlled burning and trampling reduction for conservation of *Hudsonia montana*. *Conservation Biology*, **12**(6), 1291–1301.

HALLEY, J. & INCHAUSTI, P. (2002). Lognormality in ecological time series. *Oikos*, **99**, 518–530.

HALLEY, J. M. (1996). Ecology, evolution and $1/f$-noise. *Trends in Ecology & Evolution*, **11**(1), 33–37.

HALLEY, J. M. & KUNIN, W. E. (1999). Extinction risk and the $1/f$ family of noise models. *Theoretical Population Biology*, **56**, 215–230.

HARIDAS, C. V. & TULJAPURKAR, S. (2005). Elasticities in variable environments: properties and implications. *The American Naturalist*, **166**(4), 481–495.

HASSAN, R. M., SCHOLES, R., & ASH, N., eds. (2005). *Ecosystems and human well-being: current state and trends: findings of the Condition and Trends Working Group of the Millennium Ecosystem Assessment*, volume 1. Island Press.

HASSELL, M. P. (1975). Density-dependence in single-species populations. *The Journal of Animal Ecology*, **44**(1), 283–295.

HAYS, G. C., RICHARDSON, A. J., & ROBINSON, C. (2005). Climate change and marine plankton. *Trends in Ecology & Evolution*, **20**(6), 337–344.

HEINO, M. (1998). Noise colour, synchrony and extinctions in spatially structured populations. *Oikos*, **83**(2), 368–375.

HEINO, M., RIPA, J., & KAITALA, V. (2000). Extinction risk under coloured environmental noise. *Ecography*, **23**(2), 177–184.

HORVITZ, C. C., TULJAPURKAR, S., & PASCARELLA, J. B. (2005). Plant-animal interactions in random environments: habitat-stage elasticity, seed predators, and hurricanes. *Ecology*, **86**(12), 3312–3322.

HUEY, R. B. & STEVENSON, R. D. (1979). Integrating thermal physiology and ecology of ectotherms: a discussion of approaches. *American Zoologist*, **19**(1), 357–366.

HUGHES, L. (2000). Biological consequences of global warming: is the signal already apparent? *Trends in Ecology & Evolution*, **15**(2), 56–61.

HUNT, B. G. & ELLIOTT, T. I. (2004). Interaction of climatic variability with climatic change. *Atmosphere-Ocean*, **42**(3), 145–172.

Hunter, C. M., Caswell, H., Runge, M. C., Regehr, E. V., Amstrup, S. C., & Stirling, I. (2010). Climate change threatens polar bear populations: a stochastic demographic analysis. *Ecology*, **91**(10), 2883–2897.

Inchausti, P. & Halley, J. (2001). Investigating long-term variability using the Global Population Dynamics Database. *Science*, **29**, 655–657.

Inchausti, P. & Halley, J. (2002). The long-term temporal variability and spectral colour of animal populations. *Evolutionary Ecology Research*, **4**(7), 1033–1048.

Inchausti, P. & Halley, J. (2003). On the relation between temporal variability and persistence time in animal populations. *The Journal of Animal Ecology*, **72**, 899–908.

IPCC (2007). *Climate Change 2007: Synthesis Report. Contribution of Working Groups I, II and III to the Fourth Assessment Report of the Intergovernmental Panel on Climate Change*. Geneva, Switzerland: IPCC.

Jenouvrier, S., Caswell, H., Barbraud, C., Holland, M., Strœve, J., & Weimerskirch, H. (2009). Demographic models and IPCC climate projections predict the decline of an emperor penguin population. *Proceedings of the National Academy of Sciences of the United States of America*, **106**(6), 1844.

Jenouvrier, S., Caswell, H., Barbraud, C., & Weimerskirch, H. (2010). Mating behavior, population growth, and the operational sex ratio: A periodic two-sex model approach. *The American Naturalist*, **175**(6), 739–752.

Jenouvrier, S., Holland, M., Stroeve, J., Barbraud, C., Weimerskirch, H., Serreze, M., & Caswell, H. (2012). Effects of climate change on an emperor penguin population: analysis of coupled demographic and climate models. *Global Change Biology*, n/a–n/a.

Jillson, D. A. (1980). Insect populations respond to fluctuating environments. *Nature*, **288**, 699–700.

Jonzén, N., Pople, T., Knape, J., & Sköld, M. (2010). Stochastic demography and population dynamics in the red kangaroo *Macropus rufus*. *The Journal of Animal Ecology*, **79**(1), 109–116.

Kaitala, V., Lundberg, P., Ripa, J., & Ylikarjula, J. (1997a). Red, blue and green: dyeing population dynamics. *Annales Zoologici Fennici*, **34**(4), 217–228.

Kaitala, V. & Ranta, E. (1996). Red/blue chaotic power spectra. *Nature*, **381**, 198–99.

Kaitala, V., Ylikarjula, J., Ranta, E., & Lundberg, P. (1997b). Population dynamics and the colour of environmental noise. *Proceedings of the Royal Society of London. Series B: Biological Sciences*, **264**, 943–948.

Karl, T. R., Knight, R. W., & Plummer, N. (1995). Trends in high-frequency climate variability in the twentieth century. *Nature*, **377**, 217–220.

Karlsson, B. & Wiklund, C. (2005). Butterfly life history and temperature adaptations; dry open habitats select for increased fecundity and longevity. *The Journal of Animal Ecology*, **74**(1), 99–104.

Kendall, B. E., Prendergast, J., & Bjørnstad, O. N. (1998). The macroecology of population dynamics: taxonomic and biogeographic patterns in population cycles. *Ecology Letters*, **1**, 160–164.

Koscielny-Bunde, E., Bunde, A., Havlin, S., & Goldreich, Y. (1996). Analysis of daily temperature fluctuations. *Physica A: Statistical Mechanics and its Applications*, **231**(4), 393–396.

Koscielny-Bunde, E., Bunde, A., Havlin, S., Roman, H. E., Goldreich, Y., & Schellnhuber, H.-J. (1998). Indication of a universal persistence law governing atmospheric variability. *Physical Review Letters*, **81**(3), 729–732.

Laakso, J., Kaitala, V., & Ranta, E. (2001). How does environmental variation translate into biological processes? *Oikos*, **92**, 119–122.

Laakso, J., Kaitala, V., & Ranta, E. (2003a). Non-linear biological responses to disturbance: consequences on population dynamics. *Ecological Modelling*, **162**, 247–258.

Laakso, J., Löytynoja, K., & Kaitala, V. (2003b). Environmental noise and population dynamics of the ciliated protozoa *Tetrahymena thermophila* in aquatic microcosms. *Oikos*, **102**(3), 663–671.

Lande, R., Engen, S., & Sæther, B. E. (2003). *Stochastic Population Dynamics in Ecology and Conservation.* Oxford Series in Ecology and Evolution. Oxford, UK: Oxford University Press.

Lande, R. & Orzack, S. H. (1988). Extinction dynamics of age-structured populations in a fluctuating environment. *Proceedings of the National Academy of Sciences of the United States of America*, **85**(19), 7418.

Lau, K.-M. & Weng, H. (1995). Climate signal detection using wavelet transform: how to make a time series sing. *Bulletin of the American Meteorological Society*, **76**(12), 2392–2402.

Lawler, R., Caswell, H., Richard, A., Ratsirarson, J., Dewar, R., & Schwartz, M. (2009). Demography of Verreaux's sifaka in a stochastic rainfall environment. *Oecologia*, **161**, 491–504.

Lawton, J. H. (1988). More time means more variation. *Nature*, **334**, 563.

Legendre, P. (1993). Spatial autocorrelation: Trouble or new paradigm? *Ecology*, **74**(6), 1659–1673.

Legendre, P. (2000). *Program Mod_t_test.* Département de sciences biologiques, Université de Montréal.

Legendre, P. & Fortin, M.-J. (1989). Spatial pattern and ecological analysis. *Vegetatio*, **80**, 107–138.

Legendre, P. & Legendre, L. (1998). *Numerical Ecology.* Amsterdam, The Netherlands: Elsevier Science B.V., 2nd english edition.

Legendre, P., Oden, N. L., Sokal, R. R., Vaudor, A., & Kim, J. (1990). Approximate analysis of variance of spatially autocorrelated regional data. *Journal of Classification*, **7**(1), 53–75.

Lewontin, R. C. & Cohen, D. (1969). On population growth in a randomly varying environment. *Proceedings of the National Academy of Sciences of the United States of America*, **62**(4), 1056–1060.

Mandelbrot, B. (1982). *The Fractal Geometry of Nature.* New York, USA: W. H. Freeman.

Manly, B. F. J. (2007). *Randomization, Bootstrap and Monte Carlo Methods in Biology.* Chapman & Hall/CRC.

May, R. M. (1981). *Theoretical Ecology: Principles and Applications*, chapter 2: Models for Single Populations. Oxford, UK: Blackwell Scientific Publications, 2nd edition, 5–29.

May, R. M. & Oster, G. F. (1976). Bifurcations and dynamic complexity in simple ecological models. *The American Naturalist*, **110**(974), 573.

McArdle, B. H., Gaston, K. J., & Lawton, J. H. (1990). Variation in the size of animal populations: patterns, problems and artefacts. *The Journal of Animal Ecology*, **59**(2), 439–454.

McCarty, J. P. (2001). Ecological consequences of recent climate change. *Conservation Biology*, **15**(2), 320–331.

McLaughlin, J. F., Hellmann, J. J., Boggs, C. L., & Ehrlich, P. R. (2002). Climate change hastens population extinctions. *Proceedings of the National Academy of Sciences of the United States of America*, **99**(9), 6070–6074.

Menne, M. J. & Williams Jr, C. N. (2009). Homogenization of temperature series via pairwise comparisons. *Journal of Climate*, **22**(7), 1700–1717.

Menne, M. J., Williams Jr, C. N., & Vose, R. S. (2009). The U.S. Historical Climatology Network monthly temperature data, version 2. *Bulletin of the American Meteorological Society*, **90**(7), 993–1007.

Michaels, P. J., Bailing, R. C., Vose, R. S., & Knappenberger, P. C. (1998). Analysis of trends in the variability of daily and monthly historical temperature measurements. *Climate Research*, **10**, 27–33.

Mitchell, T. (2004). *CRU TS 2.0 and time-series analysis: advice for users.*

Mitchell, T. D. & Jones, P. D. (2005). An improved method of constructing a database of monthly climate observations and associated high-resolution grids. *International Journal of Climatology*, **25**, 693–712.

Morales, J. M. (1999). Viability in a pink environment: why "white noise" models can be dangerous. *Ecology Letters*, **2**(4), 228–232.

Morris, W. F. & Doak, D. F. (2002). *Quantitative Conservation Biology: Theory and Practice of Population Viability Analysis.* Sunderland, Massachusetts: Sinauer Associates, Inc.

Morris, W. F. & Doak, D. F. (2004). Buffering of life histories against environmental stochasticity: accounting for a spurious correlation between the variabilities of vital rates and their contributions to fitness. *The American Naturalist*, **163**(4), 579–590.

Morris, W. F., Pfister, C. A., Tuljapurkar, S., Haridas, C. V., Boggs, C. L., Boyce, M., Bruna, E. M., Church, D. R., Coulson, T., Doak, D. F. *et al.* (2008). Longevity can buffer plant and animal populations against changing climatic variability. *Ecology*, **89**(1), 19–25.

Morris, W. F., Tuljapurkar, S., Haridas, C. V., Menges, E. S., Horvitz, C. C., & Pfister, C. A. (2006). Sensitivity of the population growth rate to demographic variability within and between phases of the disturbance cycle. *Ecology Letters*, **9**(12), 1331–1341.

National Climatic Data Center, National Oceanic and Atmospheric Administration (2011). The USHCN Version 2 Serial Monthly Dataset. `ftp://ftp.ncdc.noaa.gov/pub/data/ushcn/v2/monthly/`. Accessed on 16/04/2011.

NERC Centre for Population Biology & Imperial College (1999). The Global Population Dynamics Database.

New, M., Hulme, M., & Jones, P. (2000). Representing twentieth-century space-time climate variability. Part II: Development of 1901-96 monthly grids of terrestrial surface climate. *Journal of Climate*, **13**, 2217–2238.

Novak, M., Obbard, M. E., Jones, J. G., Newman, R., Booth, A., Satterthwaite, A. J., & Linscombe, G. (1987). Furbearer harvests in North America, 1600-1984. Technical report, Ministry of Natural Resources Ontario, Canada and Ontario Trappers Organisation.

Osborn, T. J. (2004). Simulating the winter North Atlantic Oscillation: the roles of internal variability and greenhouse gas forcing. *Climate Dynamics*, **22**, 605–623.

Parker, D. E., Folland, C. K., Bevan, A., & Jones, P. D. (1994). Interdecadal changes of surface temperature since the late nineteenth century. *Journal of Geophysical Research*, **99**(D7), 14373–14399.

Parmesan, C. (1996). Climate and species' range. *Nature*, **382**(6594), 765–766.

Parmesan, C. (2006). Ecological and evolutionary responses to recent climate change. *Annual Review of Ecology, Evolution, and Systematics*, **37**, 637–669.

Parmesan, C., Ryrholm, N., Stefanescu, C., Hill, J. K., Thomas, C. D., Descimon, H., Huntley, B., Kaila, L., Kullberg, J., Tammaru, T., Tennent, J. W., Thomas, J. A., & Warren, M. (1999). Poleward shifts in geographical ranges of butterfly species associated with regional warming. *Nature*, **399**(6736), 579–583.

Parmesan, C. & Yohe, G. (2003). A globally coherent fingerprint of climate change impacts across natural systems. *Nature*, **421**(6918), 37–42.

Pelletier, J. D. (1998). The power spectral density of atmospheric temperature from time scales of 10^{-2} to 10^{6} yr. *Earth and Planetary Science Letters*, **158**, 157–164.

Pelletier, J. D. (2002). Natural variability of atmospheric temperatures and geomagnetic intensity over a wide range of timescales. *Proceedings of the National Academy of Sciences of the United States of America*, **99**(1), 2546–2553.

Pelletier, J. D. & Turcotte, D. L. (1997). Long-range persistence in climatological and hydrological time series: analysis, modeling and application to drought hazard assessment. *Journal of Hydrology*, **203**(1-4), 198–208.

Petchey, O. L. (2000). Environmental colour affects aspects of single-species population dynamics. *Proceedings of the Royal Society of London. Series B: Biological Sciences*, **267**, 747–754.

Petchey, O. L., Gonzalez, A., & Wilson, H. B. (1997). Effects on population persistence: the interaction between environmental noise colour, intraspecific competition and space. *Proceedings of the Royal Society of London. Series B: Biological Sciences*, **264**, 1841–1847.

Peterson, T. C. & Vose, R. S. (1997). An overview of the Global Historical Climatology Network temperature database. *Bulletin of the American Meteorological Society*, **78**(12), 2837–2849.

Pfister, C. A. (1998). Patterns of variance in stage-structured populations: Evolutionary predictions and ecological implications. *Proceedings of the National Academy of Sciences of the United States of America*, **95**(1), 213–218.

Pike, N., Tully, T., Haccou, P., & Ferrière, R. (2004). The effect of autocorrelation in environmental variability on the persistence of populations: an experimental test. *Proceedings of the Royal Society of London. Series B: Biological Sciences*, **271**(1553), 2143.

Pimm, S. L. & Redfearn, A. (1988). The variability of population densities. *Nature*, **334**, 613–614.

Pörtner, H. O. & Farrell, A. P. (2008). Physiology and climate change. *Science*, **322**(5902), 690–692.

Pounds, J. A., Fogden, M. P. L., & Campbell, J. H. (1999). Biological response to climate change on a tropical mountain. *Nature*, **398**(6728), 611–615.

Purvis, A., Gittleman, J. L., Cowlishaw, G., & Mace, G. M. (2000). Predicting extinction risk in declining species. *Proceedings of the Royal Society of London. Series B: Biological Sciences*, **267**(1456), 1947–1952.

R Development Core Team (2009). *R: A Language and Environment for Statistical Computing*. R Foundation for Statistical Computing, Vienna, Austria. ISBN 3-900051-07-0.

Räisänen, J. (2002). CO_2-induced changes in interannual temperature and precipitation variability in 19 CMIP2 experiments. *Journal of Climate*, **15**(17), 2395–2411.

Rangel, T. F. L. V. B., Diniz-Filho, J. A. F., & Bini, L. M. (2006). Towards an integrated computational tool for spatial analysis in macroecology and biogeography. *Global Ecology and Biogeography*, **15**, 321–327.

Ranta, E., Lundberg, P., Kaitala, V., & Laakso, J. (2000). Visibility of the environmental noise modulating population dynamics. *Proceedings of the Royal Society of London. Series B: Biological Sciences*, **267**, 1851–1856.

Reuman, D. C., Costantino, R. F., Desharnais, R. A., & Cohen, J. E. (2008). Colour of environmental noise affects the nonlinear dynamics of cycling, stage-structured populations. *Ecology Letters*, **11**, 820–830.

Reuman, D. C., Desharnais, R. A., Costantino, R. F., Ahmad, O. S., & Cohen, J. E. (2006). Power spectra reveal the influence of stochasticity on nonlinear population dynamics. *Proceedings of the National Academy of Sciences of the United States of America*, **103**(49), 18860.

Ripa, J. & Heino, M. (1999). Linear analysis solves two puzzles in population dynamics: the route to extinction and extinction in coloured environments. *Ecology Letters*, **2**(4), 219–222.

Ripa, J. & Lundberg, P. (1996). Noise colour and the risk of population extinctions. *Proceedings of the Royal Society of London. Series B: Biological Sciences*, **263**, 1751–1753.

Ripa, J. & Lundberg, P. (2000). The route to extinction in variable environments. *Oikos*, **90**, 89–96.

Ripa, J., Lundberg, P., & Kaitala, V. (1998). A general theory of environmental noise in ecological food webs. *The American Naturalist*, **151**(3), 256–263.

Rodó, X., Pascual, M., Fuchs, G., & Faruque, A. S. G. (2002). ENSO and cholera: A nonstationary link related to climate change? *Proceedings of the National Academy of Sciences of the United States of America*, **99**(20), 12901–12906.

Roughgarden, J. (1975). A simple model for population dynamics in stochastic environments. *The American Naturalist*, **109**(970), 713–736.

Ruel, J. J. & Ayres, M. P. (1999). Jensen's inequality predicts effects of environmental variation. *Trends in Ecology & Evolution*, **14**(9), 361–366.

Runge, M. C. & Moen, A. N. (1998). A modified model for projecting age-structured populations in random environments. *Mathematical Biosciences*, **150**(1), 21–41.

Ruokolainen, L., Fowler, M. S., & Ranta, E. (2007). Extinctions in competitive communities forced by coloured environmental variation. *Oikos*, **116**(3), 439–448.

Ruokolainen, L., Lindén, A., Kaitala, V., & Fowler, M. S. (2009). Ecological and evolutionary dynamics under coloured environmental variation. *Trends in Ecology & Evolution*, **24**(10), 555–563.

Sæther, B.-E., Tufto, J., Engen, S., Jerstad, K., Røstad, O. W., & Skåtan, J. E. (2000). Population dynamical consequences of climate change for a small temperate songbird. *Science*, **287**(5454), 854–856.

Sakai, D., Itoh, H., & Yukimoto, S. (2009). Changes in the interannual surface air temperature variability in the Northern Hemisphere in response to global warming. *Journal of the Meteorological Society of Japan*, **87**(4), 721–737.

Sala, O. E., Stuart Chapin, F., III, Armesto, J. J., Berlow, E., Bloomfield, J., Dirzo, R., Huber-Sanwald, E., Huenneke, L. F., Jackson, R. B., Kinzig, A., Leemans, R., Lodge, D. M., Mooney, H. A., Oesterheld, M., Poff, N. L., Sykes, M. T., Walker, B. H., Walker, M., & Wall, D. H. (2000). Global biodiversity scenarios for the year 2100. *Science*, **287**(5459), 1770–1774.

Scargle, J. D. (1982). Studies in astronomical time series analysis. II. Statistical aspects of spectral analysis of unevenly spaced data. *Astrophysical Journal*, **263**, 835–853.

Schoener, T. W. & Spiller, D. A. (1992). Is extinction rate related to temporal variability in population size? An empirical answer for orb spiders. *The American Naturalist*, **139**(6), 1176–1207.

Schwager, M., Johst, K., & Jeltsch, F. (2006). Does red noise increase or decrease extinction risk? Single extreme events versus series of unfavorable conditions. *The American Naturalist*, **167**(6), 879–888.

Smith, M., Caswell, H., & Mettler-Cherry, P. (2005). Stochastic flood and precipitation regimes and the population dynamics of a threatened floodplain plant. *Ecological Applications*, **15**(3), 1036–1052.

Steele, J. H. (1985). A comparison of terrestrial and marine ecological systems. *Nature*, **313**(31), 355–358.

STEELE, J. H. & HENDERSON, E. W. (1994). Coupling between physical and biological scales. *Philosophical Transactions of the Royal Society. Series B: Biological Sciences*, **343**, 5–9.

STEINSALTZ, D., TULJAPURKAR, S., & HORVITZ, C. (2011). Derivatives of the stochastic growth rate. *Theoretical Population Biology*, **80**(1), 1–15.

STENSETH, N. C., CHAN, K.-S., TAVECCHIA, G., COULSON, T., MYSTERUD, A., CLUTTON-BROCK, T., & GRENFELL, B. (2004). Modelling non-additive and nonlinear signals from climatic noise in ecological time series: Soay sheep as an example. *Proceedings of the Royal Society of London. Series B: Biological Sciences*, **271**, 1985–1993.

STENSETH, N. C., OTTERSEN, G., HURRELL, J. W., MYSTERUD, A., LIMA, M., CHAN, K.-S., YOCCOZ, N. G., & ÅDLANDSVIK, B. (2003). Studying climate effects on ecology through the use of climate indices: the North Atlantic Oscillation, El Niño Southern Oscillation and beyond. *Proceedings of the Royal Society of London. Series B: Biological Sciences*, **270**, 2087–2096.

STOUFFER, R. J. & WETHERALD, R. T. (2007). Changes of variability in response to increasing greenhouse gases. Part I: Temperature. *Journal of Climate*, **20**(21), 5455–5467.

STUART, S. N., CHANSON, J. S., COX, N. A., YOUNG, B. E., RODRIGUES, A. S. L., FISCHMAN, D. L., & WALLER, R. W. (2004). Status and trends of amphibian declines and extinctions worldwide. *Science*, **306**(5702), 1783–1786.

STUDENT, B. (1914). The elimination of spurious corrrelation due to position in time or space. *Biometrika*, **10**, 179–181.

SUGIHARA, G. (1995). From out of the blue. *Nature*, **378**, 559–560.

SUGIHARA, G. (1996). Red/blue chaotic power spectra. *Nature*, **381**, 199.

SUN, F., RODERICK, M. L., FARQUHAR, G. D., LIM, W. H., ZHANG, Y., BENNETT, N., & ROXBURGH, S. H. (2010). Partitioning the variance between space and time. *Geophysical Research Letters*, **37**(12), L12704.

SVOMA, B. M. & BALLING, R. C. (2010). United States' interannual precipitation variability over the past century: is variability increasing as predicted by models? *Physical Geography*, **31**(4), 307–318.

TALKNER, P. & WEBER, R. (2000). Power spectrum and detrended fluctuation analysis: application to daily temperatures. *Physical Review E: Statistical, Nonlinear, and Soft Matter Physics*, **62**(1), 150–160.

TEWS, J. & JELTSCH, F. (2004). Modelling the impact of climate change on woody plant population dynamics in South African savanna. *BMC Ecology*, **4**(1), 17.

THOMAS, C. D. & LENNON, J. J. (1999). Birds extend their ranges northwards. *Nature*, **399**(6733), 213–213.

TORRENCE, C. & COMPO, G. P. (1998). A practical guide to wavelet analysis. *Bulletin of the American Meteorological Society*, **79**(1), 61–78.

TULJAPURKAR, S. (2010). Environmental variance, population growth and evolution. *Journal of Animal Ecology*, **79**(1), 1–3.

TULJAPURKAR, S., HORVITZ, C. C., & PASCARELLA, J. B. (2003). The many growth rates and elasticities of populations in random environments. *The American Naturalist*, **162**(4), 489–502.

TULJAPURKAR, S. D. (1982). Population dynamics in variable environments. III. Evolutionary dynamics of r-selection. *Theoretical Population Biology*, **21**(1), 141–165.

TULJAPURKAR, S. D. (1990). *Population Dynamics in Variable Environments.* New York, NY: Springer-Verlag.

TULJAPURKAR, S. D. & ORZACK, S. H. (1980). Population dynamics in variable environments. I. Long-run growth rates and extinction. *Theoretical Population Biology*, **18**(3), 314–342.

VAN DE POL, M., VINDENES, Y., SÆTHER, B.-E., ENGEN, S., ENS, B. J., OOSTERBEEK, K., & TINBERGEN, J. M. (2010). Effects of climate change and variability on population dynamics in a long-lived shorebird. *Ecology*, **91**(4), 1192–1204.

VAN DE POL, M., VINDENES, Y., SÆTHER, B.-E., ENGEN, S., ENS, B. J., OOSTERBEEK, K., & TINBERGEN, J. M. (2011). Poor environmental tracking can make extinction risk insensitive to the colour of environmental noise. *Proceedings of the Royal Society of London. Series B: Biological Sciences*, **278**(1725), 3713–3722.

VASSEUR, D. A. & YODZIS, P. (2004). The color of environmental noise. *Ecology*, **85**(4), 1146–1152.

VINNIKOV, K. Y. & ROBOCK, A. (2002). Trends in moments of climatic indices. *Geophysical Research Letters*, **29**(2), 14–1.

Vose, R. S., Williams Jr, C. N., Peterson, T. C., Karl, T. R., & Easterling, D. R. (2003). An evaluation of the time of observation bias adjustment in the U. S. Historical Climatology Network. *Geophysical Research Letters*, **30**(20), 2046.

Walther, G. R., Post, E., Convey, P., Menzel, A., Parmesan, C., Beebee, T. J. C., Fromentin, J. M., Hoegh-Guldberg, O., & Bairlein, F. (2002). Ecological responses to recent climate change. *Nature*, **416**(6879), 389–395.

White, A., Begon, M., & Bowers, R. G. (1996a). Explaining the colour of power spectra in chaotic ecological models. *Proceedings of the Royal Society of London. Series B: Biological Sciences*, **263**, 1731–1737.

White, A., Bowers, R. G., & Begon, M. (1996b). Red/blue chaotic power spectra. *Nature*, **381**, 198.

Wichmann, M. C., Johst, K., Schwager, M., Blasius, B., & Jeltsch, F. (2005). Extinction risk, coloured noise and the scaling of variance. *Theoretical Population Biology*, **68**(1), 29–40.

Wigley, T. M. L., Smith, R. L., & Santer, B. D. (1998). Anthropogenic influence on the autocorrelation structure of hemispheric-mean temperatures. *Science*, **282**(5394), 1676.

Yiou, P., Baert, E., & Loutre, M. F. (1996). Spectral analysis of climate data. *Surveys in Geophysics*, **17**, 619–663.